Funded by the European Union

Horizon Europe

EUROPEAN COMMISSION

European Climate, Infrastructure and Environment Executive Agency (CINEA)

Grant agreement no. 101056765

Electric Vehicles Management for carbon neutrality in Europe

Deliverable D8.5
Analysis of demonstration results in the Greek demonstration report

Document Details

Due date	30-11-2025
Actual delivery date	17-04-2026
Lead Contractor	HEDNO
Version	1.0
Prepared by	Antonios Koutounidis (HEDNO), Ilias Manitaris (HEDNO), Vasileios-Martin Nikiforidis (PPC), Christina Papapostolou (PPC), Margarita Chatzouli (DTU)
Reviewed by	Cindy Paola Lascano (INESC ID), Samuel Matias (EDP NEW)
Dissemination Level	Public

Project Contractual Details

Project Title	Electric Vehicles Management for carbon neutrality in Europe
Project Acronym	EV4EU
Grant Agreement No.	101056765
Project Start Date	01-06-2022
Project End Date	31-05-2026
Duration	48 months

Document History

Version	Date	Contributor(s)	Description
0.1	24/10/2025	Antonios Koutounidis (HEDNO), Ilias Manitaris (HEDNO), Vasileios Melissianos (PPC)	Table of Contents
0.2	13/03/2026	Antonios Koutounidis (HEDNO), Ilias Manitaris (HEDNO), Vasileios-Martin Nikiforidis (PPC), Christina Papapostolou (PPC), Margarita Chatzouli (DTU)	First Complete Draft
0.3	02/04/2026	Antonios Koutounidis (HEDNO), Ilias Manitaris (HEDNO), Vasileios-Martin Nikiforidis (PPC), Christina Papapostolou (PPC), Margarita Chatzouli (DTU)	Revision after Internal Review
1.0	03/04/2026	Antonios Koutounidis (HEDNO), Ilias Manitaris (HEDNO), Vasileios-Martin Nikiforidis (PPC), Christina Papapostolou (PPC), Margarita Chatzouli (DTU)	Final Version

Disclaimer

Acknowledgment

This document is a deliverable of EV4EU project. EV4EU has received funding from the European Union´s Horizon Europe programme under grant agreement no. 101056765.

Funded by
the European Union

[1] https://ev4eu.eu/

Executive Summary

An analysis of results from the Greek EV4EU pilot in Koropi is presented in this document, combining evidence from field operation and simulation-based assessment to evaluate smart charging services, flexibility mechanisms, grid interaction, and the performance of the supporting technical ecosystem. The impacts of Flexible Capacity Contracts (FCC), Green Charging (GC) and Vehicle-to-Grid (V2G)-related concepts on charging behaviour, charger utilisation and local grid operation are examined, while the readiness of the Open Vehicle-to-Everything Management Platform (O-V2X-MP), smart chargers, the Decision Support System (DSS), the forecasting services and the Low-Voltage (LV) monitoring infrastructure is also assessed.

The Koropi pilot and the infrastructure deployed in the demonstration area of East Attica are first introduced. Four locations were electrified and equipped with dual-outlet AC smart chargers, while the grid-side infrastructure included LV monitoring equipment installed at the relevant substations and feeders. On the software side, reliance was placed on the DSS and the O-V2X-MP, through which data exchange, forecasting, smart charging control and the implementation of the flexibility services were supported. The pilot scope also included the two flexibility mechanisms addressed in the Greek demo, namely Business Use Case (BUC) 4 GC and BUC 5 FCC.

The operational setup of the DEMO is then described, including the constraints that shaped implementation. Due to legal and licensing limitations, the charging infrastructure was operated within a controlled pilot framework and user participation was restricted to PPC's and HEDNO's personnel. A dedicated pricing scheme was designed to reproduce the economic signals associated with the flexibility use cases through dynamic Distribution Use of System (DUoS) tariff, while user wallets were periodically credited to support participation. Since the monitored transformers did not naturally exceed their operational limits during the demonstration period, a forced activation logic was adopted based on forecasted and historical transformer loading, using transformer- and month-specific thresholds. In this way, tariff-based and capacity-based flexibility activation could be tested even under relatively mild real grid conditions. It should be noted already at this stage that the V2G-related results presented in this deliverable are simulation-based only, as bidirectional operation was not validated through real-user field operation during the demonstration period.

A dedicated Key Performance Indicator (KPI) framework is then defined for the assessment. The KPIs are grouped into General, Technical Related and Service Related categories. In addition to the indicators already defined in previous work, Forecast Accuracy, Forecast Model Retraining Time and O-V2X-MP Distribution System Operator (DSO) Latency are introduced as critical indicators for the activation of flexibility services. Service-related KPIs are assessed through simulation and include Desired Flexibility, Utilised Flexibility, CO2 emissions reduction, EV users' economic impact and Renewable Energy Sources (RES) curtailment reduction. In this way, both the demonstrated pilot and the broader effects of the simulated service concepts are consistently evaluated.

The findings from the field activities and the simulations are then brought together. Interoperability of the main components under real operating conditions was confirmed, and measurable technical, economic and behavioural evidence was generated. On the grid side, LV monitoring showed different loading conditions across the charging areas, with Papasideris Stadium operating closer to a potentially critical range, while no major voltage quality violations were observed at the feeders supplying the chargers. On the charging side, the pilot recorded 39 charging sessions, corresponding to 548.753 kWh of delivered energy and an average of 14.07 kWh per session, indicating mainly medium-scale opportunity charging. A total of 13 active users engaged with the system, including a recurring core

group, while billing and tariff application functioned as intended and smart charging operation was validated through DSO-triggered charging power modulation without interrupting user service.

The KPI evaluation confirms that the pilot reached a satisfactory level of technical maturity. Four locations were electrified, the user participation target was exceeded, and user satisfaction remained high. On the technical side, data acquisition and storage accuracy reached 99.58%, charger heartbeat and meter-value sampling met the required frequency, the O-V2X-MP supported up to 28 simultaneously connected chargers, service availability was reported at 100%, and average DSS-to-platform latency was 250 ms. Forecasting performance also proved adequate for operational use, with a Mean Absolute Percentage Error (MAPE) of 8.41% for the 4-hour horizon and a retraining time of 10.42 s, showing that the forecasting service can support near-real-time flexibility activation.

The simulation analysis extends the assessment beyond the limited field conditions and shows a clear progression across the examined service configurations. FCC mainly smooths and constrains charging demand, confirming its role as a direct congestion-management mechanism. GC produces a stronger temporal shift in charging demand toward periods with more favourable tariff and photovoltaic (PV) conditions. V2G provides the strongest overall flexibility effect, since it adds bidirectional exchange and enables discharge during system-relevant periods. This progression is also reflected in the simulated KPIs. FCC utilised 23.9% of the desired flexibility, while both GC and V2G reached 78.9%. Net CO2 emissions were reduced by 12.4% in GC and 20.4% in V2G relative to Business as Usual (BaU), while average EV user cost decreased by 9.1% in GC and 21.2% in V2G. These results indicate that FCC mainly delivers technical grid support, while GC and especially V2G offer broader environmental and economic value.

The final sections synthesise these findings through the discussion and conclusions. Overall, an operationally credible ecosystem for smart and flexible EV charging was established in the Greek DEMO, with the LV monitoring system, DSS and forecasting services, O-V2X-MP and smart chargers all demonstrating readiness for practical deployment. At the same time, the simulations show that the value of this ecosystem increases significantly when moving from direct technical control toward more advanced tariff-based and bidirectional flexibility schemes. A validated implementation basis is therefore provided, together with a forward-looking assessment of how coordinated EV charging can support grid operation, RES integration and future flexibility services in Greece.

Table of Contents

List of Figures

List of Tables

Acronyms

Acronym	Meaning
AoI	Area of Interest
BaU	Business as Usual
BUC	Business Use Case
CHAdeMO	“Charge de Move” DC fast-charging standard
CPO	Charge Point Operator
DER	Distributed Energy Resources
DSO	Distribution System Operator
DSS	Decision Support System
DUoS	Distribution Use of System
eMSP	e-Mobility Service Provider
EV	Electric Vehicle
FFC	Flexible Capacity Contracts
GC	Green Charging
KPI	Key Performance Indicator
LV	Low Voltage
MAPE	Mean Absolute Percentage Error
MV	Medium Voltage
NB-IoT	Narrowband Internet of Things
OCPP	Open Charge Point Protocol
O-V2X-MP	Open Vehicle-to-Everything Management Platform
PV	Photovoltaic
REST API	Representational State Transfer Application
RES	Renewable Energy Sources
SoC	State of Charge
V1G	Unidirectional Smart Charging
V2G	Vehicle-to-Grid
V2X	Vehicle-to-Everything

1 Introduction

1.1 Scope and Objectives

This deliverable presents the analysis of results, focusing on the evaluation of innovative electric vehicle (EV) charging services, business models, and flexibility concepts demonstrated and simulated within the project. The assessment combines field data from the demonstrator with simulation results to provide a consistent and comprehensive evaluation framework.

The scope includes the impact of concepts such as flexible capacity contracts, Green Charging, and Vehicle-to-Everything (V2X) services on EV user charging behaviour, charger utilization, and grid interaction. The evaluation is carried out using the Key Performance Indicators (KPIs) defined in Tasks T8.1 and also includes an assessment of the Open V2X Management Platform (O-V2X-MP) performance.

The main objectives of this deliverable are:

- To quantify the effects of new service and business models on EV charging behaviour.
- To evaluate the impact of Green Charging and Flexible Capacity Contracts on load profiles and grid interaction.
- To assess grid-related effects, including reverse load flow under high renewable generation
- To evaluate the performance of the DEMO components under real operational conditions.
- To compare Vehicle-to-Everything (V2X) and Unidirectional Smart Charging (V1G) charging strategies.
- To consolidate and analyse results from both field demonstrations and simulation studies to derive validated conclusions

1.2 Structure

The remaining of the deliverable is structured as follows: Chapter 2 presents the Greek pilot, the demonstrator components and the services assessed. Chapter 3 describes the operational setup and the implementation approach followed in the pilot site. Chapter 4 defines the KPI framework used for the assessment of the pilot and the simulations. Chapter 5 presents the results of the field activities and the simulation analysis. Chapter 6 discusses the main findings of the demonstration and simulation results. Chapter 7 concludes the deliverable by summarising the main outcomes and implications of the Greek DEMO.

1.3 Relationship with other deliverables

Deliverable D8.5 – Analysis of Results builds on the previous WP8 deliverables by analysing the outcomes of the Greek DEMO. D8.1 [1] defined the use cases and deployment plan, D8.2 [2] reported the demonstrator start-up status, D8.3 [3] addressed the testing of the O-V2X-MP, and D8.4 [4] validated the technologies enabling the flexibility services. In this context, D8.5 assesses the actual demonstration results and KPI performance, while D1.5 [5] provides the broader use-case framework for BUC 4 and BUC 5 and D4.5 [6]

2 Pilot Overview

2.1 Pilot Area

The demonstration of this pilot project is deployed in the East Attica region of Greece — the wider area that includes Mesogeia (as decided during D 8.1 [1]). The area plays a pivotal role for research activities, and the present demonstrator builds on and continues synergies established in previous projects. Mesogeia forms an important mobility and development corridor east of Athens, combining residential zones, commercial activity, transport infrastructure, and industrial areas.

The pilot site is located in the municipality of Koropi, part of the Mesogeia area in East Attica. Koropi is strategically located southeast of Athens, serving as a connection point between the capital, the eastern coastal part of Attica, and the Athens International Airport. Major transport corridors pass through or near the city. The city hosts more than 30,000 residents, while the greater Municipality of Kropia includes one of the main industrial zones of Attica.

2.2 Equipment

2.2.1 Smart Chargers

In close cooperation with the Municipality of Koropi, five candidate charging locations were initially identified to address diverse daily mobility needs within the local community. Following the implementation process, four locations were successfully electrified and became operational. The active charging areas are **Papasideris Stadium**, **2nd Elementary School**, **Municipality**, **Platea Eleftherias**.

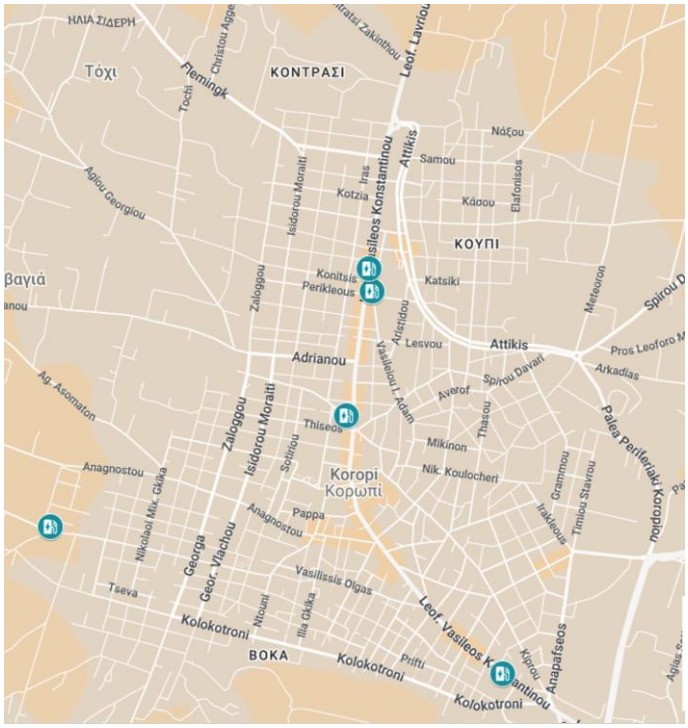

Figure 1: The locations of the 5 charging stations.

Each operational site is equipped with a dual-outlet AC charging unit featuring two Type 2 connectors, enabling the simultaneous charging of two EVs. Each connector supports a maximum charging capacity of 22 kW, allowing flexible service provision consistent with urban and semi-urban charging demand profiles.

All deployed charging stations support the Open Charge Point Protocol (OCPP) 1.6 for backend communication, ensuring interoperability with the central management system and enabling real-time monitoring, tariff management, and smart charging functionality. Figure 1 presents the locations of the installed charging stations and Figure 2 the respective photos.

Papasideris athletics

Agalmatos square

Koropi Municipality

Eleftherias square

2nd elementary school.

Figure 2: Photos of the charging points in the respective areas

2.2.2 V2G Chargers

PPC procured two Vehicle-to-Grid (V2G) enabled charging systems (Figure 3) to support bidirectional energy exchange between EVs and the distribution grid. The selected equipment includes:

Enovates Wallbox 22 kW V2G

Wallbox Quasar V2G

Figure 3: Procured V2G chargers

Connector Type and Charging Technology

The two chargers differ in connector technology and charging architecture:

- **Enovates Wallbox 22 kW V2G**
  - *AC Mode 3 charging*
  - *Type 2 connector (IEC 62196-2)*
  - *Supports three-phase AC charging up to 22 kW*
  - *Suitable for semi-public and commercial environments*
  - *Designed for integration with smart energy management systems*

- **Wallbox Quasar V2G**
  - *DC bidirectional charging*
  - *CHAdeMO connector (DC interface)*
  - *Enables true V2G functionality (vehicle-to-grid power export)*
  - *Designed for residential and controlled pilot deployments*

Nominal Power Ratings

- **Enovates Wallbox 22 kW V2G**
  - *Maximum AC charging power: 22 kW (3-phase, 400V)*
  - *Input: 3x400V AC ±10%, 50 Hz*
  - *Designed* for high-capacity AC charging applications
- **Wallbox Quasar V2G**
  - *Maximum charging power: 5 kW (AC/DC conversion integrated)*
  - *Maximum discharging power (V2G): 5 kW*
  - *Operates on single-phase AC input (230V, 50 Hz)*
  - *DC voltage range: 150–500 V*

Communication Protocols and Backend Integration
Both chargers support advanced communication standards for interoperability:

- OCPP 1.6 (Open Charge Point Protocol)
  - *Enables backend communication with the central management platform*
  - *Supports remote monitoring, transaction handling, firmware updates, and tariff management*
  - *Allows integration with e-mobility Service Provider (eMSP) platforms and smart charging algorithms*
- Additional communication capabilities (Wallbox Quasar):
  - *Wi-Fi / Ethernet connectivity*
  - *RFID authentication*
  - *App-based management*

The **Enovates Wallbox 22 kW (Vehicle-to-Grid) V2G charger is designed to support OCPP 2.0.1**, which represents the latest evolution of the Open Charge Point Protocol and includes enhanced functionalities such as improved smart charging capabilities, advanced security mechanisms, and native support for ISO 15118-based communication. However, **during the demonstration period, the OCPP 2.0.1 communication stack was not yet commercially activated by the manufacturer**.

2.2.3 LV Monitoring

The monitoring of the LV grid in the context of this project is achieving two main goals: the advanced monitoring of the grid and data-based decision making and network management, with the collection and analysis of network data for the efficient integration of electromobility in the electricity distribution network and the examination of demand response scenarios.

As defined in D8.2 [2], the main objective of the LV monitoring system is to collect accurate measurements of voltage (V), current (I), frequency (Hz), active (W) and reactive power (Var), energy consumption (Wh), and harmonics from MV/LV substations. The equipment facilitates the quick and efficient analysis of network data, with the target of improving grid performance, and the prevention of overloads and imbalances in the system. For every substation, the system includes one metering

device for the LV buses and up to 8 meters for the LV feeders, which depends on every different occasion.

More specifically, three-phase meters using Rogowski coils were installed at the selected substations to measure currents at: a) the substations' LV buses and b) their active LV feeders. Also, G-clamps were attached on the LV buses to collect the voltage, as depicted in Figure 4. In addition, the meters support wireless communication via NB-IoT technology (Narrowband Internet of things) with built-in SIM card and local memory for storing up to 3,000 records. For the pilot's LV monitoring system, the solution of the Greek company *Meazon* was selected.

Figure 4: LV monitoring installation

In total, five (5) MV/LV transformers provide power to the smart chargers. On the LV buses of each transformer, one 3-phase plus neutral meter (4 x 1000A) was installed with Rogowski coils for measuring currents. Also, thirty-two (32) 3-phase plus neutral meters (4 x 600A) were installed on the active LV feeders of those 5 substations. The total number of 32 meters was defined based on the active LV feeders that each substation has.

One additional LV monitoring solution was also implemented to complement the research purposes of this project. Two (2) distribution transformer monitoring devices were installed at the LV busbar of additional substations. Another, five (5) outage monitoring devices were installed at selected transformers including six (6) three-phase monitoring equipment of the LV feeders per substation. This system is called "Distribution Transformer Monitoring solution - DTM" and is offered by the international provider *Itron*.

2.3 Software

This section briefly presents the main software components supporting the Greek pilot. In particular, it describes the DSO side DSS and the O-V2X-MP platform, which together enable monitoring, data

exchange, smart charging operation, and the implementation of the flexibility services examined in the project.

2.3.1 DSS Overview

As reported in the previous deliverables D8.2 [2] and D8.4 [4], the DSS is a collection of software tools and capabilities, which integrates existing DSO functionalities, the LV monitoring equipment that has already been installed during the development of this project, and the Charging Point Operator's (CPO's) platform O-V2X-MP, Figure 5. The core purpose of the DSS is to enable the seamless communication between the DSS and the O-V2X-MP. This integration will facilitate the exchange of data and trigger events using standardized protocols, thereby achieving a higher level of network knowledge and visibility. Utilizing the data and the triggers delivered from the DSS, the O-V2X-MP will have the ability to realize the requirements of the BUCs proposed in the Greek demo.

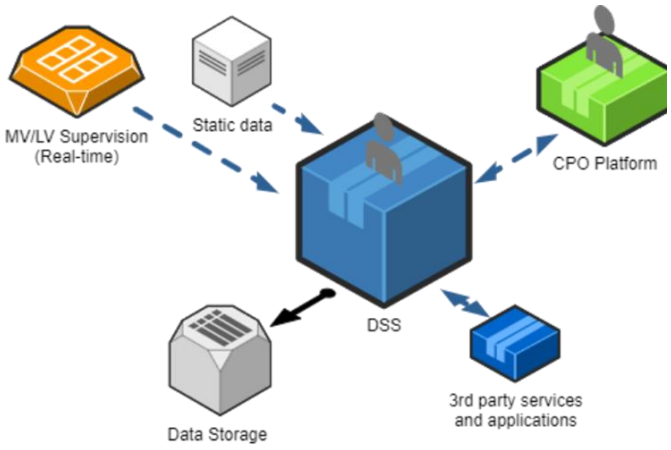

Figure 5: DSS architecture

The DSS acts as a decision support system to assist the control room and field operating personnel with the monitoring and control of the electric distribution system. It improves the efficiency and precision of many tasks, ranging from simple, such as network visualisation, to more advanced, such as dynamic decision-making on resources optimisation. In the centre of a DSS lies a software platform which can host all the required functionalities and 3rd party services, while interfacing with field equipment and other platforms.

2.3.1.1 Forecasting and Monitoring

A real time forecasting and flexibility activation framework was developed, implemented, and deployed to predict transformer loading and trigger EV flexibility actions. Using hourly aggregated monitoring data, the framework includes training a short-term probabilistic forecasting model and runs it in a rolling 4hour horizon, updating predictions every hour. A weighted trigger function evaluates the criticality of predicted limit violations, using normalized deviations across the horizon and weights reflecting decreasing forecast certainty, to activate either tariff based (BUC4) or capacity based (BUC5) flexibility. The trigger incorporates a hybrid decision strategy combining direct forecasts and percentile-based bounds near operational limits to balance false positives and false negatives. The developed forecasting framework and the detailed methodology followed are described in [4].

2.3.2 O-V2X-MP

The O-V2X-MP is an integrated digital platform designed to manage, monitor, and optimize EV charging infrastructure while enabling V2X services. Developed within the EV4EU framework, the platform acts as a central coordination layer between EV users, CPOs, charging stations, and the DSO, supporting smart charging and grid-responsive functionalities. More details can be found in D 5.5 [7].

The platform follows a modular, microservices-based architecture comprising backend services, frontend user interfaces, and interoperable APIs. It communicates with charging stations via OCPP, supports real-time WebSocket connections, and integrates with the DSS for dynamic grid interaction. This architecture ensures scalability, interoperability, and adaptability across different charging hardware and deployment contexts.

Key Functionalities

1. Charging Infrastructure Management: O-V2X-MP enables CPOs to manage charging stations, connectors, tariffs, charging profiles, and transactions. Through dedicated administrative tools, operators can remotely start/stop sessions, apply charging profiles, monitor real-time energy delivery, and export transaction data.

2. Smart Charging and Demand Response: The platform supports advanced smart charging scenarios, including charging scheduling, dynamic tariff updates, and capacity-based load allocation. Integration with the DSS allows real-time deployment of grid signals (e.g., renewable surplus or network congestion), enabling adaptive charging behavior aligned with grid conditions.

3. Real-Time Monitoring and Communication: Through WebSocket-based communication, the platform provides real-time updates on charger status, transaction progress, and power flow. Both EV users and administrators receive notifications related to tariff changes or grid constraints, enhancing operational transparency.

4. Data Analytics and Load Prediction: O-V2X-MP incorporates machine learning–based load prediction modules capable of forecasting daily charging demand per station. These predictive analytics tools support proactive grid management and infrastructure planning.

5. User Interaction and Experience Tools: The frontend interface provides routing support, charger filtering, tariff and capacity schedules, transaction history, weather integration, and reservation capabilities. Profile management tools allow users to manage identification tags and charging preferences.

6. Interoperability and Extensibility: The platform is designed to integrate with multiple charger brands and backend systems. Its modular design allows future expansion toward V2G services, advanced scheduling algorithms, and enhanced predictive functionalities.

2.4 Flexibility Mechanisms

As the penetration of EVs and RES increases, electricity grids are exposed to new operational challenges, including network congestion, reverse power flows, and more variable demand patterns [6]. Flexibility mechanisms (such as demand response, dynamic pricing, capacity management, and Vehicle-to-Grid (V2G) integration) are used to better align supply and demand and improve grid

efficiency. These mechanisms allow EVs and charging infrastructure to react dynamically, either by shifting charging demand over time or by returning stored energy back to the grid.

Within this framework, Business Use Case (BUC) 4 (Green Charging) and BUC 5 (Flexible Capacity Contracts) demonstrate how coordinated EV charging and V2G services can contribute to grid stability through incentive schemes and capacity constraints. In both use cases, flexibility is enabled through price incentives, but also, capacity contracts arranged in a monopsony market structure, where the CPO offers the DSO the option to enforce limits at substation level restricting energy imports in BUC 4 and capping load in BUC 5.

2.4.1 BUC 4 Green Charging

BUC 4 focuses on optimizing EV charging and V2G operations to support grid stability through Demand Response (DR) mechanisms [4], [6]. Its main objective is to reduce overvoltage risks, increase the use of renewable energy, and incentivize EV charging during periods of high renewable generation, while at the same time limiting V2G activity to avoid excessive power injection into the grid. The DSO procures capacity limitation contracts with CPOs through a monopsony market structure, allowing energy imports from V2G to be controlled when necessary. By dynamically adapting charging demand according to renewable energy availability, BUC 4 improves coordination between EVs and Distributed Energy Resources (DERs). When reverse power flow occurs (for example due to surplus photovoltaic (PV) generation), the mechanism activates incentives for EV users to charge at appropriate times and applies restrictions on V2G operations. In this way, demand is better aligned with supply, helping to prevent grid congestion.

Process and Implementation

BUC 4 can be described in the following steps:

1. **Identifying Potential Overvoltage Risks**
   DSO (HEDNO) through the DSS tools, that integrate the installed Low Voltage (LV) monitoring system and the forecasting services provided by Technical University of Denmark (DTU), identifies with estimated uncertainties substations where potentially overvoltage could occur due to high renewable energy injection.

2. **Dynamic Tariff Adjustment & Capacity Limitations**
   To encourage EV charging and prevent excessive power imports, the DSO:

   a. Introduces negative DUoS tariffs for charging under affected substations, making charging more attractive, and at the same time penalizing V2G.
   b. Activates capacity limits for energy imports, ensuring that EVs do not inject excessive power back into the grid.

3. **Communication & Implementation**
   The negative DUoS tariffs and V2G capacity limits are communicated to the O-V2X-MP, via a predesigned message, from DSS tools. The Charging Point Operator (CPO - PPC) receives this information and updates the pricing and V2G capacity limits for the affected charging stations accordingly.

4. **User Notification & Response**

The updated charging tariffs are displayed to EV users via the platform. This allows users to adjust their charging behavior, shifting their demand to the discounted period while keeping V2G operations within feasible capacity levels.

By implementing BUC 4, the grid can optimize EV charging, mitigate overvoltage risks, and promote renewable energy utilization, ensuring a more stable and efficient distribution system.

2.4.2 BUC 5 Flexible Capacity Contracts

BUC 5 defines a flexibility mechanism through which the DSO can regulate EV charging and V2G activity using capacity limitation contracts, with the aim of avoiding grid congestion and improving network utilization. Under this scheme, the DSO acquires capacity limitation contracts from CPOs within a monopsony market framework, ensuring that charging power can be curtailed when required. When congestion is identified in real time, the DSO applies charging capacity limits and simultaneously increases DUoS (Distribution Use of System) tariffs at the affected distribution network buses. These changes are transmitted to the O-V2X-MP platform, which accordingly updates charging station power limits as well as charging and discharging price signals, and informs EV users so they can adapt their charging behaviour while maintaining grid stability [4], [6].

Process and Implementation

BUC 5 can be described in the following steps:

1. **Identifying Grid Congestion & Forecasting Capacity Needs**
   The Distribution System Operator (DSO), using its DSS tools, integrates data from the installed LV monitoring system and forecasting services provided by DTU. With estimated uncertainties, the DSO identifies substations where congestion is likely to occur, in real-time operations.

2. **Capacity Limitation Activation**
   When congestion is detected (real-time), the DSO activates the capacity limits to prevent network overloading. The DSO activates the pre-procured contracts for the affected substations and increases the DUoS tariffs to discourage charging and incentivize V2G.

3. **Communication & Implementation**
   The capacity limits and increased tariffs are communicated via DSS tools to the O-V2X-MP. The high DUoS tariffs, and capacity limits are communicated to the O-V2X-MP, via a predesigned message, from DSS tools. The Charging Point Operator (CPO - PPC) receives this information and updates the pricing and charging power capacity for the affected charging stations accordingly.

4. **User Notification & Response**
   The platform updates EV charging availability, displaying it to EV users informing users about charging power adjustments and increased prices. Users can then modify their charging sessions based on available capacity, ensuring compliance with grid stability measures.

By implementing BUC 5, the grid can dynamically manage congestion, optimize network flexibility, balance EV charging demand, ensuring efficient energy distribution without compromising grid reliability.

3 DEMO Preparation and Operational Design

Chapter 3presents the main elements that supported the implementation and operation of the DEMO. In particular, it describes the user recruitment activities, the design of the pricing and wallet scheme, and the analysis approach used to define the activation of the BUCs, which together enabled the practical execution of the demonstration.

3.1 Recruitment

Due to legal and licensing constraints associated with the operation of the demonstration charging infrastructure, the user recruitment strategy was necessarily limited to personnel employed by the PPC and the HEDNO. Consequently, participation in the demonstration activities was restricted to employees of these two organizations.

In order to effectively disseminate information about the demonstration and encourage participation among potential EV users within these organisations, a targeted internal communication approach was adopted. Specifically, an informational poster was designed and distributed across several PPC and HEDNO facilities. The posters were placed at visible locations within buildings situated in the wider Koropi area, as well as in additional operational facilities where technical staff and field personnel operating company service vehicles are based.

The objective of this approach was to ensure that employees who regularly operate company vehicles in the surrounding area were adequately informed about the availability of the charging infrastructure and the opportunity to participate in the demonstration activities. Figure 6 presents two indicative photographs of the informational poster installed at central locations within the premises of the participating organizations, ensuring high visibility for interested personnel.

Figure 6: Informational posters displayed at PPC and HEDNO facilities to support user recruitment for the demonstration.

In addition, HEDNO organized an online event in order to inform potential users about the EV4EU project and specifically the goals of the Greek DEMO and the technologies implemented, which they will potentially use during the DEMO period.

It should be noted that the participant pool of the demonstration was restricted to PPC and HEDNO personnel due to legal and licensing constraints. As a result, the sample was limited in both size and diversity, with 13 active users recorded during the monitoring period. Therefore, the observed

behavioural and operational patterns should be interpreted as indicative findings from a controlled pilot environment rather than as statistically representative evidence of the broader EV user population.

3.2 Pricing Scheme

The demo pricing scheme was designed to reproduce the economic signals associated with the different flexibility use cases by modifying the network-use tariff around a common baseline. In the Business as Usual (BaU) scenario, the applicable network charge was set to 0.0034 €/kWh [8], while the electricity sale price was assumed to be 0.4 €/kWh. For the flexibility cases, this baseline tariff was scaled according to the active use case. In BUC 4, the tariff was set to -15 × 0.0034 €/kWh = −0.051 €/kWh in the yellow period and -45 × 0.0034 €/kWh = −0.153 €/kWh in the orange/red period. In BUC 5, the tariff was set to 30 × 0.0034 €/kWh = 0.102 €/kWh in the yellow period and 60 × 0.0034 €/kWh = 0.204 €/kWh in the orange/red period.

Accordingly, the total cost of a full 50 kWh charging session becomes 20.17 € in BaU, 17.45 € in BUC 4 yellow, 12.35 € in BUC 4 orange/red, 25.10 € in BUC 5 yellow, and 30.20 € in BUC 5 orange/red. In this way, the scheme combined rewards for grid-supportive charging with penalties for charging during stressed periods.

To support user participation during the pilot, each user wallet was credited with 45 €, renewed every two weeks, a level chosen to approximately cover expected charging needs while still making the tariff differentiation visible in user behaviour.

3.3 Forced BUCs Activation

Generally, PV generation is expected to peak around midday, creating a risk of overvoltage that would require EVs to consume more, through incentives. Conversely, EV charging demand is expected to rise in the evening hours, leading to peak loading where incentives would need to work in the opposite direction.

However, the actual transformer measurements follow a different pattern. From approximately 23:00 to 07:00 the loading reaches its daily minimum. During the middle of the day, we observe a subtle dual-peak profile, with one peak around 10:00 and a second around 16:00, followed by declining loading in the afternoon.

Importantly, none of the transformers are currently overloaded; their loading never exceeds their operational limits. Figure 7 and Figure 8, both illustrate these trends and highlight the hourly and monthly variation in loading behaviour. To meaningfully test all incentive-trigger levels, we derived **transformer-specific and month-specific limits** using forecasted values in combination with observed historical transformer loading.

- The **upper limit** (overloading risk) was defined as the 95th percentile of loading during 07:00-10:00 and 16:00-19:00, which were the periods where peaks are observed.
- The **lower limit** (overvoltage risk due to PV generation) was defined as the 5th percentile during 11:00-15:00.

Incentive messages are only allowed between 07:00 and 23:00, with the latest possible message being issued at 19:00 for the next four-hour period. This constraint reflects both the unrealistic probability of overvoltage at night and the low likelihood that consumers would respond to incentives during those hours. Overall, the trigger limits are tailored for each transformer and each month based on both

forecasting outputs and historical loading patterns. This approach enables us to **test as many relevant cases as possible,** given the uncertainty of forecasting results.

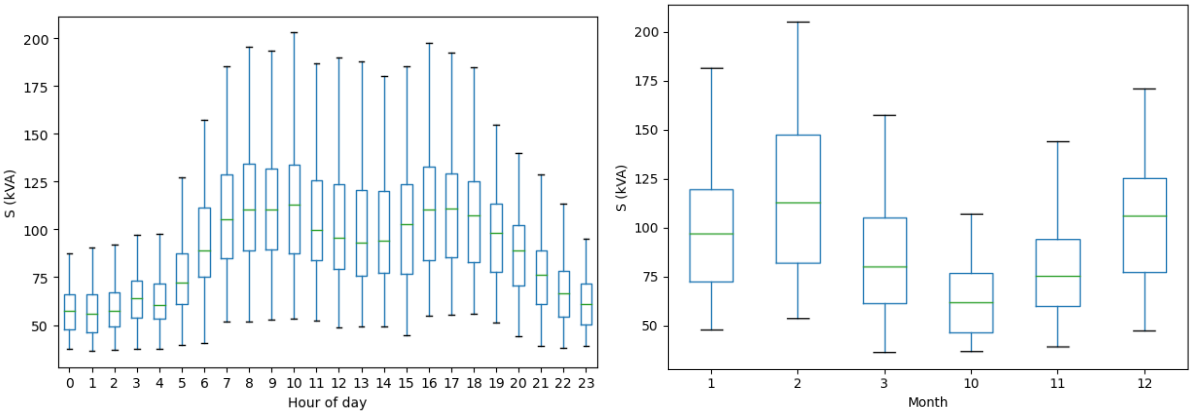

Figure 7: The apparent power of transformer at the 2nd Elementary School distributed across hours of day and across months of year.

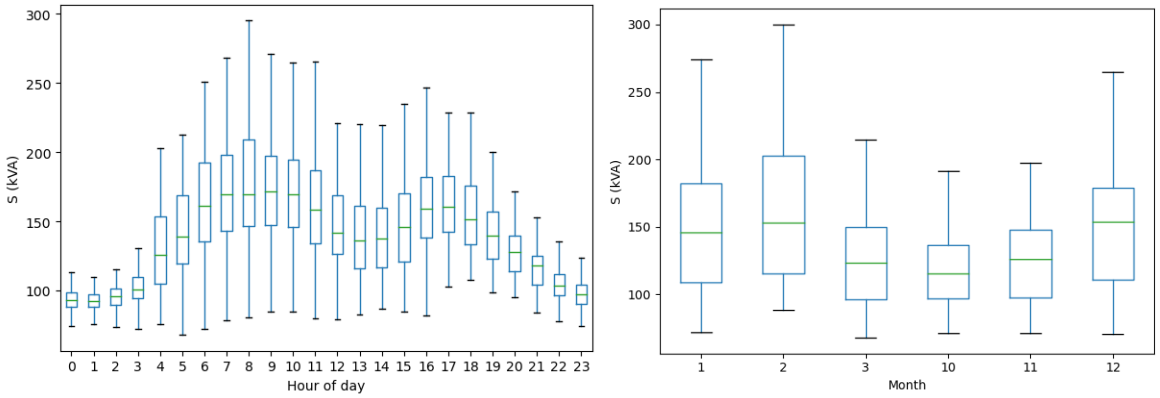

Figure 8: The apparent power of transformer at Koropi Municipality distributed across hours of day and across months of year.

4 KPIs of the Greek Demo

In this Chapter we formally describe the calculated KPIs in table form to help the reader identify the important aspects of the calculated or input value. In addition, we present any significant change compared to D 8.1.

The KPIs have been already described in D 8.1. Three (3) KPIs have been added, one (1) have been renamed, and one (1) have been removed. The three KPIs that have been added are the: Forecast Accuracy, Forecast Model Retraining Time, O-V2X-MP DSO Latency, which have been identified as critical for the accurate and seamless activation of the BUCs. The Requested Flexibility has been renamed to Desired Flexibility, since the tariff incentives that DSO signals cannot be quantified. In a request but we can see it as desire. Moreover, Peak Load Demand reduction/increase has been removed since it is a KPI relative to BUC 5 (Flexible Capacity Contracts) and the activation of such contacts is applied if the transformer's load reaches 80% of transformer's nominal capacity and this is exactly what we calculate in Desired Flexibility and Utilized Flexibility KPIs.

Also the KPIs have been recategorized to: General KPIs where we included the general information ("demo in numbers") of the DEMO, Technical Related KPIs which are insightful about the performance of individual elements of DEMOs components, and Service Related KPIs which estimate the impact of the flexibility services to important environmental, distribution network, and user metrics through state of the art simulations, combining realistic individual agents (EV user) activity schedules and real charging and grid infrastructure in Athens Metropolitan Area.

4.1 General

4.1.1 Number of Charging Points

BASIC KPI INFORMATION

KPI NAME	Number of Charging Points	**KPI ID**	KPI_GR_03
RELEVANT BUC(S)	4, 5		
RELATED PROJECT OBJECTIVE(S)	Integration of V2X in Smart Grids.		
Related GREEK DEMO OBJECTIVE (S)	Deployment and testing of the Open V2X management platform for public Charging Points.		
OWNER	PPC		
KPI DESCRIPTION	The indicator presents the number of charging points installed in the pilot.		
KPI FORMULA	CCPs = n, n ∈ ℕ CCPs: counter of CPs n: number of CPs ℕ: set of natural numbers		
UNIT OF MEASUREMENT	Number (#)		
TARGET/ THRESHOLDS	The indicator shows the total installed charging points in the grid that are fully functional. This KPI should be within the suggested number of charging points proposed in the Greek pilot, between 2 and 5 charging points.		
MEASURED/INPUT DATA	-		

4.1.2 Number of LV Monitoring Equipment

BASIC KPI INFORMATION

KPI NAME	Number of LV Monitoring Equipment	**KPI ID**	KPI_GR_04
RELEVANT BUC(S)	4, 5		
RELATED PROJECT OBJECTIVE(S)	Contributes to planning and real-time operation tools using by DSO.		
RELATED GREEK DEMO OBJECTIVE(S)	Measurements from Secondary Substations which is important for DSO to request flexibility from CPO (BUC5) and to detect the reverse flow energy (BUC4).		
OWNER	HEDNO		
KPI DESCRIPTION	This KPI measures the number of Low Voltage monitoring equipment which will be installed in HEDNOs' Secondary Substations to provide data to DSO platform.		
KPI FORMULA	$C = n, n \in \mathbb{N}$ C: number of LV monitoring equipment in operation $\mathbb{N}$: set of natural numbers		
UNIT OF MEASUREMENT	Number (#)		
TARGET / THRESHOLDS	The target is to install the LV monitoring equipment at least in three Secondary Substations and set it in fully operated mode.		
MEASURED/INPUT DATA	-		

4.1.3 EV User Participants

BASIC KPI INFORMATION

KPI NAME	EV User Participants	**KPI ID**	KPI_GR_08
RELEVANT BUC(S)	4, 5		
RELATED PROJECT OBJECTIVE(S)	The project demonstrates how the extensive use of V2X technologies affects user behaviour. The O-V2X MP is set to incorporate a series of algorithms designed for the effective management of EVs. These algorithms will be accessible to EV users, enabling them to assess the performance of these tools.		
RELATED GREEK DEMO OBJECTIVE(S)	Users will primarily be sourced from the pilot site's region, although individuals from other intriguing areas will be taken into account, to enable a comprehensive analysis.		
OWNER	PPC		
KPI DESCRIPTION	The quantity of EV users who will utilize the project-related charging stations to recharge their vehicles at least once.		
KPI FORMULA	$N_U = n, n \in \mathrm{N}$ N_U: number of EV users N set of natural numbers		

UNIT OF MEASUREMENT	Number(#)
TARGET / THRESHOLDS	At least 4
MEASURED/INPUT DATA	The O-V2X-MP tracked the distinct count of EV users who charged their vehicles at the designated project-related charging stations.

4.1.4 EV User Satisfaction

BASIC KPI INFORMATION			
KPI NAME	EV User Satisfaction	**KPI ID**	KPI_GR_10
RELEVANT BUC(S)	BUC 4,5		
RELATED PROJECT OBJECTIVE	To Evaluate the engagement of the users in V2X adoption.		
GREEK DEMO OBJECTIVE(S)	To test the activation and impact in user behaviour of platform's different services.		
OWNER	PPC		
KPI DESCRIPTION	This KPI measures the satisfaction of users with respect to their interaction with O-V2X-MP. The KPI will be measured from a questionnaire that will be distributed to the participants. Each question will accept a range from 0 to 10 (greater number indicates higher satisfaction). Therefore,		
KPI FORMULA	$$S = \frac{\sum_i^n q_i}{n}$$ q_i denotes the score for the i-th question. n denotes the total number of questions.		
UNIT OF MEASUREMENT	Percentage %		
TARGET / THRESHOLDS	> 90%		
MEASURED/INPUT DATA	A custom questionnaire was prepared using the EU Survey tool[2] and shared with the EV users participating in the BUCs.		

[2] https://ec.europa.eu/eusurvey/

4.1.5 Information Computer Technology (ICT) Cost

BASIC KPI INFORMATION			
KPI NAME	Information Computer Technology (ICT) cost	**KPI ID**	KPI_GR_14
RELEVANT BUC(S)	4, 5		
RELATED PROJECT OBJECTIVE(S)	Communications and data exchange between all stakeholders		
RELATED GREEK DEMO OBJECTIVE(S)	Interoperability of the O-V2X-MP for the management and operation of public charging with the existing infrastructure that includes charging stations, user equipment, and DMS.		
OWNER	HEDNO, PPC		
KPI DESCRIPTION	This KPI calculates the total cost incurred from the necessary use of information and communication technologies (HW and SW) to provide the flexibility services. Two formulas are presented, one for the costs of the DSO and one for the CPO.		
KPI FORMULA	$COUT_{DSO} = C_{ommunication\ equipment} + S_{erver} + SW_{\ development} + (N_{etwork\ provider} \times X) + M_{aintenance}$ **$C_{ommunication\ equipment}$:** cost of communication hardware (€) **S_{erver}:** server equipment cost (€) **$SW_{\ development}$:** software development cost (€) **$N_{etwork\ provider}$:** monthly network fees (€) **X:** total months of network contract **$M_{aintenance}$:** maintenance cost (€)		
UNIT OF MEASUREMENT	Euro (€)		
TARGET / THRESHOLDS	The target of this KPI is to keep the total cost of the installed information and communication technologies below the allocated budget for equipment and services in order to leave enough resources for the rest of the required equipment.		
MEASURED/INPUT DATA	The formulas sum up the total cost of: a) the communication hardware equipment used to facilitate the communication of the platforms with the grid equipment and between each other (modems, switches, antennas, etc.), b) the total server equipment required (PCs, miscellaneous), c) platform software development and end user application development (if applicable), d) network communication provider monthly fees, e) roaming hub provider monthly fees (for CPO) and f) maintenance of the total SW and HW technologies.		

4.2 Technical Related KPIs

4.2.1 Data Acquisition and Storage Accuracy

BASIC KPI INFORMATION

KPI NAME	Data Acquisition and Storage Accuracy (DASA)	**KPI ID**	KPI_GR_05
RELEVANT BUC(S)	4, 5		
RELATED PROJECT OBJECTIVE(S)	Real-time operation decision support tools		
RELATED GREEK DEMO OBJECTIVE(S)	To validate that the measurement data are collected and stored properly, for further process.		
OWNER	HEDNO		
KPI DESCRIPTION	This KPI assesses the precision and reliability of data collected from metering infrastructures installed at secondary substations. It focuses on ensuring that measurements from the substations are captured, recorded, and processed with a high degree of accuracy, completeness, and consistency. A series of data includes valid values of all the expected data (V, I, f, P, Q) at a certain time. To consider a series of data as accurate it should contain all the expected data, and the values of these data are within a specific reasonable range.		
KPI FORMULA	$\text{Accuracy} = \left(\frac{\text{Accurate Data Points Sored}}{\text{Total Expected Data Points}} \right) \times 100$		
UNIT OF MEASUREMENT	%		
TARGET / THRESHOLDS	95% during a month period of time, in the context 95% of the expected data has been collected and stored properly		
MEASURED/INPUT DATA	Voltage (V), Current (I), frequency (f), Active Power (P), Reactive Power (Q) from the secondary substations		

4.2.2 Data Sampling Frequency

BASIC KPI INFORMATION

KPI NAME	Data Sampling Frequency	**KPI ID**	KPI_GR_06
RELEVANT BUC(S)	4, 5		
RELATED PROJECT OBJECTIVE(S)	Real-time operation decision support tools.		
RELATED GREEK DEMO OBJECTIVE(S)	Reduced data sampling time period and capacity accuracy in flexibility contracts and green charging.		
OWNER	HEDNO, PPC		
KPI DESCRIPTION	The time period in which the CPs and the LV monitoring system send measurements and data packages from the field to the Server/platform.		
KPI FORMULA	$T = t$		

	t: time period for sampling data setting or configuring the equipment and the telecommunication with the target intervals.
UNIT OF MEASUREMENT	Time (minutes)
TARGET / THRESHOLDS	≤ 5 minutes/per data packages
MEASURED/INPUT DATA	-

4.2.3 Scalability of O-V2X-MP

BASIC KPI INFORMATION

KPI NAME	Scalability of O-V2X-MP	**KPI ID**	KPI_GR_13
RELEVANT BUC(S)	4, 5		
RELATED PROJECT OBJECTIVE(S)	The design of the open V2X management platform ensures solution scalability and reliability		
RELATED GREEK DEMO OBJECTIVE(S)			
OWNER	PPC		
KPI DESCRIPTION	The maximum number of EV charging stations (EVCS) that O-V2X-MP can support simultaneously.		
KPI FORMULA	$EVCS_{max} = n \in N$ n: The number of EV charging stations that O-V2X-MP can support.		
UNIT OF MEASUREMENT	Units (number of EVCSs)		
TARGET / THRESHOLDS	>= 25		
MEASURED/INPUT DATA	Use one or multiple instances of an EV charging station simulator [9] and configure multiple instances of EVCSs to connect to a production-ready deployed version of O-V2X-MP. While all EVCSs are connected, verify that O-V2X-MP is operational, by trying to execute OCPP commands to the underlying EVCSs. All OCPP operations must be successful.		

4.2.4 Availability of the O-V2X-MP Services

BASIC KPI INFORMATION

KPI NAME	Availability of the the O-V2X-MP Services	**KPI ID**	KPI_GR_12
RELEVANT BUC(S)	4, 5		
RELATED PROJECT OBJECTIVE(S)	The design of the open V2X management platform ensures solution scalability and reliability		
RELATED GREEK DEMO OBJECTIVE(S)	To demonstrate the interoperability of the O-V2X-MP for the management and operation of public charging with the existing		

	infrastructure that includes charging stations, user equipment, and DSM.
OWNER	PPC
KPI DESCRIPTION	The indicator measures the percentage of time that the connectivity of O-V2X-MP with the charging points is available. The availability ensures the reliability of O-V2X-MP and the fact that there are no implementation flaws that disrupt the availability of the O-V2X-MP services. External events and circumstances (e.g., bad 4G connectivity or disruptions irrelevant to O-V2X-MP) are excluded from this KPI.
KPI FORMULA	$$A = \frac{Uptime}{Uptime + Downtime} * 100\%$$ *Uptime*: the total time when the connectivity of O-V2X-MP with the charging points is available *Downtime*: the total time when the connectivity of O-V2X-MP with the charging points is not available
UNIT OF MEASUREMENT	%
TARGET / THRESHOLDS	> 99.9%
MEASURED/INPUT DATA	This KPI measured by analysing the operational logs of O-V2X-MP to determine possible disconnections during a specific observability window.

4.2.5 O-V2X-MP DSO Latency

BASIC KPI INFORMATION			
KPI NAME	OV2XMP DSO Latency	**KPI ID**	KPI_GR_16
RELEVANT BUC(S)	4, 5		
RELATED PROJECT OBJECTIVE	To measure the latency of the DSS signal from DSO to the OV2XMP platform.		
GREEK DEMO OBJECTIVE(S)	To apply DSO signal to physical chargers and set capacity limits and tariff schedules.		
OWNER	PPC		
KPI DESCRIPTION	This KPI measures the latency time of the DSO signal to reach the OV2XMPL platform.		
KPI FORMULA	$$T = t$$ t: Time period of the telecommunication with the target intervals.		
UNIT OF MEASUREMENT	Time (seconds)		
TARGET / THRESHOLDS	-		
MEASURED/INPUT DATA	-		

4.2.6 Forecast Accuracy

KPI NAME	Forecast Accuracy	KPI ID	KPI_GR_ 17
RELEVANT BUC(S)	4, 5		
RELATED PROJECT OBJECTIVE(S)	Ensure reliable short-term forecasting to support activation of flexibility services and prevent congestion/overvoltage events.		
RELATED GREEK DEMO OBJECTIVE(S)	Demonstrate accurate real-time forecasting of transformer loading to enable data-driven flexibility activation.		
OWNER	DTU		
KPI DESCRIPTION	This KPI measures the predictive performance of the short-term forecasting model used to estimate transformer apparent power over a 4-hour horizon. Performance is evaluated through rolling forecasts using unseen test data, comparing forecasted values with actual measurements. Lower error indicates higher model accuracy, which is critical for correctly triggering flexibility mechanisms.		
KPI FORMULA	Mean Absolute Percentage Error (MAPE): $$MAPE = (1/n) \sum \left\lvert \frac{y_i - \hat{y}_i}{y_i} \right\rvert \times 100\%$$ • n: number of forecasted values in the evaluation period • y_i: actual measured apparent power at timestamp i • $\hat{y}_i$: forecasted apparent power at timestamp i		
UNIT OF MEASUREMENT	% MAPE		
TARGET / THRESHOLDS	Target: **MAPE < 10%** for the 4-hour forecast horizon		
MEASURED/INPUT DATA	Forecasted and actual apparent power values of the transformer (hourly resolution), test period Feb-Mar 2025.		

4.2.7 Forecast Model Retraining Time

KPI NAME	Model Retraining Time	KPI ID	KPI_GR_ 18
RELEVANT BUC(S)	4, 5		
RELATED PROJECT OBJECTIVE(S)	Ensure that forecasting services can be updated and retrained fast enough to support real-time operation and dynamic flexibility activation.		
RELATED GREEK DEMO OBJECTIVE(S)	Demonstrate low-latency retraining and updating of forecasting models in the pilot to maintain accuracy under changing load patterns.		

OWNER	DTU
KPI DESCRIPTION	This KPI measures the time required to fully retrain or update the forecasting model using the selected historical training window. Rapid retraining is essential for operational deployment, where new data arrives hourly and the model must adapt to seasonal effects and behavioral changes caused by flexibility activation.
KPI FORMULA	Total elapsed time (in seconds) required to retrain the forecasting model on the designated training dataset.
UNIT OF MEASUREMENT	Seconds (s)
TARGET / THRESHOLDS	Target: **< 15 s** for full retraining Good: 5-15 s Acceptable: 15-30 s Not acceptable: > 30 s
MEASURED/INPUT DATA	Model training logs, runtime measurements from retraining the model using the selected historical training window (3–5 months of hourly data).

4.3 Service Related KPIs

4.3.1 Desired Flexibility

BASIC KPI INFORMATION

KPI NAME	Desired Flexibility	**KPI ID**	KPI_GR_11
RELEVANT BUC(S)	4, 5		
RELATED PROJECT OBJECTIVE(S)	Planning and real-time operation tools using by DSO.		
RELATED GREEK DEMO OBJECTIVE(S)	Testing the impact of in user behaviour of flexible capacity contracts.		
OWNER	HEDNO		
KPI DESCRIPTION	Desired Flexibility quantifies the total amount of EV charging demand that worsens grid stress conditions under the BaU uncoordinated scenario. It represents the absolute EV flexibility volume that the system would ideally shift. In our case we define it as the total amount of EV charging energy across all substations when the transformer operates at over 80% of transformer's nominal apparent power capacity. We assume a unity Power Factor (PF = 1), hence apparent power is equal to active power.		
KPI FORMULA	$$F_{des} = \sum_{s\in\mathcal{S}} \sum_{t\in\mathcal{T}} P_{charge,s}\ \Delta t, \quad \text{for } P^t_{base,s} > 0.8 \cdot C_s$$ $$P^t_{base,s} = P^t_{load,s} - P^t_{pv,s}$$ where:		

	$\mathcal{S}$: set of substations s: substation index t: time index C_s: power capacity limit of substation s (kWh) $P^t_{load,s}$: load at substation s at time t (kW) $P^t_{pv,s}$: PV generation at substation s at time t (kW)
UNIT OF MEASUREMENT	kWh
TARGET / THRESHOLDS	-
MEASURED/INPUT DATA	Simulated via realistic EV user activity schedules, real infrastructure data for substations and charging stations, and generated baseline load and PV profiles.

4.3.2 Utilised Flexibility

BASIC KPI INFORMATION

KPI NAME	Utilised Flexibility	KPI ID	KPI_GR_09
RELEVANT BUC(S)	4, 5		
RELATED PROJECT OBJECTIVE(S)	To develop planning and real-time operation tools to be used by DSOs considering V2X impact and flexibilities. To propose and evaluate different business models options promoting the integration of V2X in electricity markets and power systems.		
GREEK DEMO OBJECTIVE(S)	To test the impact of flexibility services on EV user behaviour.		
OWNER	HEDNO		
KPI DESCRIPTION	The indicator computes the total amount of flexibility offered by the EV users in the form of selecting a charging session from the options available during the activation of the capacity contract service. In this case, flexibility has the form of load shifts. That means that an EV user may shift his consumption towards or away from a time period.		
KPI FORMULA	$$F_{util} = F_{des} - F_{unshifted}$$ where: F_{util}: Utilized Flexibility F_{des}: Desired Flexibility $F_{unshifted}$: EV charging demand that remains during stress periods even after the flexibility service is applied		
UNIT OF MEASUREMENT	kWh		
TARGET / THRESHOLDS	The target is to maximise utilized flexibility, that is, to shift as much of the desired flexibility as possible away from grid stress periods. The assessment is done based on the desired flexibility of the BaU case. A 40% improvement is considered significant.		

MEASURED/INPUT DATA	Simulated via realistic EV user activity schedules, real infrastructure data for substations and charging stations, and generated baseline load and PV profiles.

4.3.3 Carbon Dioxide (CO2) Emissions Reductions

BASIC KPI INFORMATION

KPI NAME	Impact on CO2 Emissions Reductions	**KPI ID**	KPI_GR_07
RELEVANT BUC(S)	4		
RELATED PROJECT OBJECTIVE(S)	To show that the massive use of EVs will significantly contribute to carbon neutrality targets.		
RELATED GREEK DEMO OBJECTIVE(S)	To examine that the proposed solutions, contributes to CO2 emissions mitigation		
OWNER	HEDNO		
KPI DESCRIPTION	This KPI evaluates the reduction in carbon dioxide (CO2) emissions achieved by using clean, renewable energy sources for EV charging, contributing to sustainability and addressing climate change.		
KPI FORMULA	$$CO_2\ Reduction\ (\%) = \frac{Em_{BaU} - Em_{scen}}{Em_{ref}} \cdot 100$$ $$Em_{net} = Em_{gross} - Em_{avoided}$$ $$Em_{avoided} = \sum_{t \in \mathcal{T}} \left(P^t_{discharge}\right) \cdot EF(t)$$ $$Em_{gross} = \sum_{t \in \mathcal{T}} \left(P^t_{charge}\right) \cdot EF(t)$$ t: timestep (Hours) $EF(t)$: Greek hourly grid emission factor at hour t gCO_2eq/kWh P^t_{charge}: total aggregated EV charging power at hour t, in kW $P^t_{discharge}$: total aggregated EV discharging power at hour t, in kW Em_{gross}: gross CO_2 emissions from EV charging $Em_{avoided}$: avoided CO_2 emissions due to V2G discharging Em_{net}: net CO_2 emissions Em_{BaU}: net CO_2 emissions of the BaU scenario Em_{scen}: net CO_2 emissions of the examined scenario		
UNIT OF MEASUREMENT	%		
TARGET / THRESHOLDS	> 10% is considered significant.		
MEASURED/INPUT DATA	Greek hourly grid carbon intensity values in gCO_2eq/kWh and the simulated charging demand results.		

4.3.4 EV users' Economic Impact

BASIC KPI INFORMATION

KPI NAME	EV users' Economic Impact	**KPI ID**	KPI_GR_15
RELEVANT BUC(S)	4		
RELATED PROJECT OBJECTIVE(S)	Demonstrate the impact of mass deployment of V2X technologies considering users behaviour. To evaluate the engagement of the users in V2X adoption and DR programs.		
RELATED GREEK DEMO OBJECTIVE(S)	To test the impact of V2X and flexibility services on EV user's economic output To investigate the proposed solutions exploitation plan and marketability strategy, resulting in the broadest possible user acceptance and societal added value.		
OWNER	HEDNO		
KPI DESCRIPTION	This KPI calculates the average net financial profit or loss of EV users. In specific, EV Users may experience discomfort (pains) or extra financial costs while participating in V2X. User discomfort can be translated to financial cost and is measured in euros. On the other hand, they may be remunerated for their participation in V2X. by selling energy back to the grid.		
KPI FORMULA	$$C_{avg} = \frac{1}{N_{EV}} \sum_{i \in I} C_i$$ where: I: set of EV users N_{EV}: number of EV users C_i: daily cost of charging/discharging for EV user i		
UNIT OF MEASUREMENT	Euro (€)		
TARGET / THRESHOLDS	The target is to have a net positive financial impact on the EV users, in order to incentivize participation in Green Charging and V2X. A 10% total cost reduction is considered adequate.		
MEASURED/INPUT DATA	The economic impact on EV users is assessed via simulations. Comparing the BaU with the rest of the scenarios.		

4.3.5 RES Curtailment Reductions

BASIC KPI INFORMATION

KPI NAME	RES Curtailment Reductions	**KPI ID**	KPI_GR_01
RELEVANT BUC(S)	4		
RELATED PROJECT OBJECTIVE(S)	To develop planning and real-time operation tools to be used by DSOs considering V2X impact and flexibilities.		
RELATED GREEK DEMO OBJECTIVE(S)	To test the activation and impact in user behaviour of different services.		
OWNER	HEDNO		

KPI DESCRIPTION	The indicator compares the amount of energy from Renewable Energy Sources (RES) that is not injected to the grid (even though it is available) due to operational limits of the grid, between the Green Charging scenario BaU.
KPI FORMULA	$$\Delta C_{RES}^{\%} = \frac{\Delta C_{RES}}{\sum_{t\in T}\sum_{i\in I} E_{g,i,t}^{BaU}} \cdot 100$$ $$\Delta C_{RES} = \sum_{t\in T}\sum_{i\in I} E_{g,i,t}^{BaU} - \sum_{t\in T}\sum_{i\in I} E_{g,i,t}^{GC}$$ where: $E_{g,i,t}^{BaU}$: energy curtailment of the i-th RES facility at time period t in the BaU, (kW) $E_{g,i,t}^{GC}$: energy curtailment of the i-th RES facility at time period $t$in the Green Charging scenario (kW) I: set of RES facilities T: Time ΔC_{RES}: absolute reduction in RES curtailment (kWh) $\Delta C_{RES}^{\%}$: percentage reduction in RES curtailment (%)
UNIT OF MEASUREMENT	%
TARGET / THRESHOLDS	The size of the fleet, the RES curtailment in BaU scenario, and the spatial distribution of charging demand and RES curtailment occurrence, are the drivers of this KPI's performance. A target is not trivia to be defined. A detailed discussion about the performance of this KPI is in the simulation's result section.
MEASURED/INPUT DATA	Simulated via realistic EV user activity schedules, real infrastructure data for substations and charging stations, and generated baseline load and PV profiles.

5 Results

5.1 Pilot Overview

Due to prevailing legal and regulatory requirements applicable during the implementation period, the charging infrastructure in Koropi site were operated within a time-defined pilot framework rather than as a continuously open public network. Importantly, this arrangement did not impose functional limitations on the system's capabilities; all technical, economic, and smart charging features were fully operational during the demonstration window. The demonstration was therefore conducted with a selected group of end users over a defined operational window from 28 January to 20 February 2026.

Within this controlled deployment environment, the LV monitoring and charging systems operated under real usage conditions, enabling the systematic collection of technical, economic, and behavioural performance data. The monitoring phase generated quantifiable indicators, substation and feeder monitoring, charging sessions, delivered energy, charging duration profiles, tariff application records, and wallet-based transaction data. In addition, the pilot enabled validation of smart charging functionality and grid interaction mechanisms. Dynamic tariff signals were applied during peak conditions, and controlled load modulation was activated in response to DSO requests. These operational events provided empirical evidence of interoperability between grid infrastructure, the DSS platform, the O-V2X-MP, the charging infrastructure and finally the EV users.

5.1.1 Substation monitoring

Every substation of the pilot area is monitored both in the LV buses as well as in every LV feeder. The pilot's chargers are located under some of these feeders. Thus, during the pilot implementation phase we were able to collect electrical data from each of these feeders and substations of interest. The data presented below showcase the loading of each one of the substations of interest and the corresponding feeders, in essence the apparent power in kVA. Additionally, the voltage deviations were also collected during the pilot activities from each of the feeders supplying the EV chargers. The charging infrastructure whose electrical datasets were collected consists of three main distinct charging areas, Papasideris Stadium, 2nd Elementary School, and Eleftherias Square.

- **2nd Elementary School**

In general, the secondary substations of the distribution network converting MV to LV are over-dimensioned, meaning that their total capacity is much larger than their daily loading conditions especially during the winter months. This statement is depicted below during the monitoring of the substation supplying the EV charger located at the 2nd Elementary School. The substation there has a total capacity of 630 kVA, although the maximum loading does not exceed 200 kVA during the demonstration, as plotted in Figure 9. A closer look into the diagram shows that the fluctuations of the apparent power grow bigger during the weekdays and decrease during the weekends. Hence, the loading of the transformer increases from Monday to Friday.

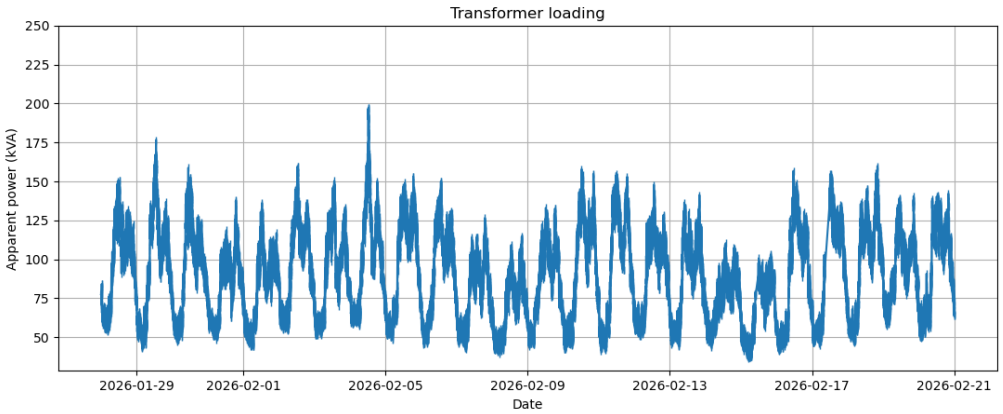

Figure 9: 2nd ElementarySchool substation plot during demo

Similar fluctuation pattern can be seen during the monitoring of the LV feeder that supplies the 2nd Elementary School's EV charger. In this case the loading is depicted two times more than the weekends' state, reaching 40 kVA in the peak load compared to no more than 20 kVA in some cases, Figure 10.

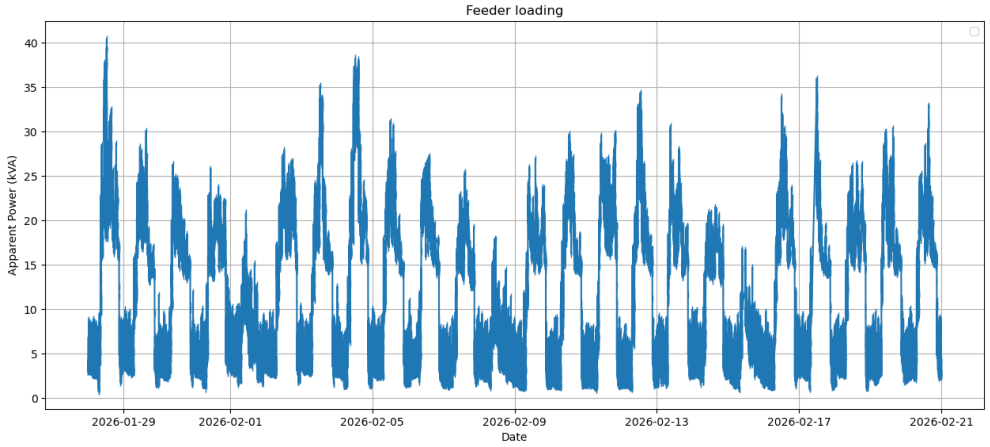

Figure 10 :Feeder supplying the2ndElementary School's EV charger

The voltage diagram of the Feeder supplying the 2nd Elementary School's EV charger is depicted in Figure 11. No essential violations arise from the collection and analysis of the data, from any of the three phases A, B and C.

- Phase A has an average value of 236.1 V, with standard deviation 1.9 V.
- Phase B has an average value of 234.9 V, with standard deviation 2.1 V.
- Phase C has an average value of 235.6 V, with standard deviation 1.9 V.

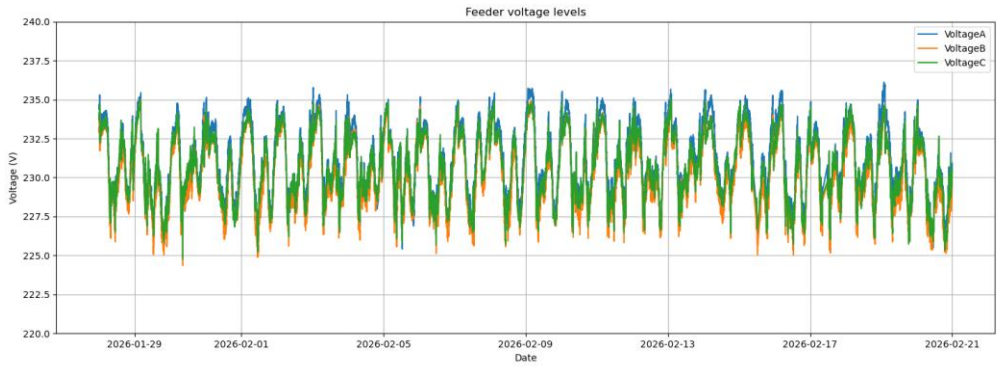

Figure 11: Voltage plot of the Feeder supplying the 2nd Elementary School's EV charger

- **Papasideris Stadium**

The over-dimensioning argument does not apply to every situation, though. In contrast with the previous substation, the one supplying the EV charger located at the Papasideris Stadium has a total capacity of 400 kVA. During its monitoring the maximum loading reaches 300 kVA nearly 75% of the total transformer capacity, Figure 12. More violations might occur in overloading during weekdays compared to weekends, as before.

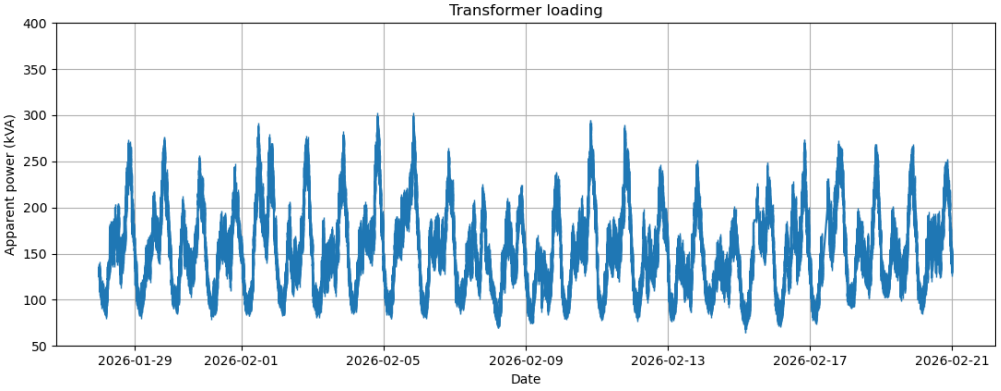

Figure 12: Papasideris Stadium substation plot during demo

Similar fluctuations can be seen during the monitoring of the LV feeder that supplies the Papasideris Stadium's EV charger. In this case the loading a maximum of more than 40 kVA on some occasions with peak value more than 50 kVA. The business-as-usual loading is depicted between 20-30 kVA, Figure 13.

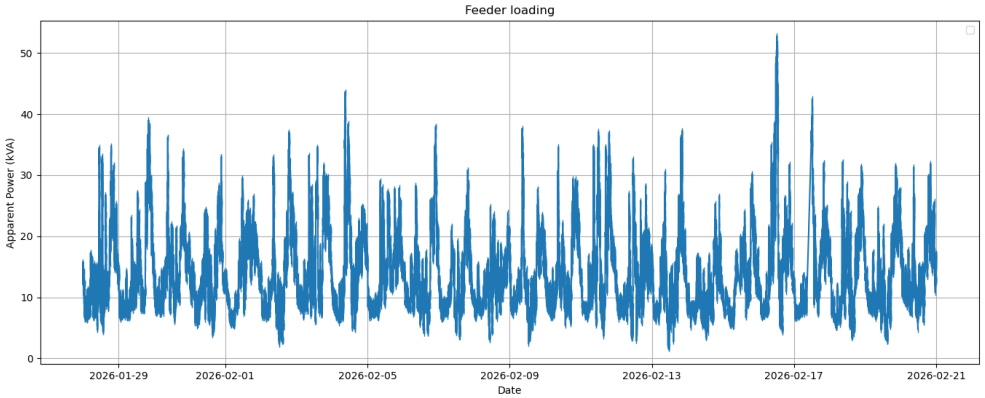

Figure 13: Feeder supplying the Papasideris Stadium's EV charger

The voltage diagram of the Feeder supplying the Papasideris Stadium's EV charger is depicted in Figure 14. No essential violations arise from the collection and analysis of the data, from any of the three phases A, B and C.

- Phase A has an average value of 231.1 V, with standard deviation 2.3 V.
- Phase B has an average value of 230.2 V, with standard deviation 2.2 V.
- Phase C has an average value of 230.7 V, with standard deviation 2.1 V.

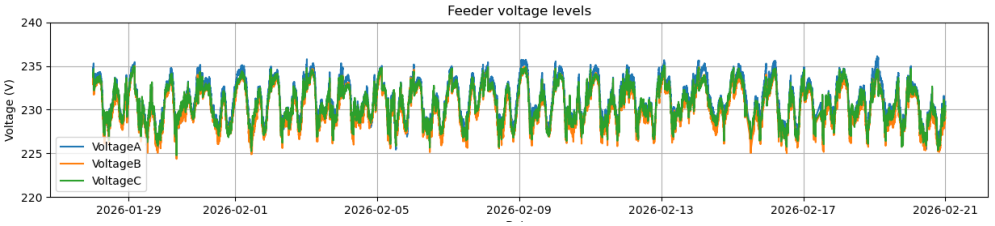

Figure 14: Voltage plot of the Feeder supplying the Papasideris Stadium's EV charger

- **Eleftherias Square**

Finally, the monitoring of the the substation supplying the EV charger located at the Eleftherias Square reveals the usual over-dimensioning scenario of the distribution grid. This transformer has a nominal capacity of 630 kVA and its loading during the pilot activities does not even reach 200 kVA, Figure 15.

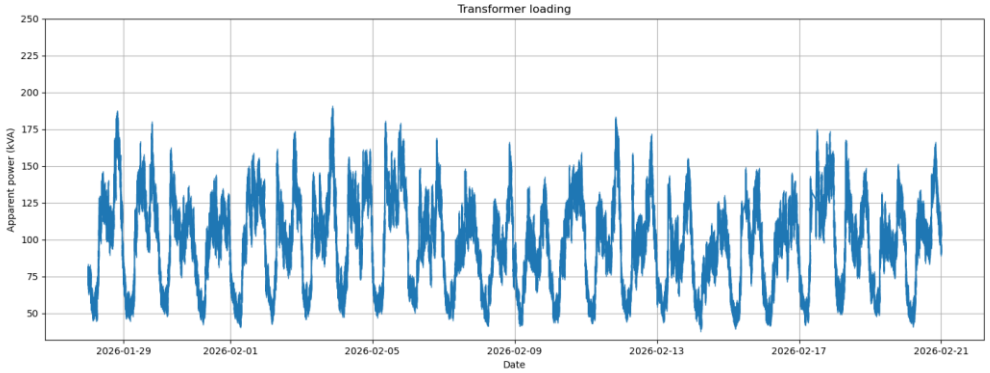

Figure 15: Eleftherias Square substation plot during demo

Similar conditions are revealed during the monitoring of the LV feeder that supplies the Eleftherias Square's EV charger. In this case the maximum loading rarely reaches 25 kVA, far less than the previous scenarios, Figure 16.

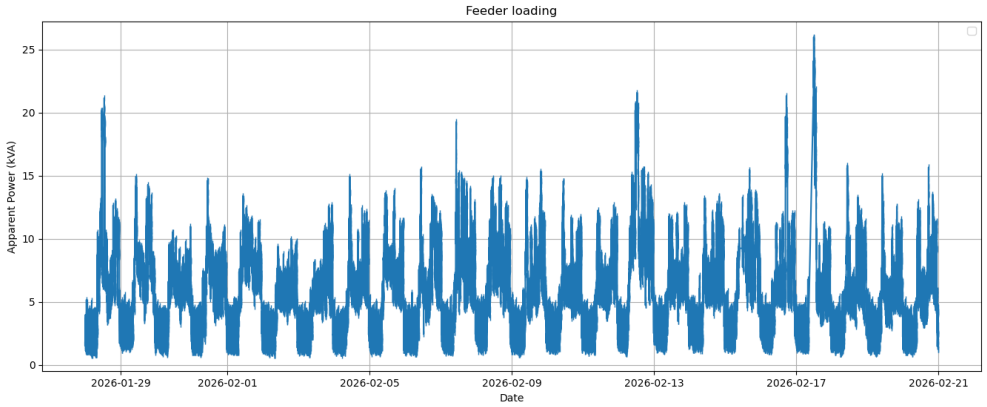

Figure 16: Feeder supplying the Eleftherias Square's EV charger

The voltage diagram of the Feeder supplying the Eleftherias Square's EV charger is depicted in Figure 17. No essential violations arise from the collection and analysis of the data, from any of the three phases A, B and C.

- Phase A has an average value of 235.8 V, with standard deviation 2.0 V.
- Phase B has an average value of 234.4 V, with standard deviation 2.2 V.
- Phase C has an average value of 235.2 V, with standard deviation 2.0 V.

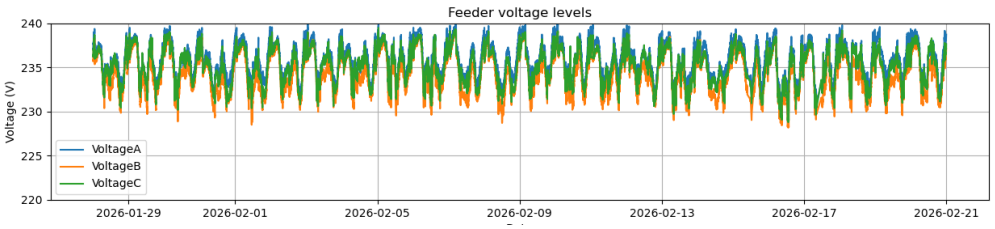

Figure 17: Voltage plot of the Feeder supplying theEleftherias Square'sEV charger

- **Zoom in a specific charging session**

Additionally, we zoomed into the timeframe of a specific charging session. The session took place in Papasideris Stadium on 11 February 2026, including two charging EVs on both sockets of the EV charger, spanning from 16:26 until 17:48 and from 16:41 until 17:45 correspondingly. As depicted in Figure 18, there is a ramp-up on the measured apparent power consumed from the feeder supplying the charger between this timeframe. In Figure 19 the feeder current levels also showcase a rise in their values in all 3 phases during the session. Then a drop occurs, before the end of the sessions, due to the activation of BUC 5 (flexible capacity contracts) and the power and current remain dropped until the end of the charging sessions.

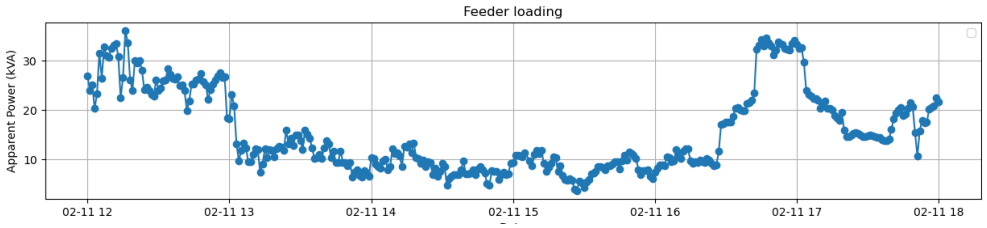

Figure 18: Papasideris Stadium's feeder loading during session

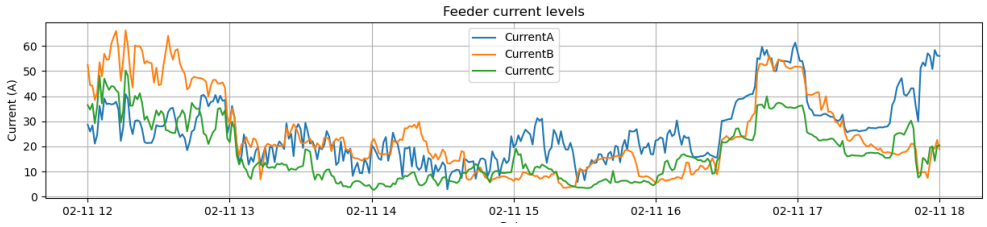

Figure 19: Papasideris Stadium's feeder current levels during session

5.1.2 BUC Activations

As mentioned in paragraph 3.3, in business-as-usual (BaU) scenarios in none of the pilot transformers their loading exceeds their operational limits, thus inducing triggering signals. For that reason, the operational limits were lowered, and the trigger limits were tailored for each transformer and each month based on both forecasting outputs and historical loading patterns. This approach enabled us to test as many relevant cases as possible**,** given the uncertainty of forecasting results.

In the following paragraphs we have summarized the number of events occurred from each substation during the demonstration period. In connection with the diagrams presented in the previous paragraph with the substations' monitoring, we were able to get a clear picture of the violations occurred in each situation, the occurrence of events within a day, providing lessons learned for future practises.

The demonstration lasted for 24 days spanning through January and February 2026. The trigger events were enabled during the daytime starting at 08:00 and lasting usually until 23:00, with the latest 4-hour triggers being observed no later than 19:00. Three distinct plots are presented below for the different demo locations where the EV charging took place, and only one indicative trigger activation diagram for the rest of the locations with no charging operations. The column diagram presents the total number of trigger events per category (yellow, orange, red) and per event (overvoltage, overloading). Histogram summarizes the trigger events per time of occurrence within the day during demo, showcasing each event for the 4 hours that it lasts. Finally, the pie chart presents the total activation time of each event in comparison with the BaU activity of the transformers during the demo.

- **2nd Elementary school**

In the 2nd Elementary school, 44 total triggers were identified during the demo. Most of which were overvoltages with severity 'red' [4], while overloading events were fewer and clearly of lower importance compared to voltage-related violations. Figure 20. Peak triggers can be observed between hours 10:00 – 12:00, Figure 21, indicating the beginning of PV production activity within the day with

some crucial overloading events taking place after 15:00. Lastly, Figure 22, presents the total activation percentage of each event during the whole demo phase, showing that the largest share corresponds to **BaU operation**, while overvoltage activation occupies a clearly larger portion than overloading. Overall, the figures confirm that this substation is affected mainly by overvoltage conditions, with overload issues appearing more occasionally and mostly later in the day.

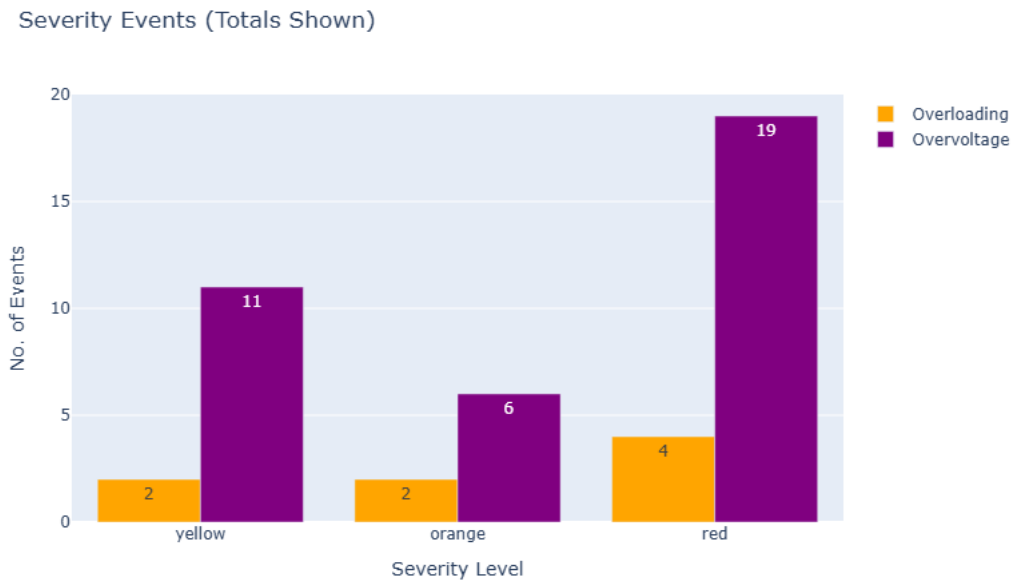

Figure 20: Bar graph of Severity Events 2nd Elementary school

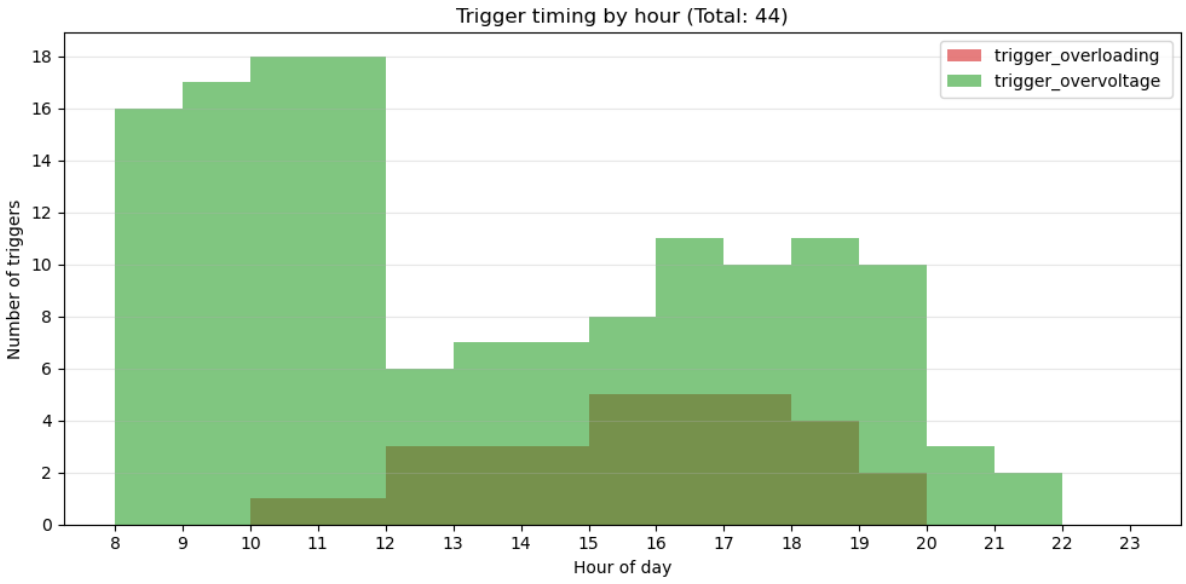

Figure 21: Histogram Trigger Timing by hour2ndElementary school

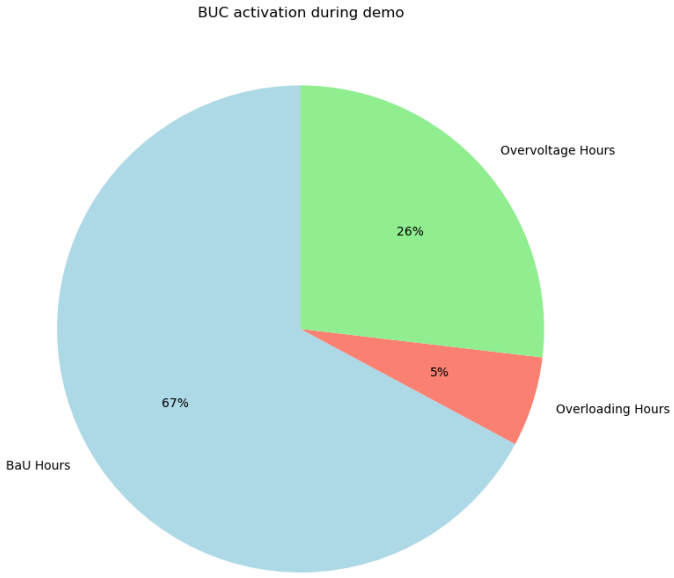

Figure 22: Total activation time percentage of events 2nd Elementary school

- **Papasideris stadium**

In Papasideris stadium, 59 total triggers were identified during the demo. Most of which were overvoltages with severity 'red', Figure 23, while overloading events were very limited and only appear in a few cases. Peak triggers can be observed between hours 11:00 – 12:00, Figure 24, indicating the beginning of PV production activity, although severe overvoltages can be observed throughout the day and until 20:00, some crucial overloading events take place after 19:00. Lastly, Figure 25, presents the total activation percentage of each event during the whole demo phase. The largest share of the activation period corresponds to **BaU operation**, while overvoltage hours account for a significant additional portion and overloading hours remain very small. Overall, the figures confirm that this substation is affected mainly by persistent and often severe overvoltage conditions.

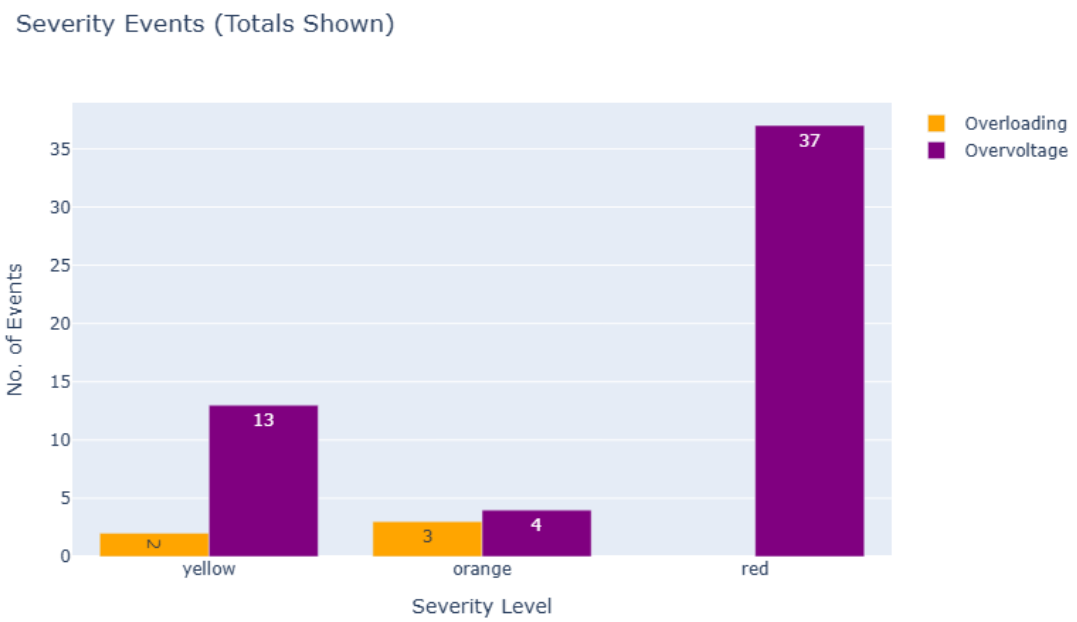

Figure 23: Bar graph of Severity Events Papasideris stadium

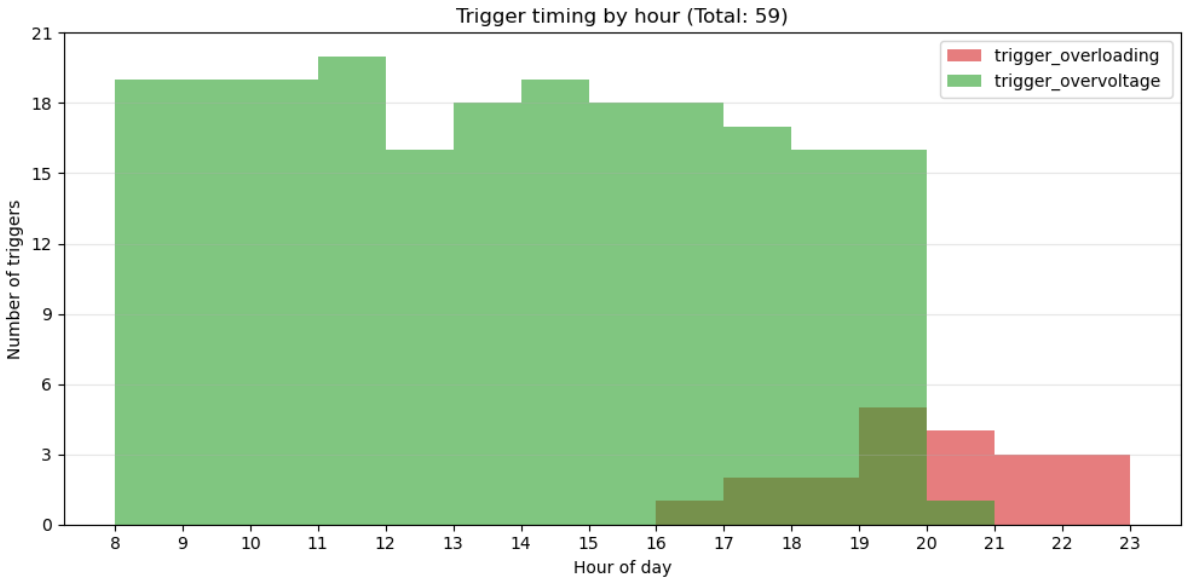

Figure 24: Histogram Trigger Timing by hour Papasideris stadium

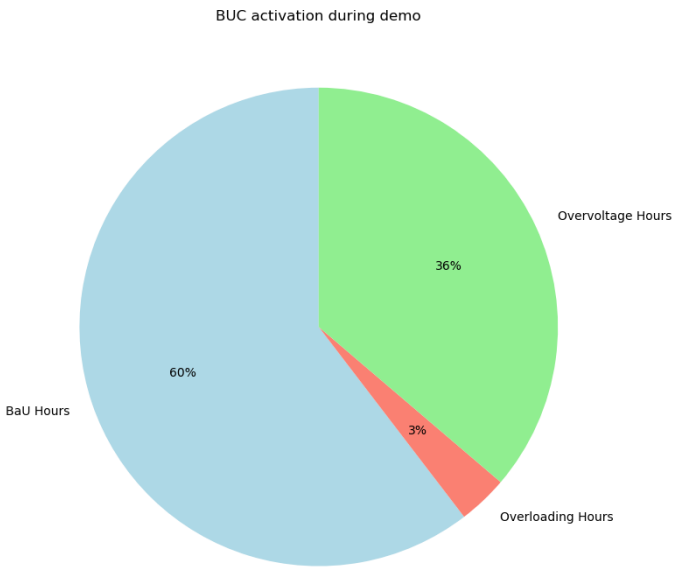

Figure 25: Total activation time percentage of events Papasideris stadium

- **Eleftherias square**

In Eleftherias square, 64 total triggers were identified during the demo. Most of which were overvoltages with severity 'yellow', Figure 26. Peak triggers can be observed between hours 10:00 – 12:00, Figure 27, indicating the beginning of PV production activity, although severe overvoltages can be observed throughout the day and until 20:00, some crucial overloading events take place after 19:00. Lastly, Figure 28, presents the total activation percentage of each event during the whole demo phase. most of the total activation time still corresponds to BaU operation, while overvoltage hours occupy a large additional share and overloading remains comparatively low. Overall, the figures show that Eleftherias Square is also driven mainly by voltage-related issues, although loading-related events appear slightly more pronounced than in the Papasideris Stadium substation.

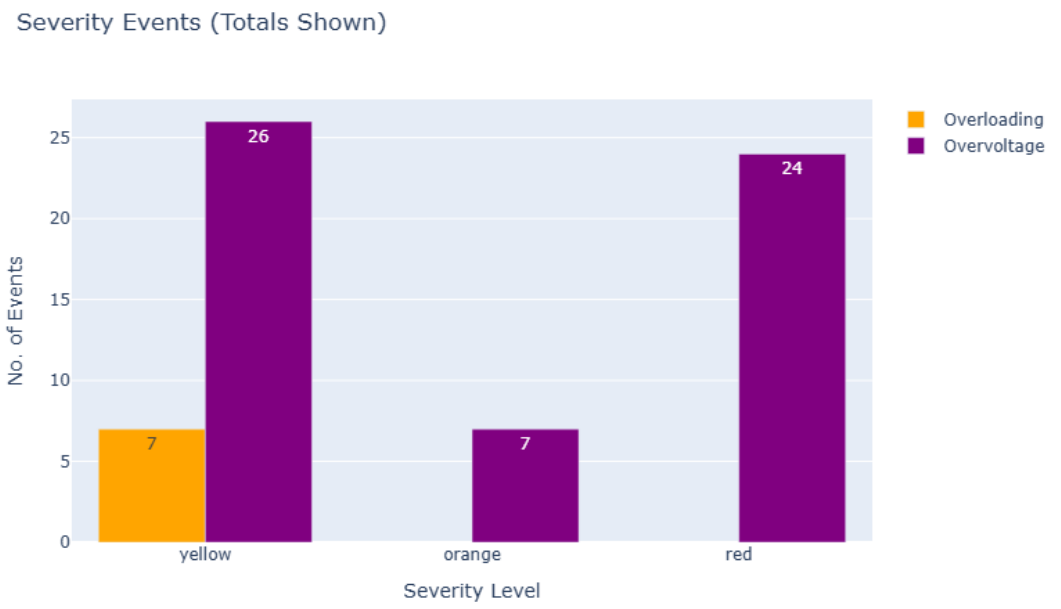

Figure 26: Bar graph of Severity Events Eleftherias square

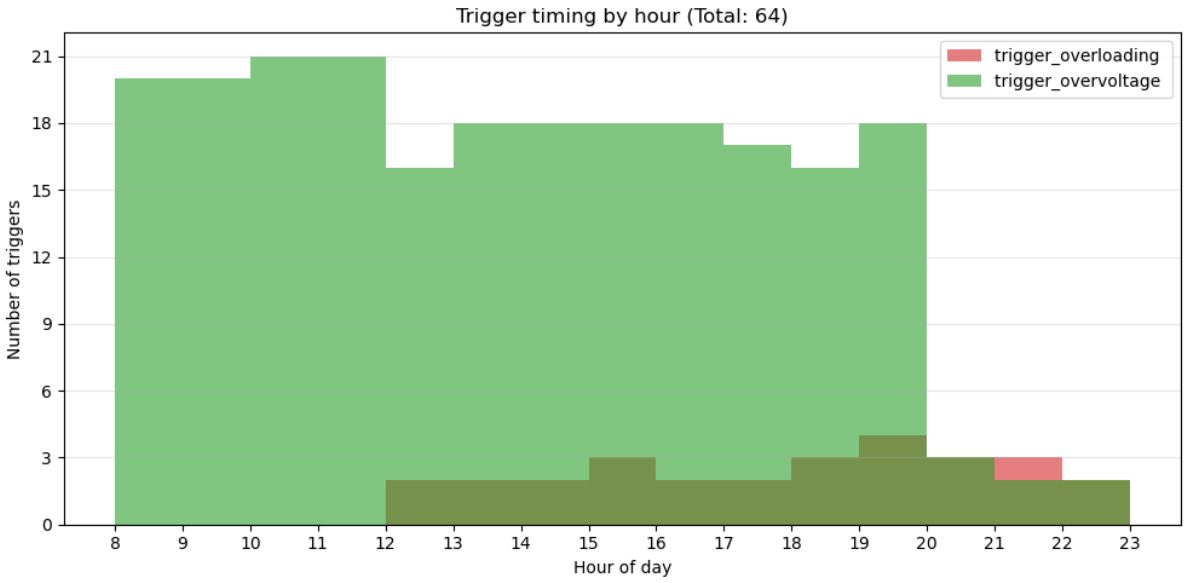

Figure 27: Histogram Trigger Timing by hour Eleftherias square

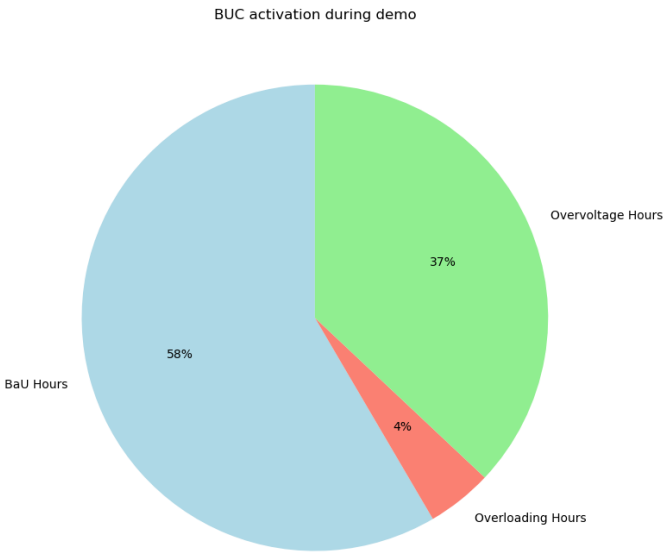

Figure 28: Total activation time percentage of events Eleftherias square

In the following locations no EV charging took place during the demo activity. Nevertheless, the substation monitoring behind each charger worked in normal operating conditions issuing triggering events whenever an overvoltage or overloading appeared.

- **Koropi Municipality & Agalmatos square**

In Koropi Municipality, 31 total triggers were identified during the demo. Most of which were overloading with severity 'red', Figure 29. This is the only location that issued more overloading events than overvoltages, indicating heavy loads at the LV side. In Agalmatos square, 56 total triggers were identified during the demo. Most of which were overvoltages with severity 'red'.

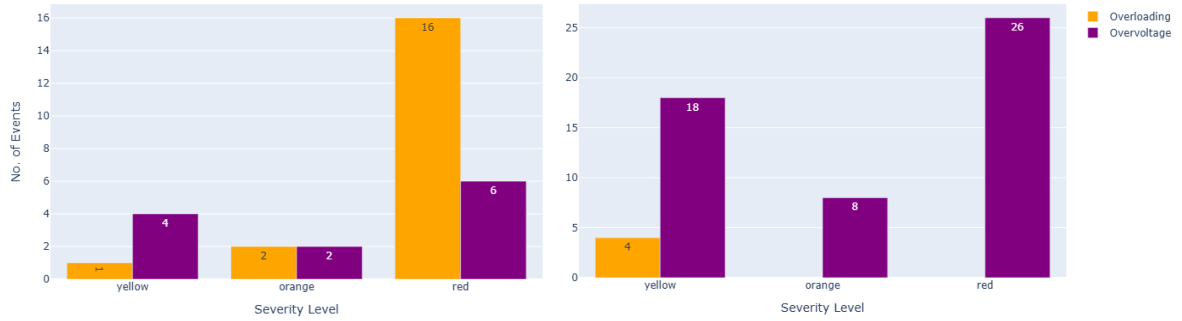

Figure 29: Bar graphs of Severity Events for Koropi Municipality and Algamatos square substations.

5.1.3 Charging Activities in a Nutshell

The operational assessment of the Koropi charging pilot is based on a dataset comprising 39 total recorded charging sessions, of which 27 correspond to February activity (Figure 30).

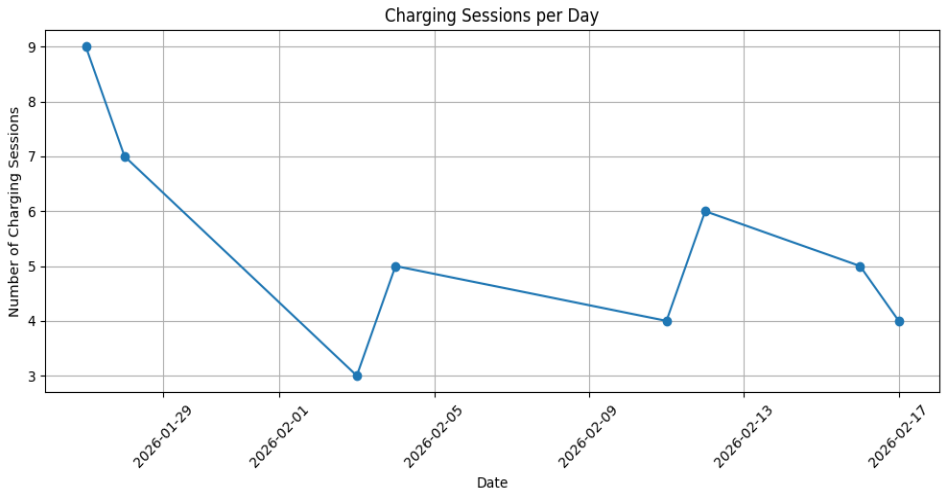

Figure 30: Temporal Distribution of Daily Charging Sessions at the Koropi Demonstration Site

The temporal distribution of charging sessions per day demonstrates moderate variability in usage patterns. Daily session counts fluctuate within a limited range, with peak activity reaching nine sessions and minimum daily activity remaining above three sessions. This variation reflects typical demand dynamics rather than operational disruptions. Importantly, the zero-activity days indicates that users where not using the charging stations in a daily basis during the monitoring period.

The charging infrastructure consists of three distinct charging areas, i.e. Papasideris Stadium, 2nd Elementary School, and Platea Eleftherias, each equipped with two charging slots, resulting in a total of six individual charging points. The distribution of charging sessions per station, as illustrated in the following diagram (Figure 31), reveals a non-uniform utilisation pattern across the three locations.

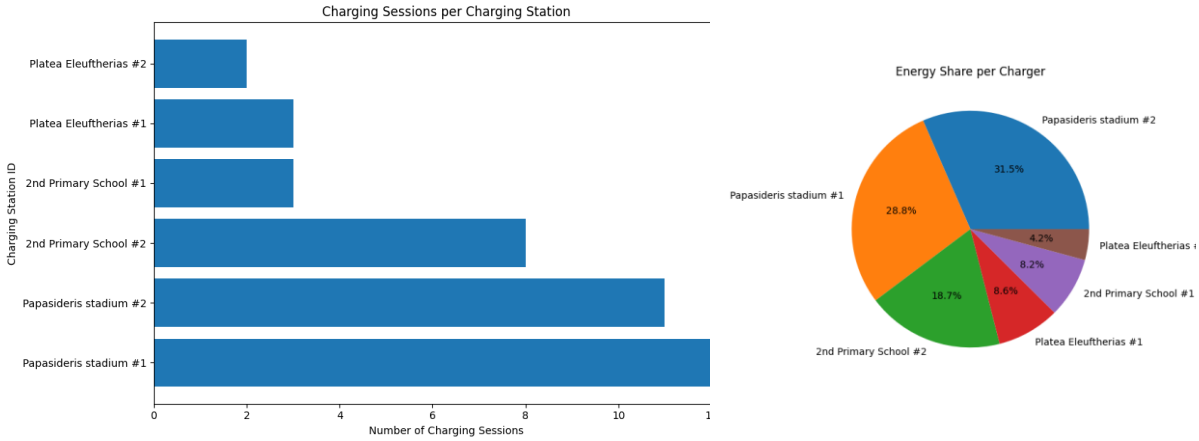

Figure 31: Spatial Distribution of Daily Charging Sessions at the Koropi Demonstration Site

The Papasideris Stadium area exhibits the highest level of activity. Specifically, Papasideris Stadium #1 recorded 12 charging sessions, while Papasideris Stadium #2 recorded 11 sessions. Combined, this area accounts for 23 charging sessions, representing the largest share of total usage among the three areas. This indicates strong demand concentration in this location. The 2nd Elementary School area demonstrates moderate utilisation. Charging Station #2 registered 8 sessions, whereas Charging Station #1 recorded 3 sessions. The internal imbalance between the two slots implies possible differences in accessibility. The Platea Eleftherias area shows comparatively lower overall activity. Charging Station #1 recorded 3 sessions and Charging Station #2 recorded 2 sessions. With a total of 5 sessions across both slots, this area presents the lowest utilisation among the three locations.

From an operational perspective, the distribution indicates that charging demand is geographically concentrated rather than evenly dispersed. The Papasideris Stadium area functions as the primary usage hub, likely due to higher traffic density, longer dwell times, or increased local attractiveness. In contrast, Platea Eleftherias appears to operate below its potential capacity. The observed intra-area asymmetries (e.g., 8 vs. 3 sessions at the 2nd Elementary School) may be influenced by micro-location factors such as parking layout and ease of manoeuvring. These findings suggest that utilisation is not solely dependent on area-level characteristics but also on slot-specific conditions. In conclusion, the current usage pattern highlights a clear spatial demand imbalance across the three charging areas. The Papasideris Stadium location demonstrates strong adoption and could serve as a benchmark for optimal siting conditions. Conversely, the lower utilisation observed at Platea Eleftherias indicates potential need for targeted measures such as improved signage, awareness campaigns, parking policy adjustments, or local stakeholder engagement.

During the demonstration period, the charging stations delivered a total of 548.753 kWh of electrical energy across 39 sessions. This corresponds to an average energy transfer of 14.072 kWh per charging event. The observed average indicates that users primarily engaged in partial or opportunity charging rather than full battery charging cycles. Such behaviour is typically associated with urban or semi-urban public charging patterns, where vehicles are connected for medium-duration stays. This is also the case in the Koropi demo site. Figure 32 presents the total energy delivered per individual charging session, expressed in kilowatt-hours (kWh), across all recorded sessions. The sessions are ordered in descending magnitude, allowing clear visualization of the distribution profile and variability in charging behaviour.

The highest recorded session delivered approximately 38 kWh, representing the maximum energy transfer observed during the reporting period. A limited number of sessions exceed 25 kWh, indicating that full or near-full charging events occurred but were not dominant. The majority of sessions cluster within the range of approximately 10–20 kWh, which aligns with the previously calculated average energy per session (14.07 kWh). This confirms that most users engaged in medium-scale charging events rather than full battery replenishment.

A gradual decline in energy per session is observed across the dataset, with several sessions delivering between 5–10 kWh and a small number of sessions below 5 kWh. These lower-energy sessions may correspond to short dwell times, top-up charging, or early session termination. Importantly, no extreme outliers or irregular spikes are visible, suggesting stable system performance and consistent user charging patterns.

From a statistical distribution perspective, the dataset demonstrates a moderately right-skewed profile, with a small number of high-energy sessions and a larger concentration of mid-range values. This pattern is typical of public charging infrastructure in urban environments, where charging duration is often constrained by parking time or user scheduling constraints.

In operational terms, the energy distribution indicates that the charging infrastructure supports a range of user needs, from short opportunistic charging to higher-capacity sessions. The absence of excessive clustering at very low energy values suggests that sessions are generally meaningful and not prematurely interrupted due to technical issues. In conclusion, the energy-per-session distribution confirms stable operational performance, realistic urban charging behavior, and absence of abnormal system variability. The results reinforce the characterization of the pilot as functionally reliable and demand-responsive.

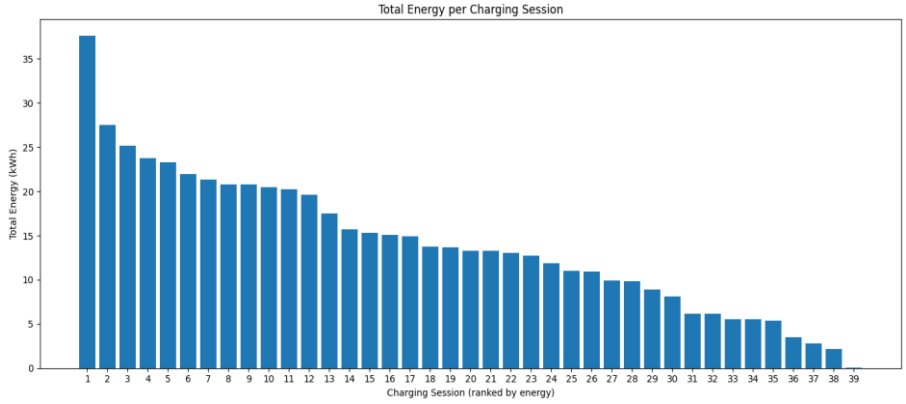

Figure 32: Session-Level Energy Consumption Profile (kWh) at the Koropi Demonstration Site

From an economic perspective, the total recorded revenue amounts to €210.99. This results in an average revenue of €5.41 per session and an average revenue per kilowatt-hour of €0.384, lower than the electricity price (€0.4), due to many overvoltage events triggered by BUC 4 (see 5.1.2), resulting in negative DUoS tariffs. The proportional relationship between total energy delivered and total revenue generated indicates correct metering functionality and coherent tariff implementation. The average price per kWh falls within the expected range for public AC charging infrastructure, suggesting pricing stability and user acceptance. No irregularities in billing consistency are observed in the aggregated metrics.

Overall. the pilot charging points demonstrate stable operational behaviour and provide a validated baseline for further performance monitoring. The results support the conclusion that the infrastructure is functioning as intended and has entered an early but stable utilisation phase.

5.1.4 Session-Level Operational Analysis – CPO Perspective

Figure 33 presents a comparative session-level analysis of energy delivered (kWh) and charging duration (minutes) for each individual charging point across the three charging areas of the Koropi pilot site. For each charger, energy per session is plotted alongside the corresponding charging duration, allowing simultaneous evaluation of utilisation intensity and temporal occupancy.

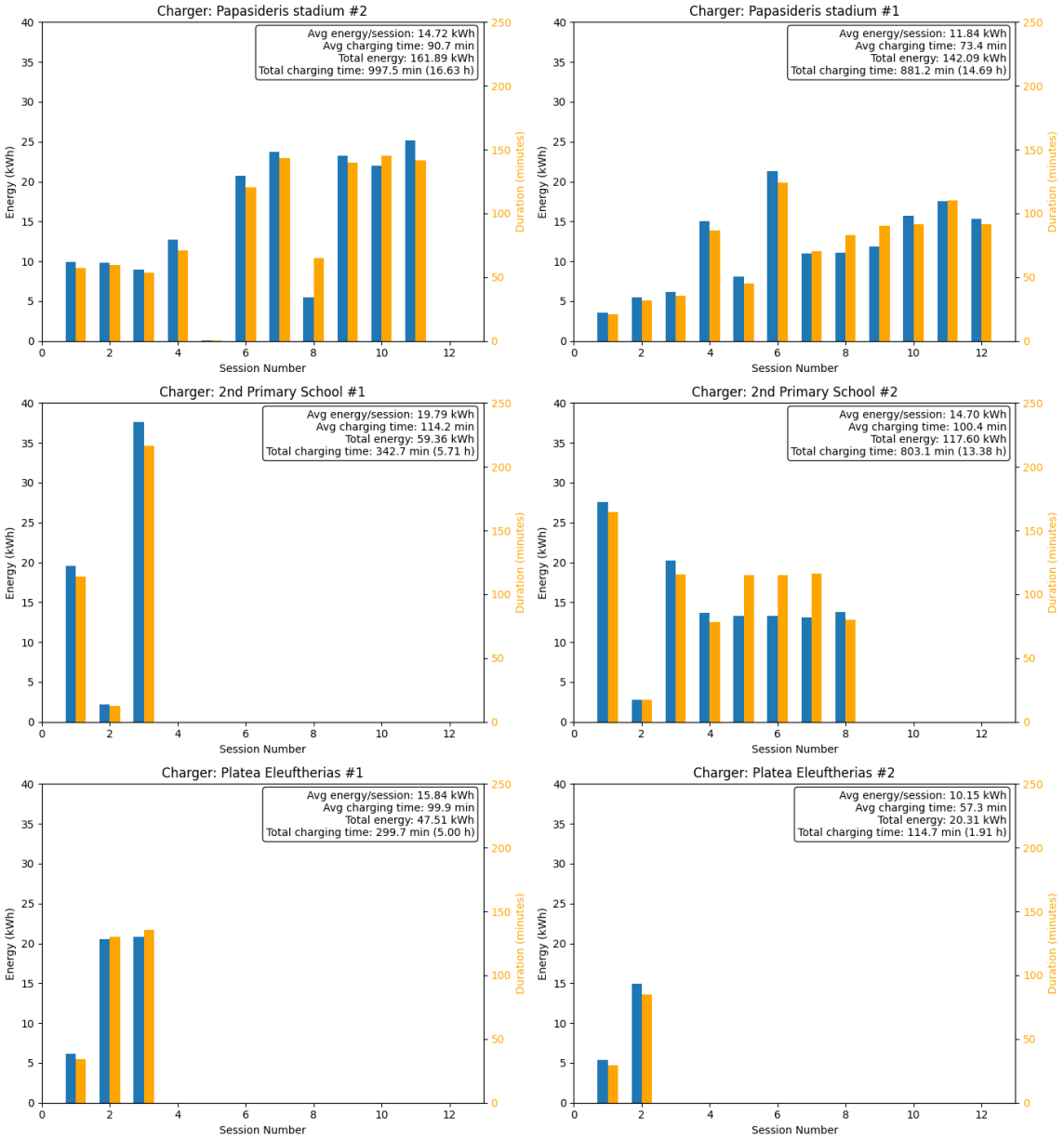

Figure 33: Session-Level Energy Delivery and Charging Duration per Charging Point at the Koropi Pilot Site

At the Papasideris Stadium location, both charging points exhibit the highest operational activity among all monitored sites. Papasideris Stadium #2 records an average energy per session of 14.725 kWh and an average charging duration of 90.7 minutes, with a total delivered energy of 161.89 kWh and cumulative charging time of 16.63 hours. Papasideris Stadium #1 shows slightly lower but comparable performance, with an average energy per session of 11.842 kWh and average duration of 73.4 minutes, delivering a total of 142.091 kWh over 14.69 hours of cumulative charging time. The proportional relationship between session energy and duration indicates consistent charging power delivery and stable operational performance at this location.

The 2nd Elementary School charging area demonstrates differentiated behaviour between its two charging points. Charging Point #2 shows moderate utilisation, with an average energy per session of 14.707 kWh and an average duration of 100.4 minutes, resulting in 88.310 kWh delivered over 13.36 total charging hours. In contrast, Charging Point #1 records fewer but significantly higher-energy sessions, with an average of 19.79 kWh per session and an average duration of 114.2 minutes.

Although total energy delivered (59.36 kWh) and cumulative charging time (5.71 hours) are lower than other locations, the higher per-session energy indicates longer and deeper charging events when utilized.

The Platea Eleftherias area shows the lowest utilisation levels overall. Charging Point #1 records an average of 15.84 kWh per session with an average duration of 99.9 minutes, delivering 47.512 kWh over 5.00 hours of cumulative operation. Charging Point #2 exhibits the lowest activity among all units, with an average energy per session of 10.159 kWh and average duration of 57.3 minutes, corresponding to 20.31 kWh delivered and only 1.91 cumulative charging hours. This indicates limited demand and shorter dwell times at this site.

Across all charging points, energy delivered per session shows a strong positive relationship with charging duration, suggesting consistent power output and absence of performance degradation or charging interruptions. No irregular spikes or inconsistencies are observed between energy and time variables, supporting the conclusion of technical reliability. Moreover, the figure highlights three principal findings: (i) spatial concentration of demand at the Papasideris Stadium location, (ii) moderate and heterogeneous utilisation at the 2nd Elementary School area, and (iii) comparatively low demand at Platea Eleftherias. The results provide evidence of location-dependent usage intensity and confirm stable operational behaviour across all installed charging units. These findings contribute to infrastructure performance benchmarking and inform future siting, optimization, and scalability strategies within the Horizon project framework.

Figure 34 illustrates the cumulative energy delivered (kWh) as a function of elapsed charging time (minutes) for each individual charging session. For most sessions, the relationship between energy and time is approximately linear, indicating stable and constant charging power throughout the session duration. The consistent slope observed in these sessions confirms steady power delivery and reliable charger performance.

However, Sessions 23 and 24 exhibit a distinctly non-linear behaviour compared to the rest of the dataset. In these two cases, the energy–time curves show a visible change in slope, characterized by a reduced incline during part of the charging process. This lower slope directly corresponds to a reduction in instantaneous charging power. The observed non-linear relationship is the result of an implemented smart charging intervention. Specifically, a load shedding request was generated by the local Distribution System Operator (DSO) due to peak demand conditions in the network. Prior price-based incentives (i.e., network tariff increase signals) were not sufficient to achieve the desired peak load reduction. Consequently, an active power limitation strategy was triggered. The reduction in the angle (slope) of the cumulative energy curve indicates a controlled decrease in charging power, demonstrating successful implementation of demand response functionality. Importantly, energy delivery continues during the power limitation phase, confirming that the intervention resulted in moderated charging rather than complete interruption.

The non-linear profiles observed in Sessions 23 and 24 should therefore be interpreted not as anomalies, but as intentional grid-supportive behavior. This validates the interoperability of the charging system with grid management strategies and demonstrates compliance with demand-side flexibility objectives. From a technical perspective, these two sessions provide clear evidence of:

- Functional smart charging capability.
- Real-time responsiveness to external grid signals.
- Effective load modulation without service discontinuity.
- Operational integration between charging infrastructure and DSO grid management mechanisms.

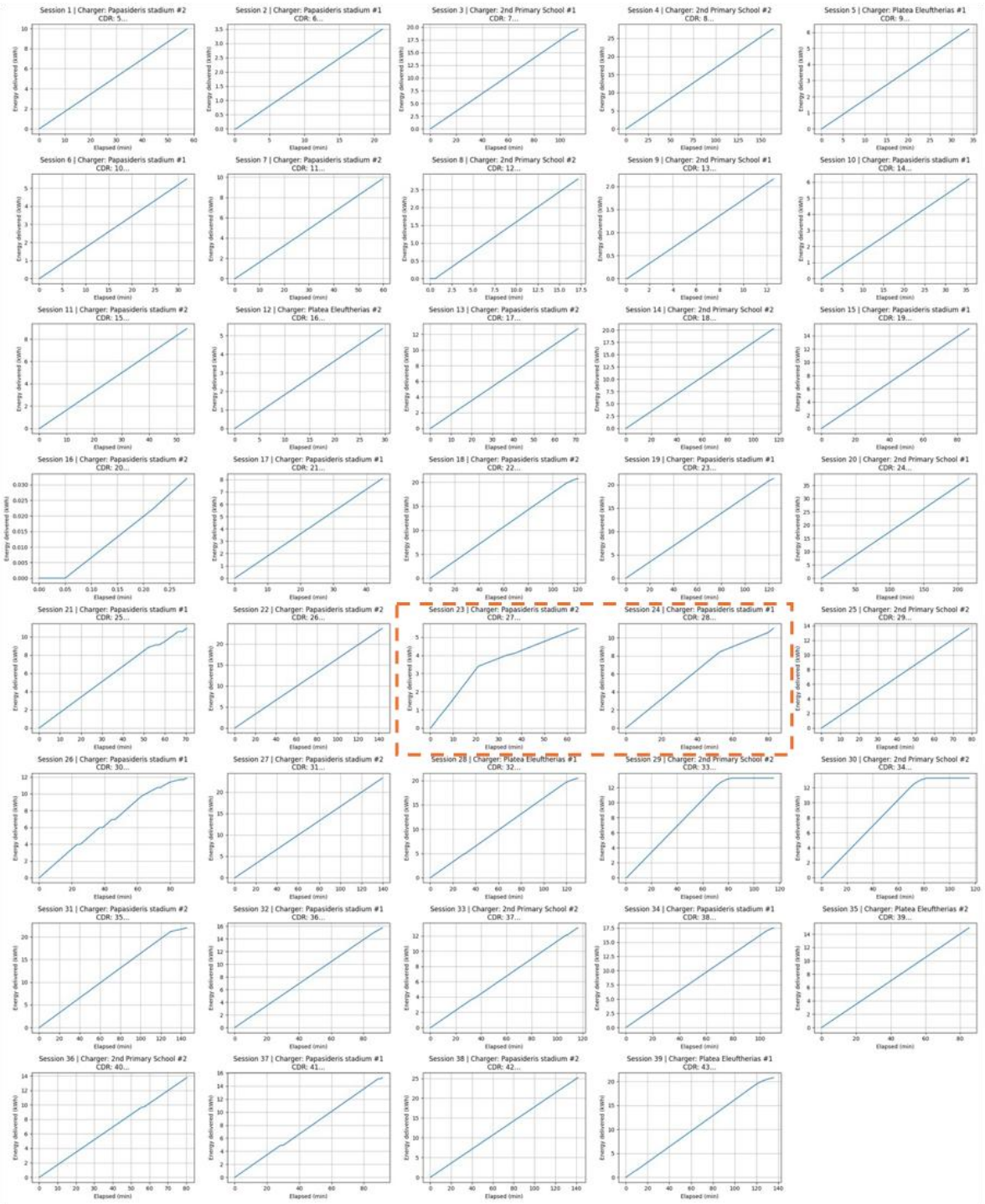

Figure 34: Power Delivery Profiles and Cumulative Energy Curves per Charging Session at the Koropi Pilot Site

Figure 35 presents the economic performance of each charging point through session-level cost (€) distribution, accompanied by aggregated indicators including total delivered energy, total revenue, average cost per session, and average cost per kWh.

At the Papasideris Stadium location, both charging points demonstrate the highest cumulative revenue generation. Papasideris Stadium #2 delivered 161.891 kWh and generated €57.09 in total revenue, with an average session cost of €5.19 and an average tariff of €0.353/kWh. Papasideris Stadium #1 delivered 142.090 kWh, generating €50.91 in revenue, with an average session value of €4.24 and an

average price of €0.358/kWh. The relatively consistent average cost per kWh between the two units indicates stable tariff application and uniform pricing structure within this location.

The 2nd Elementary School charging area exhibits differentiated economic behavior between its two charging points. Charging Point #2 delivered 117.601 kWh and generated €49.33 in revenue, corresponding to an average cost of €6.17 per session and €0.419/kWh. Charging Point #1, despite delivering lower total energy (59.362 kWh), generated €31.80 in revenue, resulting in a significantly higher average cost per session (€10.60) and the highest average cost per kWh (€0.536/kWh) among all units. This suggests that the sessions at this charger were associated with higher-duration or peak-time pricing conditions, since tariff structures are identical for chargers in the same charging location.

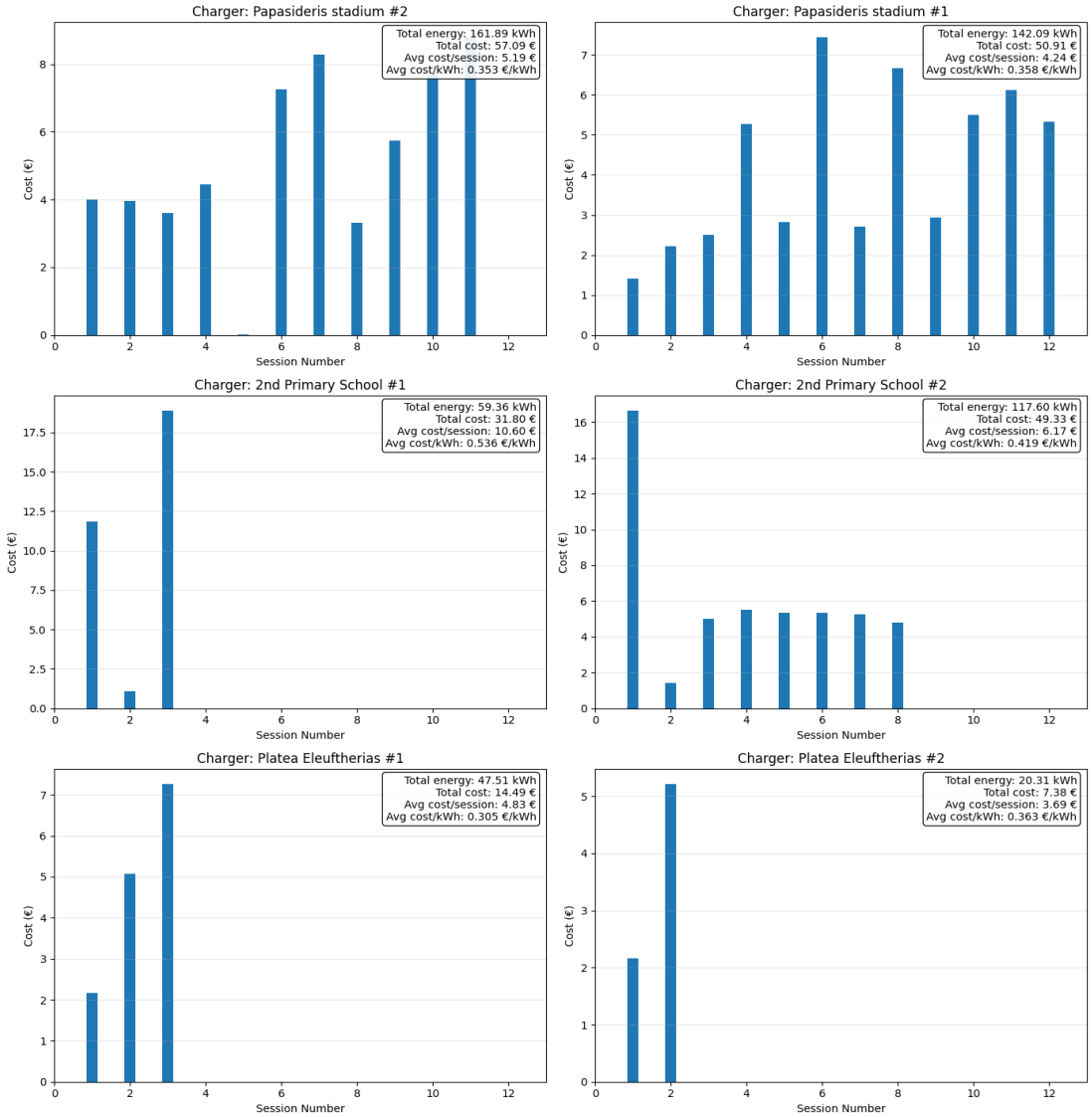

Figure 35: Session-Level Revenue Distribution and Economic Performance per Charging Point at the Koropi Pilot Site

The Platea Eleftherias location demonstrates lower overall economic activity. Charging Point #1 delivered 47.51 kWh with €14.49 total revenue (average €4.83 per session, €0.305/kWh), representing the lowest average price per kWh across all units. Charging Point #2 delivered 20.312 kWh and generated €7.38 in revenue (average €3.69 per session, €0.363/kWh). These values reflect lower utilisation intensity and comparatively shorter or lower-energy sessions.

Across all charging points, revenue scales proportionally with delivered energy, confirming pricing consistency and correct metering operation. Variations in average cost per kWh suggest location-dependent pricing effects, time-of-use differentiation, or demand-related tariff adjustments. Importantly, no irregular cost spikes unrelated to delivered energy are observed. The highest cost per kWh was observed in the Papasideris Stadium area, reflecting the high consumption level of the local substation (the maximum loading reaches 75% of the total transformer capacity, as illustrated in Figure 9).

Figure 36 presents a detailed session-level breakdown of the price structure applied during each charging event. For every recorded session, the total charging price is decomposed into its constituent components, typically including the energy tariff and the network tariff (including dynamic adjustments where applicable). Each subplot illustrates the relative contribution of these pricing elements over the duration of the session. Most sessions demonstrate a stable tariff structure, where the total price is primarily composed of the base energy tariff, with a consistent network tariff component. In these cases, the proportionality between total price and session duration reflects predictable pricing behaviour and confirms transparency in billing implementation.

However, variability in the contribution of the network tariff component is observed across certain sessions. Sessions affected by dynamic pricing signals exhibit a visible shift in the tariff composition, where the network tariff component increases relative to the base energy tariff. This reflects the application of time-dependent or grid-condition-dependent pricing mechanisms. In sessions where smart charging or grid-support interventions were triggered, the tariff composition aligns with the applied demand-response logic. Specifically, when network price incentives were activated to mitigate peak demand, the network tariff share increases. Where these price signals were insufficient to reduce charging demand, load shedding interventions were implemented, as previously documented in Sessions 23 and 24. In these cases, the pricing structure is complemented by active power modulation, demonstrating integrated economic and technical flexibility mechanisms.

Across the full dataset, no inconsistencies between applied tariff structure and recorded session duration are observed. The total price per session scales logically with both energy consumption and applied tariff conditions. The absence of abrupt or unjustified pricing deviations confirms correct tariff configuration and billing integrity. From an operational perspective, the figure demonstrates: i) successful implementation of dynamic pricing mechanisms, ii) transparent decomposition of total charging costs, iii) integration between tariff-based incentives and technical demand-response actions. And iv) alignment of economic signals with grid-support objectives.

In conclusion, the session-level tariff analysis confirms that the pricing framework operates as designed, combining static energy tariffs with dynamic network components to influence user behaviour and support grid stability. The figure provides evidence of the pilot's capability to integrate economic demand-response signals with technical load management strategies, reinforcing its contribution to smart grid interoperability objectives within the Horizon project framework.

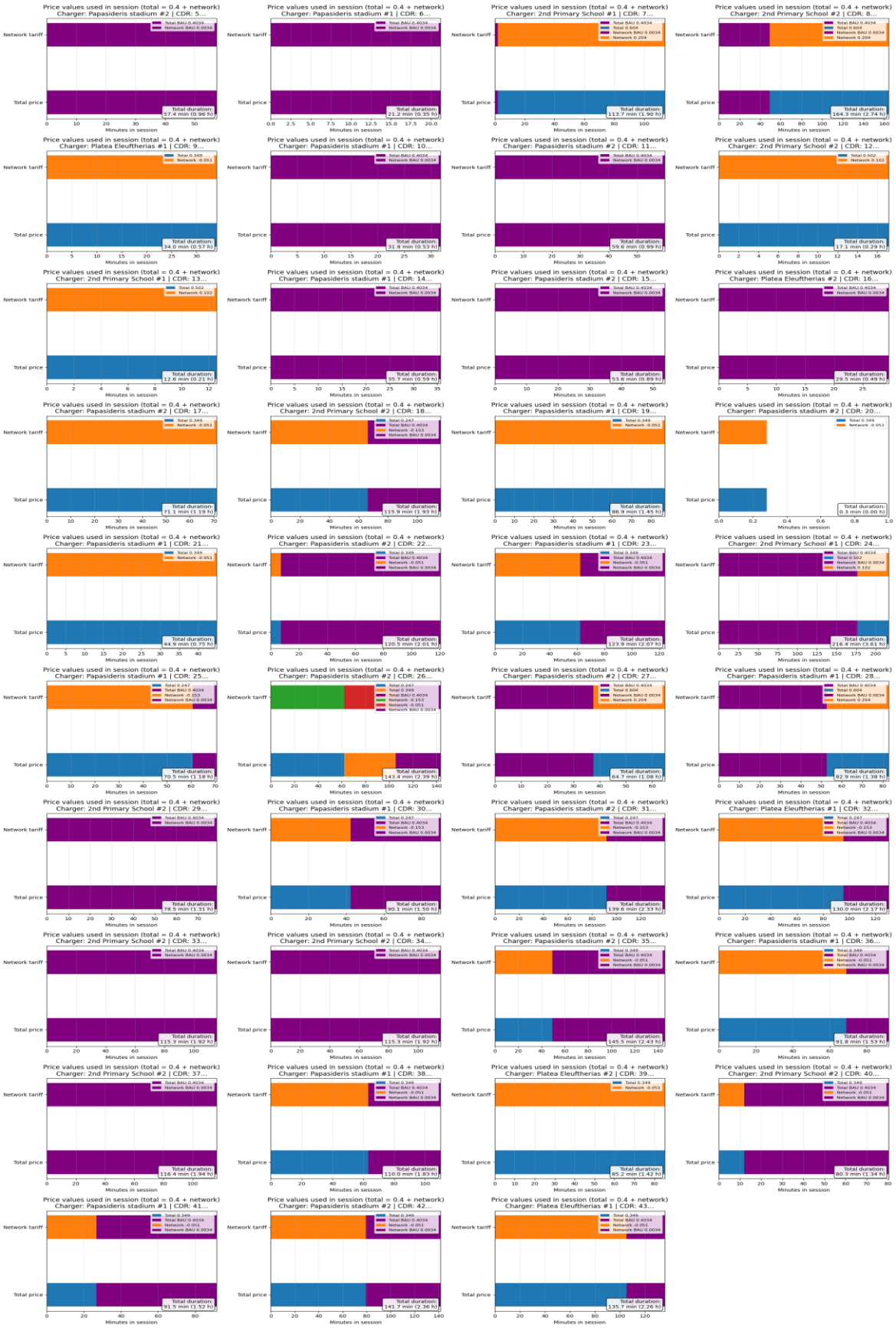

Figure 36: Decomposition of Total Charging Price into Energy Tariff and Network Tariff Components per Session

5.1.5 User Engagement Consumption Patterns, and Economic Indicators – eMSP Perspective

Table 1 tabularises aggregated user-level performance indicators at the e-Mobility Service Provider (eMSP) level, covering total sessions, total energy consumption, total cost, and derived average metrics per user. A total of 13 active users were recorded during the monitoring period. User engagement shows moderate concentration, with a subset of users accounting for a significant share of total sessions and energy consumption.

Table 1: User-Level Charging Activity and Economic Performance Indicators

USER_NUMBER	TOTAL_SESSIONS	TOTAL_ENERGY_KWH	TOTAL_COST_EUR	AVG_ENERGY_PER_SESSION	AVG_COST_PER_SESSION	AVG_COST_PER_KWH
1	4	49.374	20.048766	12.343500	5.012191	0.406059
2	3	42.239	13.530569	14.079667	4.510190	0.320334
3	5	87.895	44.218089	17.579000	8.843618	0.503079
4	4	40.795	20.602639	10.198750	5.150660	0.505029
5	1	20.247	5.001009	20.247000	5.001009	0.247000
6	1	14.935	5.212315	14.935000	5.212315	0.349000
7	3	39.586	15.968992	13.195333	5.322997	0.403400
8	1	5.497	3.320188	5.497000	3.320188	0.604000
9	5	63.444	21.865992	12.688800	4.373198	0.344650
10	5	67.501	22.395688	13.500200	4.479138	0.331783
11	1	0.032	0.011168	0.032000	0.011168	0.349000
12	2	48.933	17.077617	24.466500	8.538808	0.349000
13	4	68.275	21.735955	17.068750	5.433989	0.318359

- ***User Activity Distribution***

The most active users in terms of total sessions are Users 3, 9, and 10 (five sessions each), followed by Users 1, 4, and 13 (four sessions each). This distribution indicates the emergence of a core user group demonstrating repeated engagement with the charging infrastructure, reflecting early-stage user retention and service acceptance. Figure 37 presents the ranked distribution of charging sessions per user, illustrating the frequency of charging activity in descending order.

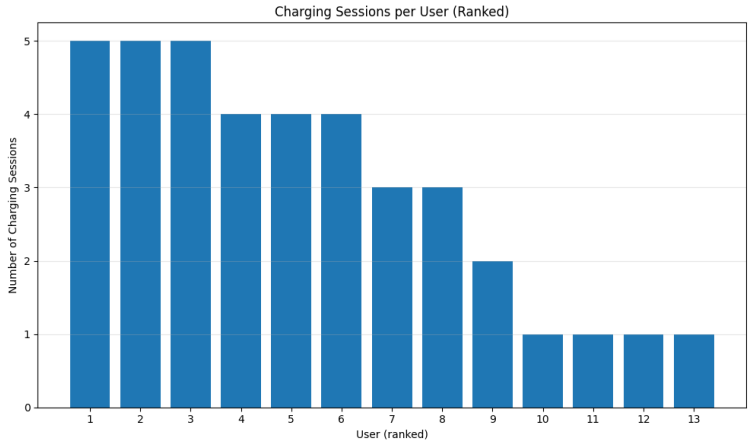

Figure 37: User Activity Ranking Based on Total Number of Charging Sessions

The distribution reveals moderate concentration without excessive dependency on a single user. While three users reached the maximum observed activity level (five sessions), a second cluster recorded four sessions, followed by users with three, two, or one session. This structure reflects a balanced early adoption profile rather than a highly skewed utilization pattern. The absence of extreme dominance by a single user indicates healthy diversification of usage across participants. At the same time, the presence of recurring high-frequency users suggests the gradual formation of a stable demand base. Such a distribution is typical of pilot-phase deployments, where user engagement is developing but not yet fully consolidated.

In terms of total energy consumption, User 3 recorded the highest demand (87.895 kWh), followed by User 13 (68.275 kWh) and User 10 (67.501 kWh). These users also contribute significantly to overall revenue generation, confirming proportionality between delivered energy and incurred cost. The alignment between session frequency, energy consumption, and revenue contribution suggests consistent usage patterns among the most engaged users.

Overall, the ranked activity profile confirms the establishment of an emerging core user segment while maintaining a broad participation base, supporting both infrastructure utilization and revenue stability.

- ***Energy Consumption Behaviour***

Average energy per session varies significantly across users, ranging from very low usage (User 11: 0.032 kWh) to high-intensity charging behaviour (User 12: 24.473 kWh per session). Most users fall within the 12–18 kWh per session range, which aligns with the overall system average (~14 kWh/session). This confirms predominantly medium-scale charging events, characteristic of opportunity or partial charging patterns. Higher average energy per session (e.g., Users 12 and 3) may indicate longer dwell times, higher battery capacity vehicles, or deeper charging cycles.

- ***Economic Indicators***

Average cost per session ranges between €3.32 and €8.84, with User 3 showing the highest average session cost (€8.84), consistent with higher energy consumption. The average cost per kWh varies between €0.247 and €0.604 per kWh. Notably:

- User 8 shows the highest average cost per kWh (€0.604/kWh), potentially reflecting dynamic tariff application or short-duration charging under specific pricing conditions.
- Users 4 and 3 also exhibit relatively high average tariffs (>€0.50/kWh).
- Lower average tariffs are observed for Users 5 and 13, indicating possible off-peak charging or favourable pricing windows.

The variation in average cost per kWh suggests the influence of dynamic pricing mechanisms, time-of-use differentiation, or network tariff components.

Indicative User Activity Patterns

Based on session frequency and energy consumption, users can be broadly categorized into:

1. High-frequency users **(**≥4 sessions): Core recurring customers contributing significantly to system utilisation.
2. Medium-frequency users (2–3 sessions): Occasional but recurring users.
3. Low-frequency users (1 session): Sporadic users or first-time adopters.

These descriptive groupings are useful for interpreting pilot usage heterogeneity and for informing future hypotheses on engagement strategies, but they are not sufficient to support formal behavioural segmentation of the broader EV user population.

The figure below illustrates the evolution of individual user wallet balances (€) over consecutive charging sessions. Each trajectory represents a single user, starting from an initial preloaded balance and progressively decreasing according to session-related charging costs.

At the initial reference point, all users exhibit a similar wallet balance (45€), indicating a standardised initial credit allocation. As sessions accumulate, wallet balances decrease proportionally to charging expenditures. The slope of each curve reflects the economic intensity of user charging behavior: steeper declines correspond to higher per-session costs or more frequent charging activity. Users with five recorded sessions demonstrate more pronounced wallet depletion patterns. Among them, certain users show moderate and steady declines, indicating relatively stable and predictable charging costs per session. In contrast, one user exhibits a significantly sharper decline in later sessions, with wallet balance approaching near-zero levels. This pattern reflects high-energy charging events occurring under elevated tariff conditions, i.e. increased network tariff schemes Users with fewer sessions (one or two) show limited wallet variation, consistent with sporadic usage patterns. The dispersion among curves after the third session highlights heterogeneous charging behaviors and economic engagement levels.

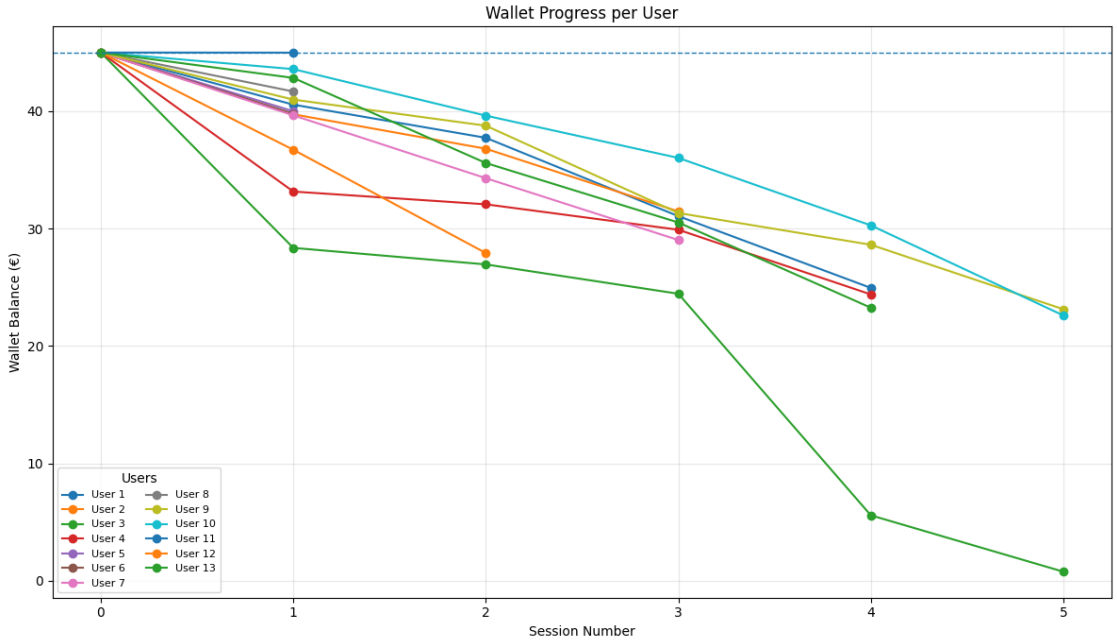

Figure 38: Wallet Balance Evolution per User across Charging Sessions

From an economic and user management perspective, Figure 38 demonstrates:

1. Clear proportionality between charging activity and wallet expenditure.
2. Absence of irregular or unexplained balance fluctuations, confirming billing consistency.
3. Differentiated user engagement intensity.
4. Potential identification of high-value users (rapid wallet turnover) versus low-intensity users.

The wallet trajectories provide insight into user liquidity dynamics and charging frequency patterns. Rapid balance depletion may signal strong engagement but could also suggest the need for automated top-up mechanisms or optimized pricing incentives to ensure continued participation.

5.2 KPIs Evaluation

5.2.1 General KPIs

5.2.1.1 Number of Charging Points

Within the Koropi pilot deployment, four charging locations were successfully electrified. Each location is equipped with one dual-outlet AC charging unit, featuring two Type 2 connectors with a nominal charging capacity of up to 22 kW per connector. Consequently, the deployment resulted in a total of **8 operational AC charging points** available for simultaneous vehicle charging.

5.2.1.2 Number of LV Monitoring Equipment

As reported in D 8.2 [2], in the pilot area five **(5**) MV/LV transformers provide power to the smart chargers. On the LV buses of each transformer, one 3-phase plus neutral meter has been installed. Also, thirty-two (32) 3-phase plus neutral meters have been installed on the active LV feeders of those 5 substations. The total number of 32 meters was defined based on the active LV feeders that each substation has.

One additional LV monitoring solution was also implemented to complement the research purposes of this project. Two (2) distribution transformer monitoring devices were installed at the LV busbar of additional substations. Another, five (5) outage monitoring devices were installed at selected transformers including six (6) three-phase monitoring equipment of the LV feeders per substation.

5.2.1.3 EV user participants

During the demonstration window (28 January – 20 February), a total of **13 unique EV users** were recorded at the eMSP level. Each user completed at least one charging session, confirming active engagement with both the charging infrastructure and the O-V2X-MP platform.
The distribution of participation indicates:

- 3 users completed 5 sessions each
- 3 users completed 4 sessions each
- 2 users completed 3 sessions
- 1 user completed 2 sessions
- 4 users completed 1 session

This pattern demonstrates the emergence of a core group of recurring participants alongside a broader base of occasional users. The absence of extreme concentration in a single user confirms diversified engagement.

5.2.1.4 EV User Satisfaction

Figure 39 presents the distribution of user ratings regarding the evaluated aspect of the demonstration. A total of 23 responses were collected, out of 39 charging sessions realised during the demo activities. ***The results indicate a very high level of user satisfaction, with an average rating of 4.74 out of 5.*** More specifically, 78.3% of respondents (18 users) assigned the maximum rating of 5/5, while 17.4% (4 users) rated the experience 4/5. Only one respondent (4.3%) provided a rating of 3/5, and no ratings of 2/5 or 1/5 were recorded.

Overall, 95.7% of the respondents evaluated the experience positively (ratings of 4 or 5), indicating a very strong acceptance of the demonstrated solution. The absence of low ratings suggests that users perceived the system as reliable and satisfactory during the demonstration period.

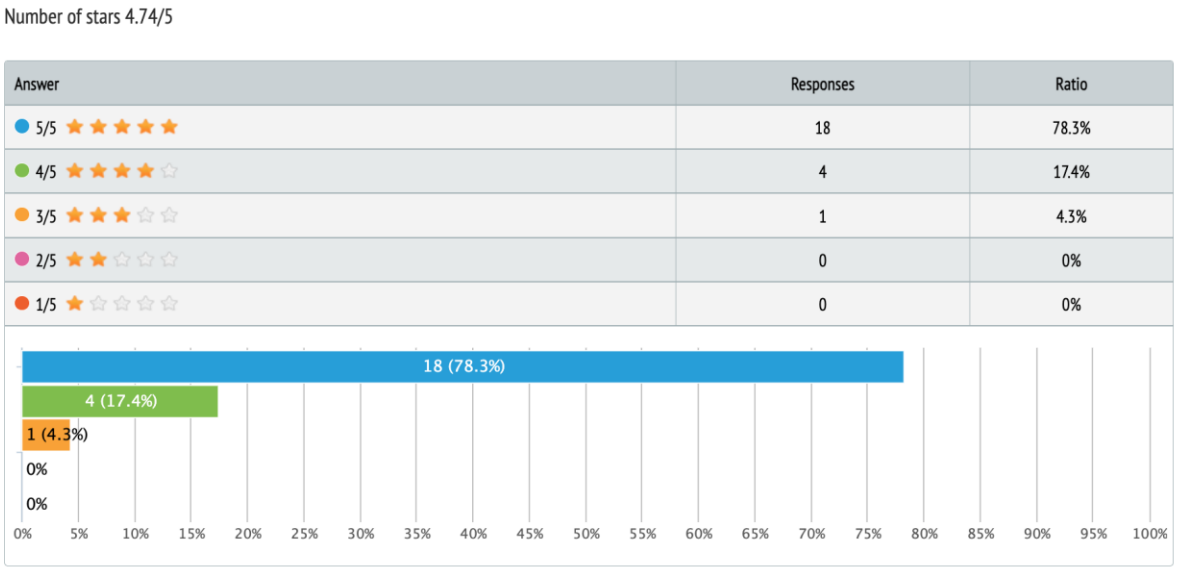

Figure 39: EV user satisfaction ratings collected during the demonstration

5.2.1.5 Information Computer Technology (ICT) cost

The cost of DSO's HW and SW technologies used

- **$C_{communication\ equipment}$:** Data exchange between field equipment and DSS was part of the LV monitoring equipment.
- **S_{erver}:** Server costs were included in the development costs.
- **$SW_{development}$:** DSS software development cost was € 59.900,00.
- **$N_{etwork\ provider}$:** No network fees included.
- **X:** It is assumed that the demo activities were executed for 12 months.
- **$M_{aintenance}$:** No maintenance costs, they are included in the development costs.

$COUT_{DSO}$ =

$C_{communication\ equipment} + S_{erver} + SW_{development} + (N_{etwork\ provider} \times X) + M_{aintenance}$

$= 0 + 0 + 59900 + (0 \times 12) + 0$

$=$ ***€ 59.900,00***

The development of DSS tool was performed during the implementation of GR demonstration, but it was not considered in the initial equipment budget. It was funded by EV4EU's budget in combination with HEDNO's own fund whenever required.

The cost of CPO's HW and SW technologies used

- ***C**ommunication equipment*:** The cost of communication equipment is € 2 / SIM card / month. There are 3 public IP addresses corresponding to EV chargers, and time execution (X) is 12, therefore the total cost is 2*3*12 = € 72,00
- ***S**erver:* The cost (CAPEX) of the server is estimated at € 2.500,00.
- ***SW development & application*: The cost for developing the O-V2X-MP software is estimated at € 40.000,00 (mainly including personnel cost of the people involved in the software design and development).
- ***N**etwork provider*:** The fees of the network provider is at € 30,00/month.
- ***X***: It is assumed that the demo activities were executed for 12 months.
- ***R**oaming hub*:** Roaming hub fees not applicable, so € 0.
- ***M**aintenance*: No maintenance costs, since they are included in the personnel costs.

Therefore,

$COUT_{CPO}$ =

$C_{communication\ equipment} + S_{erver} + SW_{development\ \&\ application} + N_{etwork\ provider} * X + R_{oaming\ hub} * X + M_{aintenance}$

= 72 + 2500 + 40000 + 30*12 + 0*12 + 0

=€ 42.932,00

5.2.2 Technical Related KPIs

5.2.2.1 Data Acquisition and Storage Accuracy

The python client software, which is also an MQTT subscriber service, received asynchronous messages in its own process. It received 99.58% of the expected messages. The same software provides three database workers for processing the inserts into the database. The appropriate logging mechanism reports 100% successful stored messages. Thus, the Data Acquisition and Storage Accuracy is 99.58%.

5.2.2.2 Data Sampling Frequency

The data sampling frequency for the **O-V2X-MP** platform varies per measurand obtained from the CPs. More specifically:

- The heartbeat interval is at 10 seconds
- The interval for obtaining Meter Values (i.e. electricity measurements) during an ongoing transaction is at 5 seconds.

The Data Sampling Frequency of the **DSS platform** is 1 minute by design.

5.2.2.3 Scalability of O-V2X-MP

To evaluate this KPI, two Linux-based Virtual Machines (VMs) were deployed, with each one of those utilizing the e-mobility charging stations simulator from SAP [9].

Each simulator was configured to deploy 10 virtual charging stations; therefore 20 virtual chargers were simulated in total. Those simulated chargers were configured to establish WebSocket/OCPP 1.6J

session with the O-V2X-MP platform. At the same time, 8 more virtual and physical charging stations were already connected with the platform as part of the Greek demo activities. In total, **28** chargers were connected to O-V2X-MP.

The KPI was evaluated successfully by conducting testing charging sessions and interacting with the O-V2X-MP REST API (Representational State Transfer Application), verifying that the O-V2X-MP is able to operate normally and carry out the charging transactions without exhibiting any errors.

5.2.2.4 Availability of the O-V2X-MP services

After analyzing the log files of the O-V2X-MP platform for the interval 01 January 2026 to 31 January 2026, the availability was determined at 100%, since no downtime events were detected that were relevant to the platform's implementation.

5.2.2.5 O-V2X-MP DSO Latency

By executing multiple HTTPS requests at the DSO endpoint of the O-V2X-MP platform, ***the average latency was measured at 250 msec***. It should be noted that this KPI greatly depends on external factors.

5.2.2.6 Forecast Accuracy

This KPI assesses the accuracy of the short-term forecasting model used to predict transformer apparent power up to 4 hours ahead. Forecast performance is evaluated using rolling predictions on unseen test data, measured through the Mean Absolute Percentage Error (MAPE). The project target was to keep the 4-hour forecast horizon below 10% MAPE. Across the evaluation period, the model achieved an average MAPE of 8.41%, remaining well within the required threshold. As shown in Figure 40, both MAPE and Pinball Loss increase slightly with forecast horizon, which is something expected for time-series forecasting. Yet the error growth remains moderate. Overall, the model demonstrates stable accuracy and satisfies the reliability requirements needed.

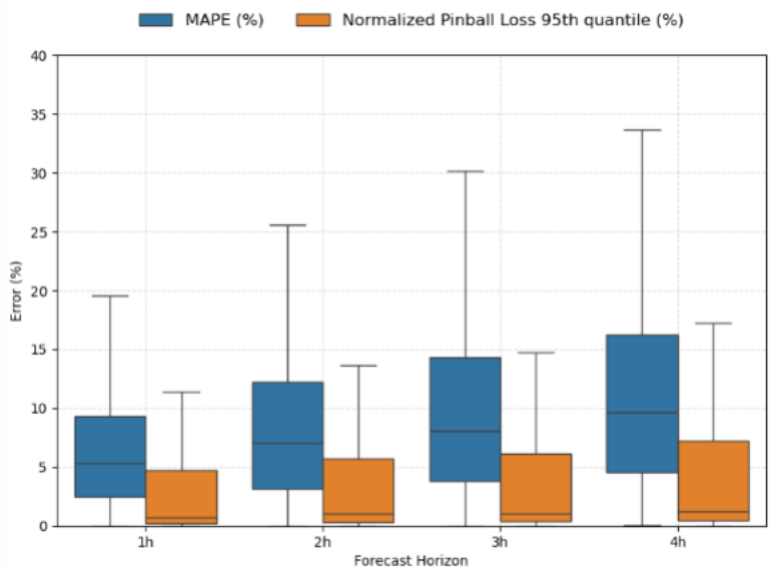

Figure 40: Distribution of MAPE and Pinball Loss for 95th quantile across forecast horizons (1h–4h).

5.2.2.7 Forecast Model Retraining Time

This KPI measures how long it takes to fully retrain the forecasting model, which is important because the model needs to stay updated as new data arrives every hour. The target was to keep retraining time below 15 seconds. To balance model accuracy and computational load, several training window sizes (3-5 months) were evaluated. Based on MAPE analysis across multiple forecast horizons (Figure 41), a 2-month training window offered the best balance between short and medium-term forecast performance.

With this setup, the model retrained in 10.42 seconds, meeting the target and fitting well within the "Good" performance band (5-15 seconds). This confirms that the model can be updated frequently enough to support real-time operation.

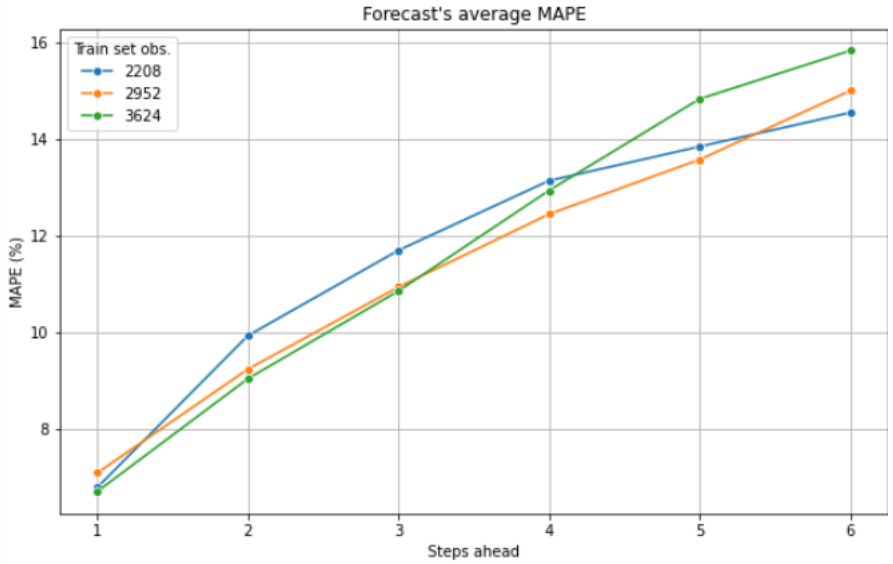

Figure 41: Forecast accuracy measured as MAPE for different forecast steps ahead, using models trained on three different dataset sizes: 2208, 2952, and 3624 observations (corresponding to approximately 3, 4, and 5 months of data). The x-axis indicates the forecast horizon in hourly steps ahead (1-6), while the y-axis shows the corresponding MAPE in percentage.

5.3 Simulations

The pilot demonstration provided valuable initial insights into EV charging sessions and user interactions with smart charging technology. However, the demo site involved a limited number of EV users and covered a relatively small geographical area. Due to this restricted scale, it is challenging to draw robust, generalized conclusions regarding the broader system impacts of the proposed solutions such as their effectiveness in large-scale congestion management, grid flexibility provision, and the system-wide integration of V2G technologies.

To bridge the gap between demonstration findings and city-level flexibility assessment, large-scale simulations are essential. Simulations allow us to model a wider, diverse population with heterogeneous mobility profiles (e.g., varying commuting distances and schedules). Ensure robustness by evaluating different charging infrastructures (public, and private) and pricing schemes (fixed versus dynamic tariffs) under varying load conditions. By employing simulations, we can effectively obtain

comprehensive insights into the flexibility potential of EVs across a realistic, dynamic urban environment.

5.3.1 Area of Interest

The Area of Interest (AoI) selected for the simulations encompasses a substantial portion of the northern and eastern suburbs of the Athens Metropolitan Area in Greece (see Figure 42). The simulated region covers 27 diverse municipal units in total; this spans from central-adjacent municipalities like Zografos and Galatsi, branching out to major northern commercial hubs such as Marousi, Kifissia, and Chalandri, and extending towards eastern suburbs like Aghia Paraskevi and Pallini.

This specific region was chosen because it presents a rich, highly representative mix of urban residential neighbourhoods, significant commercial centres, and major business districts. This structural diversity is critical for ensuring a realistic variety in daily commuting patterns, activity schedules, and charging behaviours within the simulation. Furthermore, encompassing such a broad and varied geographical area allows the model to accurately capture the complex spatio-temporal distribution of EV charging demand. By focusing heavily on behavioural modelling across these diverse zones, the simulations effectively capture how different demographic groups, varied urban layouts, and distinct mobility needs influence both the localized charging dynamics and the aggregate flexibility available at distinct nodes, without necessitating the simulation of the underlying grid topology.

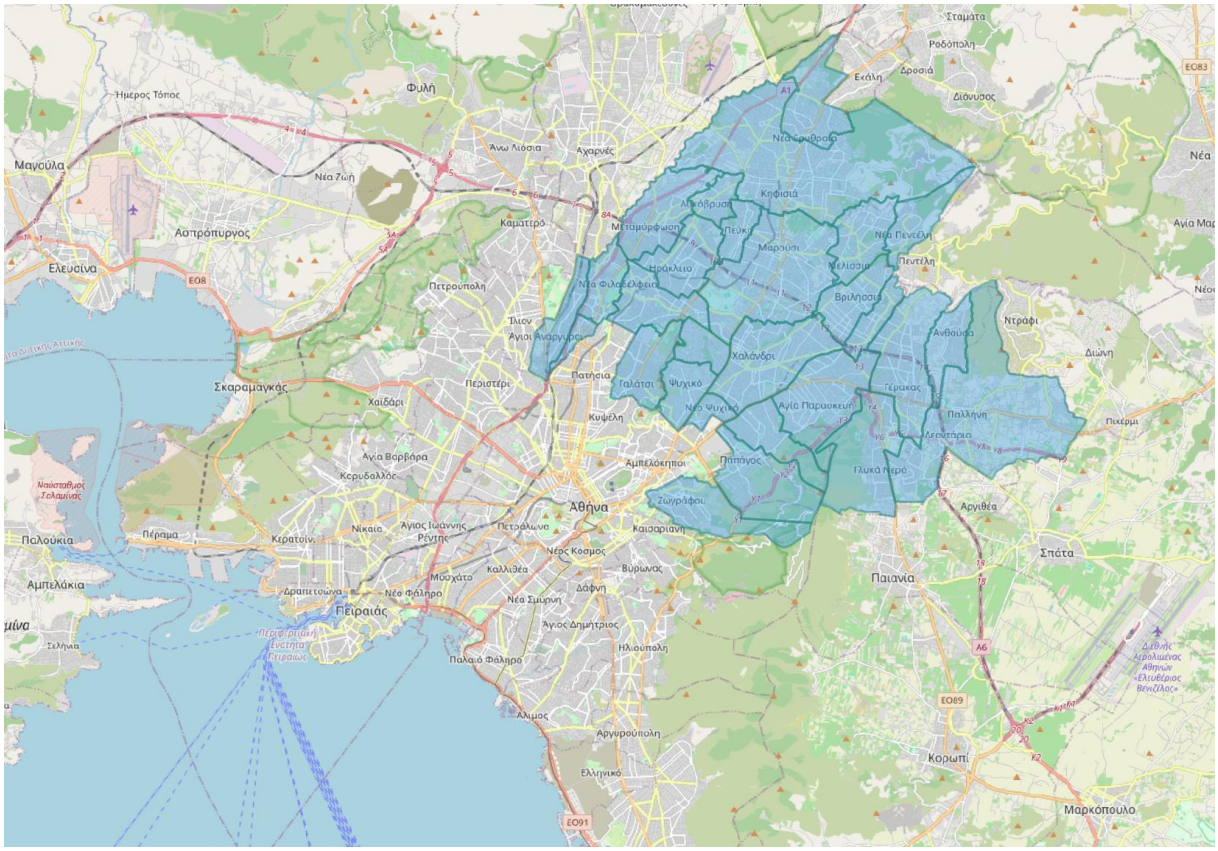

Figure 42: Area of Interest: The 27 municipal boundaries in light blue shade.

To represent charging demand within this area, the simulation leverages the AthensPop model [10], an open-source synthetic population and travel demand generator for the Athens Metropolitan Area. Specifically, a 1% population sample was extracted and subsequently filtered to isolate only passenger car trips, retaining exclusively those agents whose daily travel activities remain strictly within the 27

selected municipalities. This filtration yielded a subset of 992 individual driver profiles. Given that the current EV penetration rate in Greece stands at approximately 0.5%, treating this entire 1% synthetic sample group as EV owners effectively models an aggregate 1.0% EV penetration rate across the real-world population of the area, that their car trips are limited to the selected area boundaries. While this represents a slight overestimation relative to the current day, it provides a proportionately conservative and computationally feasible sample size required to capture the heterogeneous and complex intra-city mobility behaviours.

On average, each driver performs approximately 2.32 trips per day. The dataset captures a comprehensive spectrum of travel purposes, categorized into primary daily activities. Among the tracked activities, returning home represents the majority of trip destinations (accounting for roughly 55% of all activity ends), followed sequentially by commuting to workplaces (20%), recreation (13%), as well as shopping, educational, and other miscellaneous activities.

From an energy perspective, the mobility profile demonstrates charging requirements highly characteristic of an intra-city environment. The average distance per individual trip is relatively short, recorded at 6.19 km. By translating these distances into energy consumption (factoring in realistic driving conditions and vehicle efficiencies), the average daily energy demand per EV is approximately 3.5 kWh. Another critical metric for flexibility potential is the parking duration between consecutive trips; the data indicates that drivers remain parked and potentially connected to a charger for an average of 5.33 hours between activities. In aggregate, the simulated region introduces a baseline daily EV charging demand of over 3.4 MWh, distributed dynamically across the various activity locations and timeframes.

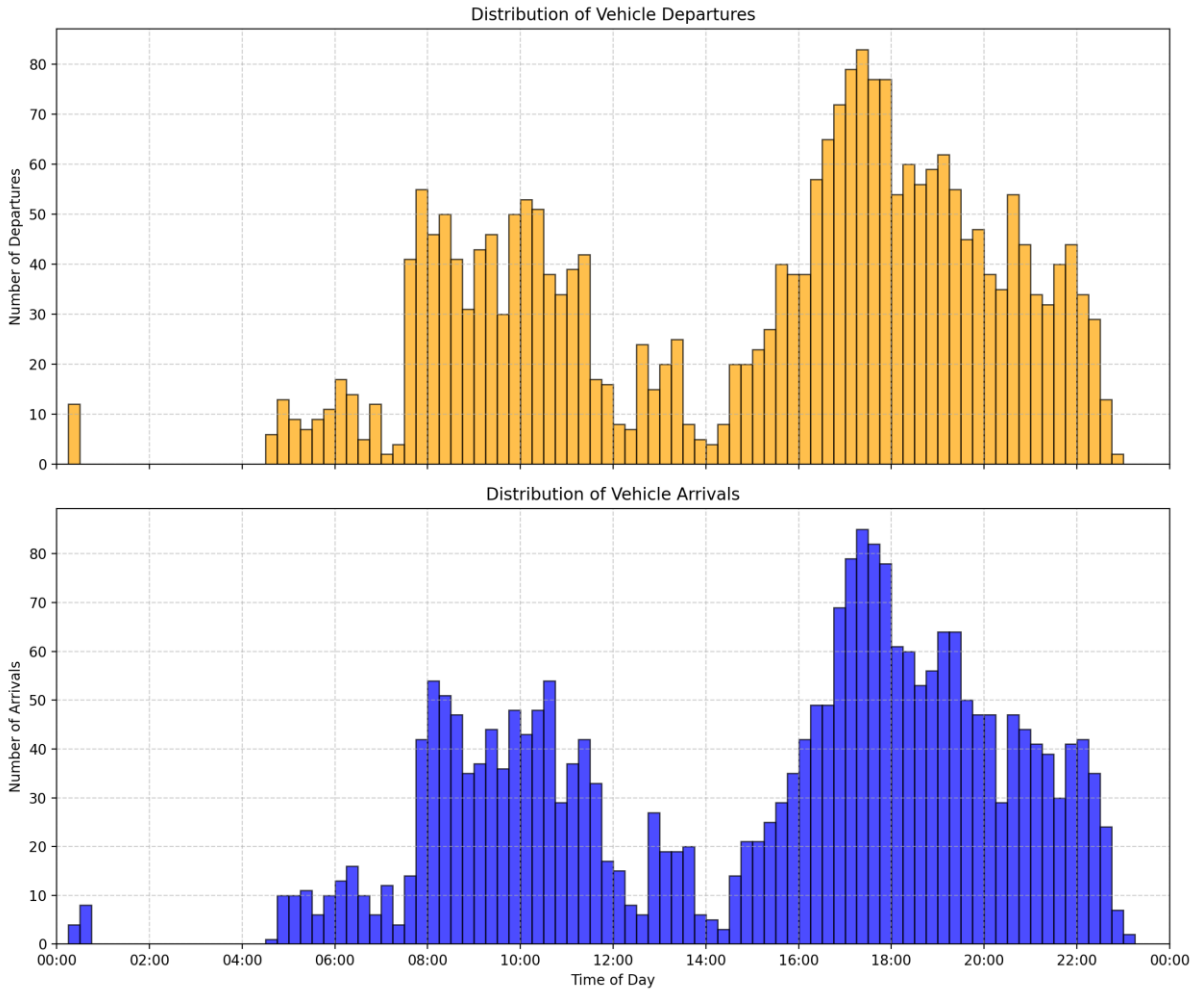

Figure 43: Distribution of Vehicle Departures and Arrivals of the population of interest.

Figure 43 illustrates the aggregate temporal distribution of vehicle departures and arrivals across the 24-hour simulation period, modelled in 15-minute intervals. The top panel ("Distribution of Vehicle Departures") clearly captures the morning commuting peak, with a dense cluster of vehicles leaving their initial locations (predominantly homes). A secondary, broader wave of departures occurs in the late afternoon and early evening as users conclude work or secondary daily activities. Correspondingly, the bottom panel ("Distribution of Vehicle Arrivals") mirrors these patterns but shifted temporally; a sharp influx of arrivals at first destinations (such as workplaces) is visible during the mid-morning hours, followed by a sustained, high-volume peak of vehicles arriving back at their final residential locations throughout the evening and into the night.

To evaluate how charging demand impacts the grid, the simulation incorporates 254 real-world public charging stations distributed across the 27 municipalities. This data was extracted directly from the official Greek Government Registry of Electric Vehicles Chargers [11], ensuring the simulation utilizes the exact geographical coordinates and technical specifications of the current infrastructure.

These public stations offer a wide variety of charging power capacities. Capacities start at 11.0 kW for standard AC charging and scale up to 110 kW for fast DC hubs. Across the entire public network, the average charging power capacity is approximately 30.0 kW.

To further enhance the simulation's realism, in addition to the public chargers, we have also distributed private home chargers. In the AoI 52% of the households possess at least one private parking slot [12]. Hence, we distributed 446 4 kW private home chargers to the population. Both home and public chargers location on the map are shown in Figure 44.

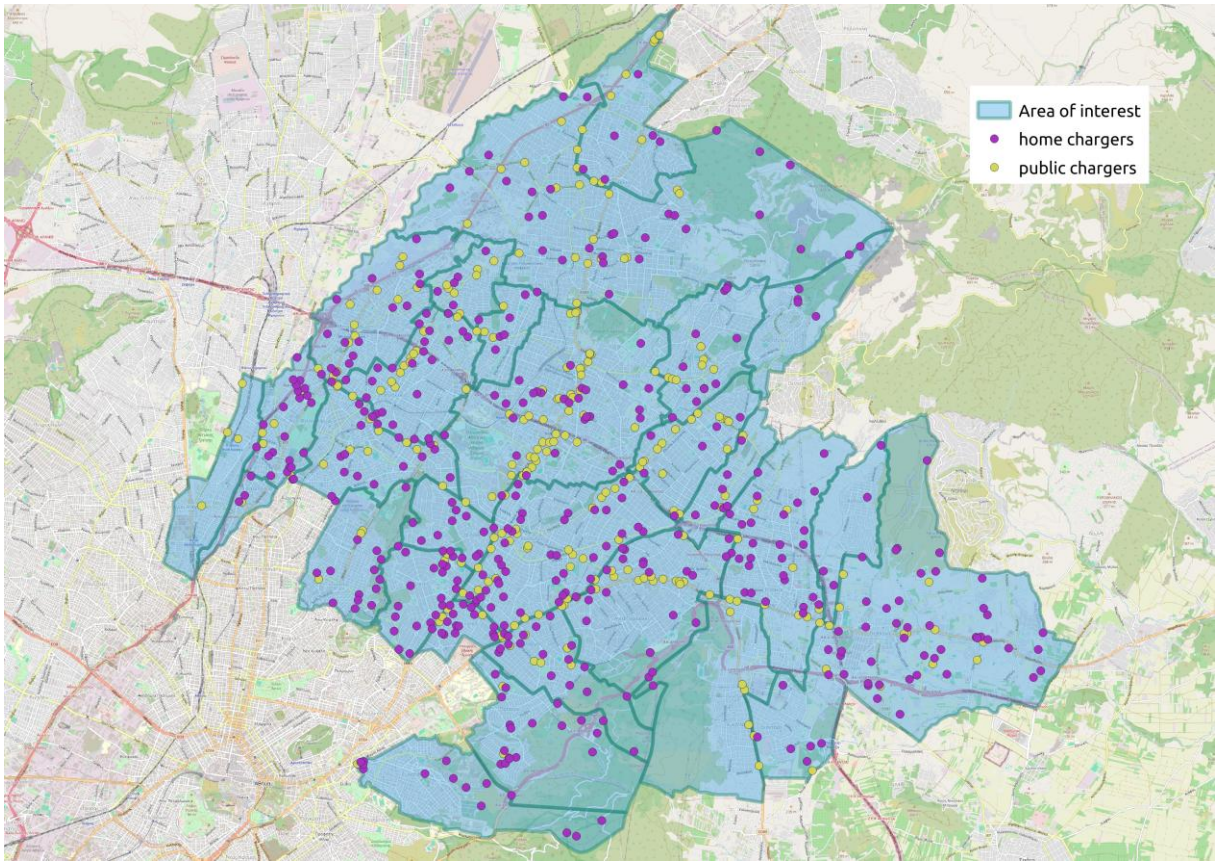

Figure 44: Home and public chargers across the AOI.

To properly evaluate the EV local charging impact, the simulation incorporates official, real-world substation data for the AoI. The exact locations, installed capacities, and technical specifications of these substations are real data points representing the actual regional infrastructure. The simulation actively monitors a network of 529 real-world substations. The power capacity varies significantly depending on whether they serve dense commercial zones or residential neighbourhoods. The capacities of these targeted nodes range from smaller 25 kVA units up to large 1,260 kVA transformers, with a network average of approximately 533 kVA.

Rather than modelling the entirety of the regional grid, the analysis focuses exclusively on the exact substations tasked with supplying the simulated EVs. However, because detailed topology of the underground distribution low voltage grid is not available for the AoI, the simulation does not model the exact topology.

5.3.2 Geographical Mapping

The mapping procedure employs a geographical heuristic: each of the 700 charging points is assigned to its geographically closest secondary substation. Consequently, the 700 charging points are paired with 529 distinct substations within the AOI.

The infrastructure is relatively distributed across the grid, with an average of 1.28 chargers per active substation. When focusing specifically on the public charging network, 222 substations are utilized, with a high degree of decentralization: 88.3% of these substations host exactly one public charging point, while only 11.7% host two or more, with a maximum concentration of 4 chargers at a single node.

To model realistic charging opportunities, the simulation pairs agent activities (e.g., Education, Work, Other) with public chargers located within a 300-meter radius. A total of 1,631 unique activities performed by the population were found to have at least one public charging option. On average, each of these activities is within reach of 1.66 public chargers, with some highly accessible locations providing up to 7 distinct charging options to the agent.

The mapping results suggest the potential for local dynamic tariffs. Because a single activity location can be within the proximity of multiple chargers, those chargers are often connected to different secondary substations. This allows agents to shift their electrical load between different nodes of the grid even without changing their destination. The mapping reveals significant spatial flexibility potential, as 35.3% of all charging-eligible activities (575 activities) are within reach of chargers connected to multiple different substations. On average, an activity with public charging access can choose between 1.50 distinct substations, while in the most diverse locations, a single activity location provides access to chargers connected to as many as 6 different substations.

This spatial distribution of activities, chargers, and substations strongly indicates the possibility that local price signals (dynamic DUoS tariffs) can effectively redirect charging demand between transformer nodes.

5.3.3 Simulation Model

The core of the simulation relies on a Mixed-Integer Linear Programming (MILP) model implemented in Pyomo [13]. This model simulates the decision-making process of an individual EV owner.

The primary objective of the model is to minimize the total cost for the EV user over a 24-hour period (discretized into 15-minute intervals). The model decides where to charge (charger selection) and when/how much to charge or discharge (V2G) to meet the user's mobility needs while minimizing costs.

The objective minimizes a sum of actual monetary costs and monetized inconveniences:

- **Charging Costs**: The cost of electricity bought from the grid (base price + DUoS tariff).
- **Discharging Revenue (V2G):** Revenue gained from selling energy back to the grid (V2G price + DUoS).
- **Battery Degradation**: A penalty cost applied to every kWh discharged to the grid from the battery.
- **Walking Cost**: A monetized inconvenience penalty for the time spent walking between a selected public charger and the actual activity location.

Model Assumptions
The following assumptions are integrated into the simulation model to define the behavioural and operational framework of the EV fleet:

Perfect Foresight and Determinism: The optimization problem is formulated with a 24-hour horizon under deterministic conditions. It is assumed that EV users have full knowledge of all future parameters, including: Their complete mobility schedule (trip durations, arrival/departure times, and energy consumption). The exact evolution of electricity prices and dynamic network tariffs across all 96-time intervals.

Daily Energy Neutrality:
To ensure that the vehicle maintains its operational readiness for subsequent days, a strict energy balance is maintained. It is assumed that the total energy charged over the 24-hour period (accounting for losses and V2G discharge) must exactly compensate for the total energy consumed during driving. Consequently, the battery State of Charge (SoC) at the end of the simulation period is constrained to be equal to the SoC at the beginning of the day.

Guaranteed Socket Availability:
The model assumes that whenever a user reaches a destination with charging infrastructure (private or public), there is always a free socket available for their use. The user is granted immediate and uninterrupted access to the charger for the entire duration of their stay.

5.3.4 Substation Profile Generation

The substation profiles generated in this step represent the background (static) electrical state of each secondary transformer node in the distribution grid. These profiles (comprising both load demand and PV generation) remain entirely fixed throughout the simulation. The EV charging or discharging actions that occur during the simulation do not modify these baseline curves; they are applied on top of them. For simplicity, and to focus the analysis on active power flows, we assume a unity Power Factor (PF = 1) for all profiles.

It is important to note that the Greek distribution grid is typically highly over dimensioned: under normal operating conditions, secondary transformers rarely approach their thermal limits. The additional burden from EV charging demand in this simulation is sufficient to cause meaningful grid congestion. Therefore, to create conditions where transformers can realistically reach their capacity limits during the simulation, we artificially inflate the background loads. Similarly, to observe reverse power flows at the transformer level, the PV installations are also sized aggressively, though capped at the transformer's rated capacity. The net demand profile is then computed as the difference between the load and PV profiles. Positive values indicate net import (demand exceeds generation), while negative values indicate net export (reverse power flow from PV surplus).

Load Profile Generation
The daily load curve for each substation is constructed in three steps:

1. **Standard Load Profiles (LPs)**: We use a set of standardized Load Profiles (LP1–LP12) [14], sourced from published quarter-hourly consumption data. Each LP represents a different consumer category (e.g., residential, commercial). All LP curves are normalized so that their daily energy integral equals 1.0, making them dimensionless and directly comparable.

2. **Random Linear Combination:** To reflect the fact that each substation serves a unique mixture of consumer types, we create a distinct load shape per transformer by forming a random weighted sum of the available LPs. A subset of LPs is randomly assigned zero weight (introducing sparsity), while the remaining LPs receive random positive weights summing to 1.0. The result is a unique, normalized daily demand curve for each node.

3. **Scaling via the Activity Factor**: The normalized curve must then be scaled to an absolute kW magnitude. We define an Activity Factor per substation, a score from 0 to 1 representing the total time EVs spend parked at chargers connected to that node, derived from the synthetic population's daily schedules. For a substation with zero EV activity, the load curve is scaled so that its peak reaches 95% of the transformer's kVA capacity. As the Activity Factor increases, the peak is pushed proportionally higher, up to 100% of the transformer's capacity for the busiest nodes. This ensures that all transformers operate near their limits before any EV load is added.

PV Profile Generation

The PV generation profile for each substation is constructed as follows:

1. **Normalized PV Curve**: A real annual PV production dataset is used, from which the daily generation profile of the peak solar production day is extracted. This 96-point (quarter-hourly) curve is normalized to [0, 1], providing a dimensionless daily solar generation shape.

2. **PV Capacity Sizing (Log-Normal Distribution)**: Each substation is assigned a PV installation whose capacity is drawn from a log-normal distribution. The Activity Factor influences the mean of this distribution: substations with higher EV activity (and hence more surrounding human activity) are assigned larger PV capacities, reflecting the correlation between urban density and rooftop solar adoption. Since real-world rooftop PV installations rarely exceed the local transformer's capacity — and to avoid unrealistic levels of curtailment — the drawn capacity factor is capped at 100% of the transformer's kVA rating.

3. **Final PV Profile:** The installed PV capacity (in kW) is multiplied by the normalized solar curve to produce the quarter-hourly PV generation profile for each substation.

Simulated Grid

Based on the provided distribution charts and the underlying data, the net load peak and net export peak figures (see Figure 45, Figure 46) illustrate the maximum loading conditions relative to the transformer capacities across the 529 analyzed substations.

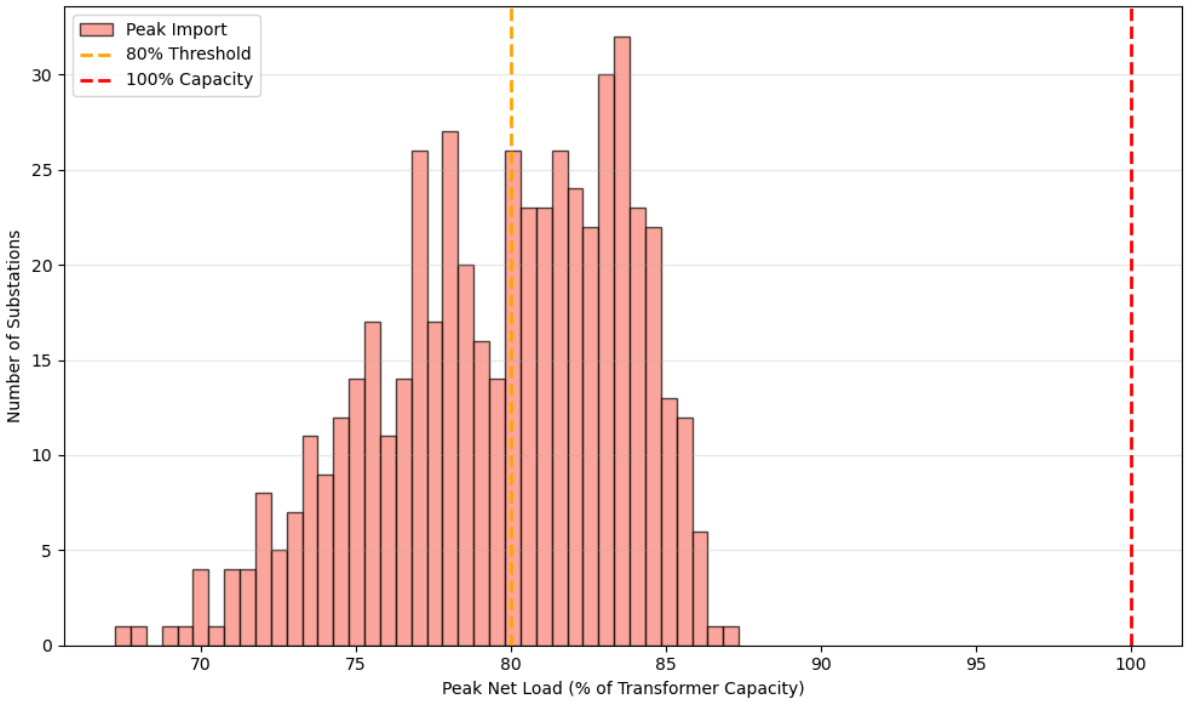

Figure 45: The distribution of peak load demand of the substations relative to the substations' nominal capacity limit.

The peak net load distribution (import) indicates a loaded network, with the average peak demand reaching 79.30% of transformer capacity and peaking at a maximum of 87.75%, which represent the assumptions of the inflated loads. Conversely, the peak export distribution, which represents reverse power flows driven by excess PV generation, shows remarkably less stress on the grid infrastructure. The vast majority of substations experience minimal reverse flow, yielding an average peak export of just 5.69% of capacity. While the maximum peak export reaches 79.44%, PV over-generation remains safely within the thermal limits of all transformers, with zero substations risking overload (0% exceeding the 100% capacity limit) from renewable energy exports.

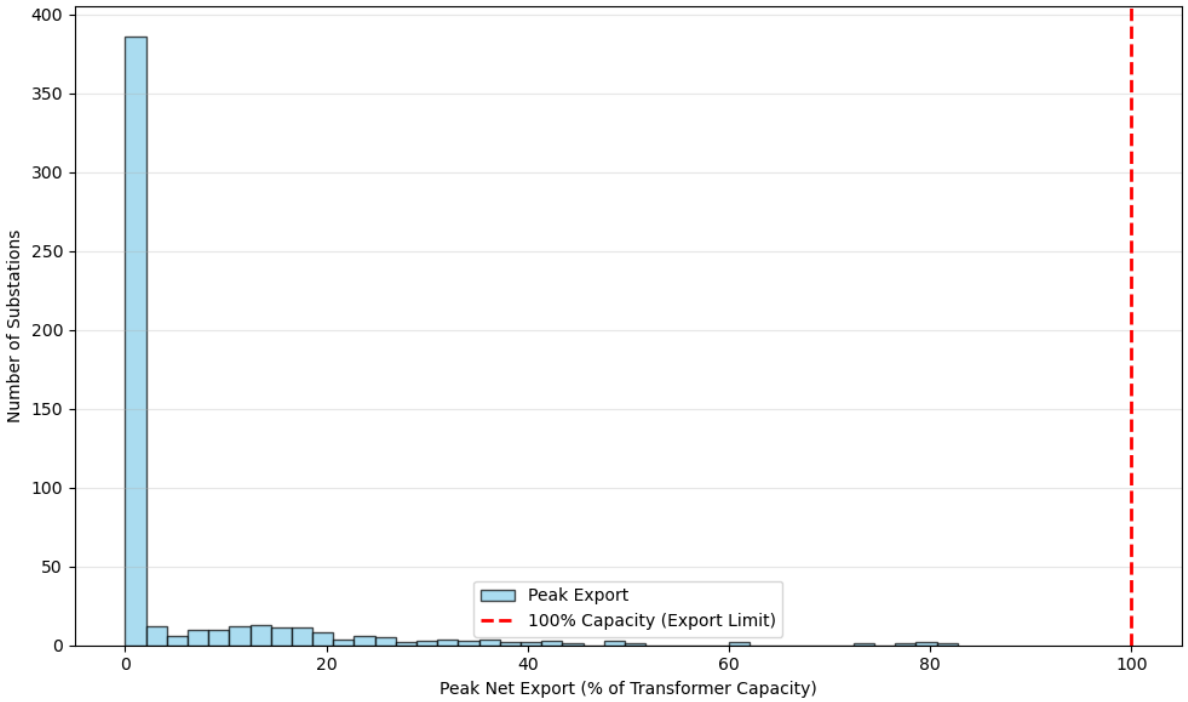

Figure 46: The distribution of peak net export of the substations relative to the substations' nominal capacity limit.

5.3.5 DUoS Tariff Function

The DUoS tariff serves as the price signal that the optimization model uses to incentivize or penalize EV charging and discharging behaviour at each substation. The core idea is simple: the tariff should reflect the stress level of the transformer at any given moment. When a transformer is lightly loaded, electricity should be cheap (encouraging charging). When it is heavily loaded or experiencing reverse power flows from excess PV, the tariff should increase significantly (discouraging additional burden and/or rewarding corrective V2G discharge).

The tariff for each substation at each 15-minute timestep is a function of the transformer's apparent power.
The tariff function (see Figure 47) is a hybrid piecewise sigmoid with three distinct regions, simulating the tariff used for the DEMO activities:

1. Safe Zone (0% to 80% loading): A flat, minimal fixed tariff of 0.0035 €/kWh. Within this range the transformer is operating well within its limits, so there is no incentive to shift load.

2. Overload Region (>80% loading): A sigmoid curve that rises steeply beyond the 80% threshold, saturating at +0.204 €/kWh. This punishes EV charging when the transformer is approaching or exceeding its capacity, strongly discouraging additional demand at congested times (typically evening peaks).

3. Export/Reverse Flow Region (<0% net demand): A separate sigmoid that drops into negative tariff territory, saturating at −0.153 €/kWh. Negative tariffs effectively act as a reward: when PV surplus causes reverse power flow, V2G-capable EVs that were previously charged can now discharge and get rewarded for alleviating the export stress (or alternatively, EVs are incentivized to charge during PV surplus to absorb the excess generation).

Both sigmoid curves are shifted so they cross through zero at the origin. The steepness parameters (K=4 for positive, K=8 for negative) control how rapidly the tariff ramps up or down beyond the safe zone thresholds.

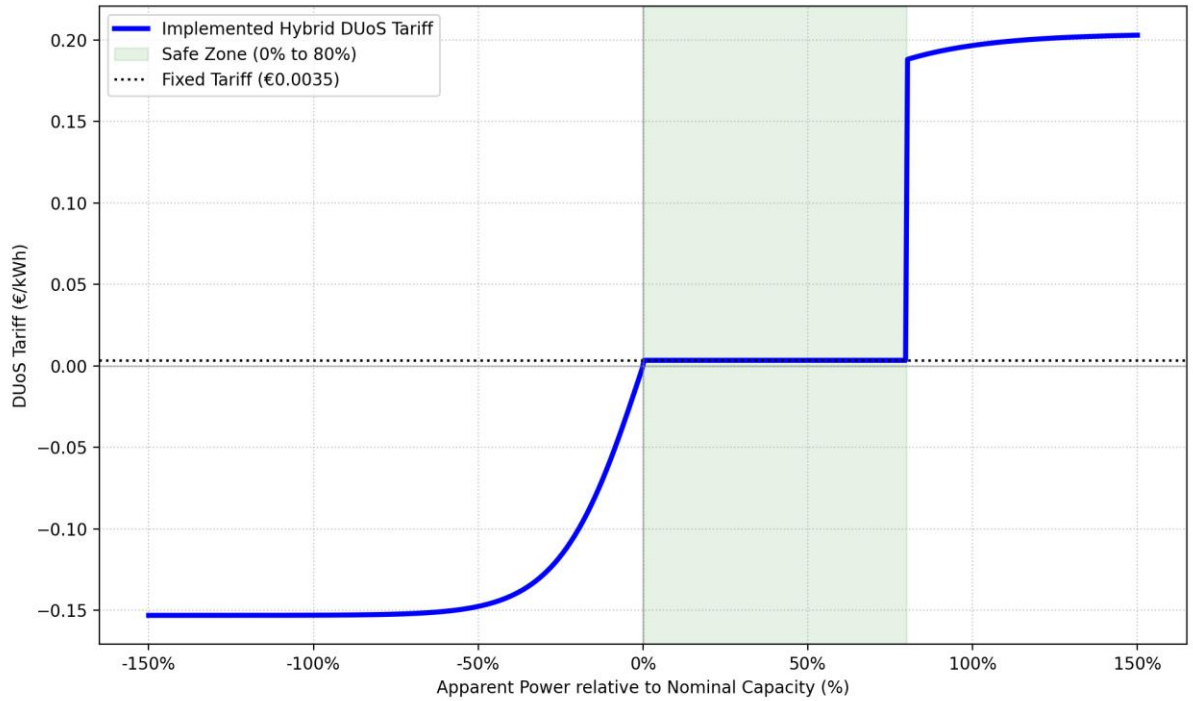

Figure 47: Tariff function of the simulation for Green Charging and V2G scenarios.

5.3.6 Simulation Setup

Electricity costs are differentiated by charger type and power capacity, reflecting a realistic pricing structure where faster public charging is more costly (see Table 2).

Table 2: Electricity price per type of charger

Charger Type	Power Rating	Price (€/kWh)
Private (Home)	~4 kW	0.15
Public AC	≤ 22 kW	0.35
Public Fast DC	≤ 50 kW	0.45
Public Ultra-Fast DC	> 50 kW	0.65

When an EV discharges energy back to the grid (V2G), the owner receives a V2G price of 0.15 €/kWh as revenue, in addition to any negative DUoS tariff reward. This creates a financial incentive for V2G participation, particularly during periods of high grid stress where the combined V2G price + negative DUoS reward can make discharging profitable. For this study V2G is restricted to private home chargers only.

Each charging/discharging cycle contributes to battery degradation. This is modelled as 0.05€ /kWh penalty [15]. This cost directly discourages unnecessary cycling and ensures V2G discharge only occurs when the combined revenue (V2G price + DUoS reward) exceeds the degradation penalty.

When an EV user parks at a charger that is not co-located with their activity, they must walk from the charger to their destination. This walking time introduces a discomfort cost penalized in the objective function with a coefficient equal to 7.5 €/h [16]. Walking speed is assumed at 5.0 km/h [17], and distances are scaled by a detour multiplier of 1.3 [18] to account for non-straight-line paths. This cost discourages the optimizer from selecting distant chargers unless their electricity price advantage is significant enough to justify the inconvenience. The battery parameters are described in Table 3.

Table 3: Battery specifications and parameters used for the simulation.

Parameter	Value	Description
Battery Capacity	50 kWh	Default EV battery size
Initial SoC	50% (25 kWh)	Initial State of Charge at start of day
Min SoC	10% (5 kWh)	Minimum allowed SOC – healthy battery usage
Max SoC	90% (45 kWh)	Maximum allowed SOC – healthy battery usage
Charging Efficiency	0.90	Charging efficiency (10% energy loss)
Discharging Efficiency	0.90	Discharging efficiency (10% energy loss)

5.3.7 Simulation Scenarios

To systematically assess the impact of progressively advanced EV-grid integration strategies, we define four simulation scenarios. Each scenario builds incrementally upon the previous one by introducing an additional mechanism, allowing us to isolate and quantify the contribution of each component.

Business as Usual (BaU)
The BaU scenario represents the current state of EV charging with no grid-aware coordination. A flat, fixed DUoS tariff is applied uniformly across all substations and timesteps, providing no locational or temporal price signal. Flexible Capacity Contracts are not active, meaning chargers always operate at their full rated power regardless of transformer loading. V2G is disabled (in fact, even if V2G was enabled the agents would not discharge since it is always not profitable in the BaU scenario). In this scenario, EVs charge opportunistically based solely on electricity price and user convenience, with no awareness of grid constraints. This serves as the baseline against which all subsequent scenarios are compared.

Flexible Capacity Contracts (FCC)
Building on BaU, this scenario introduces Flexible Capacity Contracts. When the apparent power at a substation exceeds 80% of its rated capacity, FCCs are activated for all chargers electrically connected to that specific transformer. Under FCC activation, the charging power capacity of each affected charger is curtailed to 50% of its nominal rating. This is a direct, hardware-level (charger) intervention that physically limits the demand EVs can place on a congested transformer, preventing thermal

overloads. The tariff remains fixed and V2G is still disabled. This scenario isolates the effect of a simple, rule-based congestion management mechanism.

Green Charging (GC)
This scenario adds the dynamic DUoS tariff pricing scheme (as described in the DUoS Tariff Function section) on top of the previous FCC mechanism. Instead of a flat tariff, each substation now broadcasts a time-varying price signal that reflects its real-time loading condition. During periods of low utilization or PV surplus, the tariff drops incentivizing EV charging to absorb excess renewable generation. During peak demand periods approaching the transformer's limits, the tariff rises sharply discouraging additional charging load.

Vehicle to Grid (V2G)
The final scenario enables Vehicle-to-Grid (V2G) discharging on top of all previous mechanisms. V2G is restricted to private home chargers only. When discharging, the EV owner receives a V2G revenue of 0.15 €/kWh, while the battery degradation cost penalizes the action. V2G discharge is only economically rational when the combined revenue (V2G price + DUoS tariff) exceeds the degradation penalty.

V2G is not permitted at public chargers. Public charging infrastructure involves significant installation and operational costs for the CPOs, and the discharging revenue model cannot straightforwardly compensate for these expenses. Determining a fair V2G compensation scheme at public chargers would require the development of specialized V2G products and business models distinct from simply selling energy back to the grid which falls outside the scope of this demonstration and study. By restricting V2G to the home environment, where the infrastructure is simpler and the cost structure more transparent, we focus on the most immediately deployable and economically justifiable V2G use case.

5.3.8 Results

In this section, we present the general results of the simulation across the four defined scenarios, together with the KPIs defined for the Greek DEMO. While the simulation assumptions and input data have been constructed to be as realistic as possible, the primary goal of this simulation is to serve as a proof of concept for the mechanisms investigated in the Greek DEMO. The results are intended to demonstrate the impact and relative effectiveness of Flexible Capacity Contracts, dynamic DUoS tariffs, and V2G strategies on MV\LV substation load, renewable energy integration, emissions impact, and user costs, rather than to make definitive claims about the precise economic or environmental outcomes that would be observed in a real-world deployment. Accordingly, the KPI values reported below should be interpreted as indicative of the trends and trade-offs that each scenario introduces, rather than as exact predictions of operational performance.

5.3.8.1 Scenarios Overview

This subsection discusses the simulation results based on the visual evidence provided by the figures, focusing on the temporal and spatial behaviour of the different scenarios. The interpretation is therefore initially centred on the aggregate charging/discharging demand, the evolution of the average fleet state of charge, and the geographical redistribution of demand relative to the BaU case. The quantitative assessment based on KPI calculations follows.

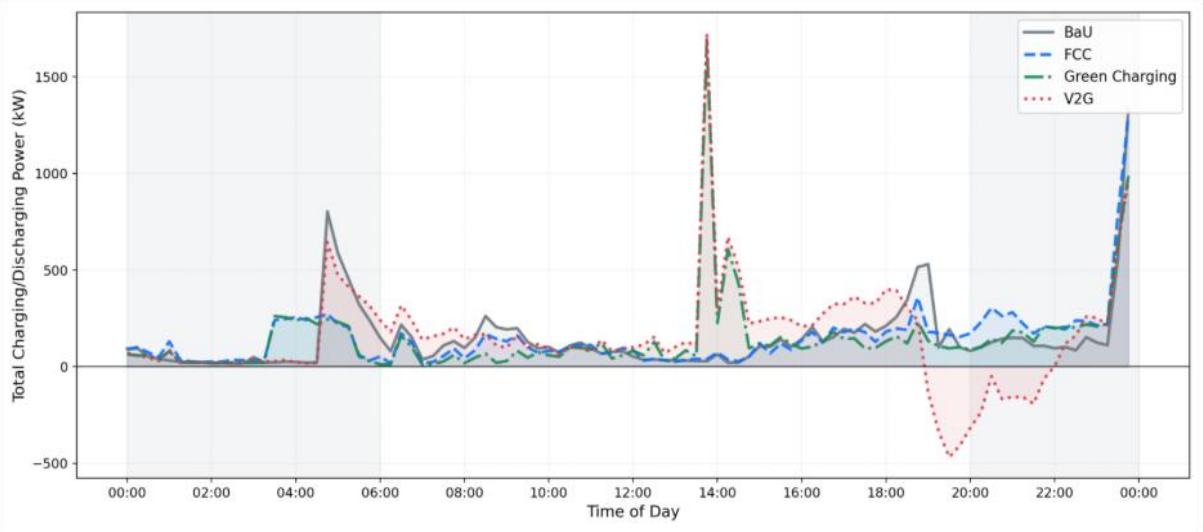

Figure 48: Total charging and discharging power time series across all simulation scenarios.

Figure 48 presents the total charging/discharging power for all scenarios over the course of the day. The BaU case follows the expected pattern of unidirectional charging demand and remains strictly positive throughout the day. The FCC scenario preserves a similar overall shape, but with a generally smoother and lower profile during several intervals, indicating that its primary effect is to constrain charging power rather than fundamentally shift charging activity. In contrast, Green Charging produces a more visible reshaping of the demand curve, with charging activity being shifted clearly. This is particularly evident in the pronounced mid-afternoon increase, which suggests a coordinated concentration of charging activities during the peak PV generation, which is expected since the DUoS tariffs incentivize the EV users to have this behavioral output. The V2G scenario shows the strongest deviation from the other cases, especially in the evening period, where total power becomes negative. This indicates net discharge from EVs back to the grid and confirms the bidirectional nature of this strategy. It should be noted that the very large spike at the end of the day should not be interpreted as a realistic operational effect, but rather as a mathematical artifact of the optimization. Because the electricity tariff remains perfectly flat during these hours. Without any price incentive to begin charging earlier in the evening, the solver mathematically defers this required energy recovery until the final available timesteps, creating an artificial, synchronized spike at midnight.

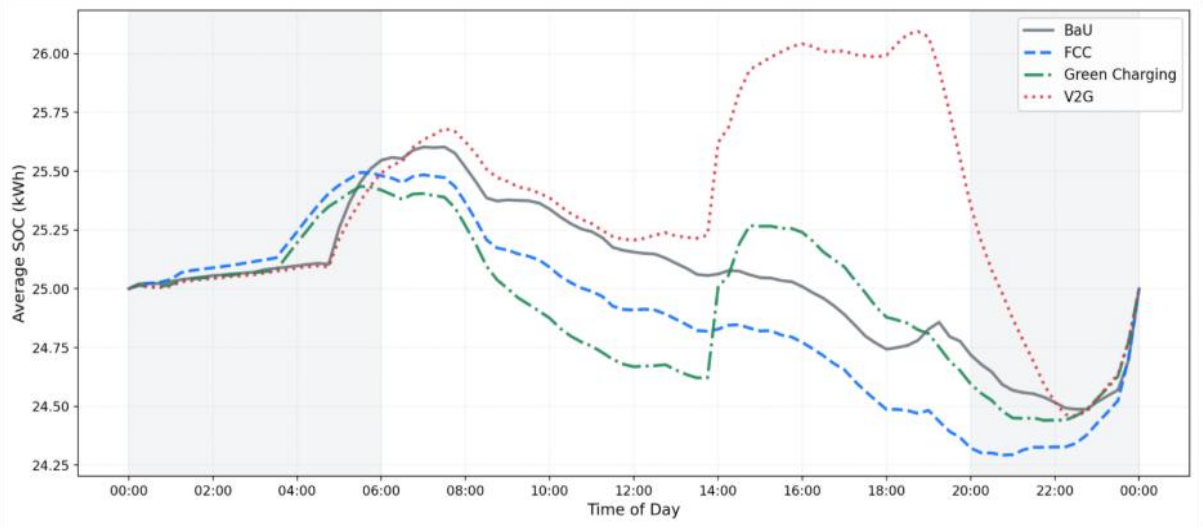

Figure 49: Average fleet SoC evolution across simulation scenarios.

Figure 49 shows the average fleet state of charge for all scenarios. Since all curves begin from nearly identical initial conditions, the subsequent divergence can be directly attributed to the charging strategy applied in each case. The BaU profile rises during the early hours and then gradually declines during the day, reflecting standard charging and vehicle use patterns. The FCC scenario follows a similar trend, but remains below BaU for much of the day, suggesting that charging constraints reduce or delay energy replenishment. Green Charging exhibits a more dynamic trajectory, with a stronger decline during the late morning and midday, followed by a clearer recovery in the afternoon, which is consistent with the concentrated charging activity already observed in the aggregate power profile. The V2G scenario is again the most distinct, maintaining a higher average SoC during much of the afternoon and early evening before declining sharply during the period in which aggregate power becomes negative. This indicates that energy is intentionally accumulated before being discharged back to the grid, highlighting the most strategic charging scheduling across all scenarios.

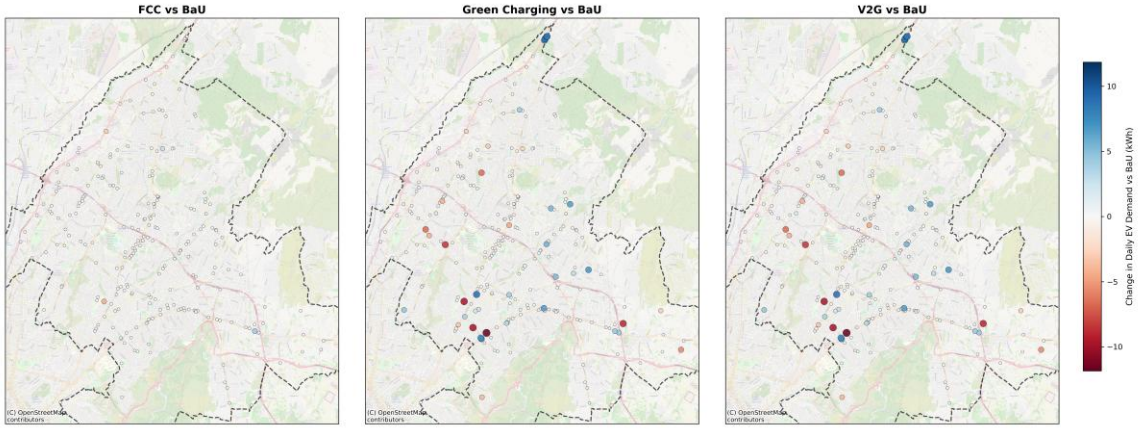

Figure 50: Spatial redistribution of public charging demand relative to the BaU scenario.

Figure 50 illustrates the spatial shift in daily public EV charging demand relative to the BaU case. More specifically, the figure isolates the effect of the 205 “spatial shifters”, i.e. users who do not have access to a private home charger and who visit more than one location with a public charger during the day. Since these are the only EV users who have multiple public charging options, they are the group that we expect to see a change in their spatial charging scheduling in response to price signals. The dots in the figure correspond to the locations of public EV chargers. Chargers connected to the same substation are represented with the same colour and marker size, so that the visualisation reflects the net daily change at substation level. Blue markers indicate locations where daily charging demand decreased compared to BaU, while red markers indicate locations where demand increased. The marker size reflects the magnitude of the shift in total charged energy.

The FCC vs BaU comparison shows almost no spatial redistribution. Only a very small number of public charging locations gain or lose demand, indicating that the flat capacity tariff is not sufficient to induce users to change charging location. In this case, users may adjust charging behaviour in time, but they largely continue charging at their usual public charging points. By contrast, the Green Charging vs BaU comparison shows a much stronger spatial reallocation, with a substantial number of public chargers gaining demand and others losing it. This indicates that dynamic tariffs successfully encourage this specific user group to abandon chargers used during less favourable, typically evening, periods and instead shift charging to alternative public charging locations visited during cheaper daytime hours, such as workplaces or commercial areas. The large red and blue markers confirm that this is not a marginal effect, but a measurable transfer of charging energy between specific parts of the public charging network.

The V2G vs BaU map is effectively identical to the Green Charging case, and this should be expected. Since V2G is only enabled for home chargers, and the present figure includes only public chargers, no additional V2G-specific effect can appear in this spatial comparison. In addition, the EV users will not increase the demand in these chargers in order to benefit from V2G later since, simply they do not have the opportunity to plug their vehicles in a V2G home charger. Therefore, the spatial pattern shown for V2G reflects only the same public-charging relocation mechanism already observed under Green Charging.

Overall, the visual analysis suggests a clear progression across the scenarios: **FCC** mainly moderates charging demand, **Green Charging** reshapes it more substantially in both time and space, and **V2G** extends this behaviour further by enabling active discharge back to the grid.

5.3.8.2 KPI Calculation and Comparison

Following the visual interpretation of the scenario behaviour, the KPI comparison (Table 4) provides a quantitative assessment of the effect of each control strategy.

Table 4: KPI comparison across the 4 different scenarios.

KPI	BaU	FCC	Green Charging	V2G
Desired Flexibility (kWh)	192.84	—	—	—
Utilized Flexibility (kWh)	—	46.11 (+23.9%)	152.18 (+78.9%)	152.18 (+78.9%)
Net CO_2 Emissions ($kgCO_2eq$)	998.92	1021.31 (−2.2%)	875.05 (+12.4%)	795.27 (+20.4%)
Avg EV User Cost ($)	952.35	952.35 (+0.0%)	865.42 (+9.1%)	750.88 (+21.2%)

The first KPI concerns desired flexibility, estimated at 192.84 kWh in the simulated system. This represents the total amount of charging demand shift that would ideally be useful from the grid perspective. Against this benchmark, the FCC scenario delivers 46.11 kWh of utilized flexibility, corresponding to 23.9% of the desired flexibility. This shows that rule-based charging demand curtailment can activate some flexibility, but only to a limited extent. When dynamic tariffs are introduced in the Green Charging scenario, utilized flexibility rises sharply to 152.18 kWh, or 78.9% of the desired flexibility. The same utilized flexibility value is reported for V2G, indicating that the additional benefit of V2G is not expressed as a further increase in shifted charging demand, but rather through the ability to discharge energy during system-relevant periods.

The net CO_2 emissions KPI shows a clear ranking across the scenarios. BaU results in 998.92 $kgCO_2eq$, while FCC increases emissions to 1021.31 $kgCO_2eq$ (+2.2% vs BaU). By contrast, Green Charging reduces emissions to 875.05 $kgCO_2eq$ (−12.4%), and V2G achieves the best result with 795.27 $kgCO_2eq$ (−20.4%). Figure 51 explains these differences by plotting EV power together with the grid carbon intensity profile. In BaU and FCC, charging still occurs largely outside the low-carbon midday window and remains significant during the more carbon-intensive evening period. In Green Charging, charging is shifted more clearly toward midday hours, which lowers emissions. V2G further improves performance by also discharging during the evening peak, when carbon intensity is highest, thereby providing the strongest emissions reduction.

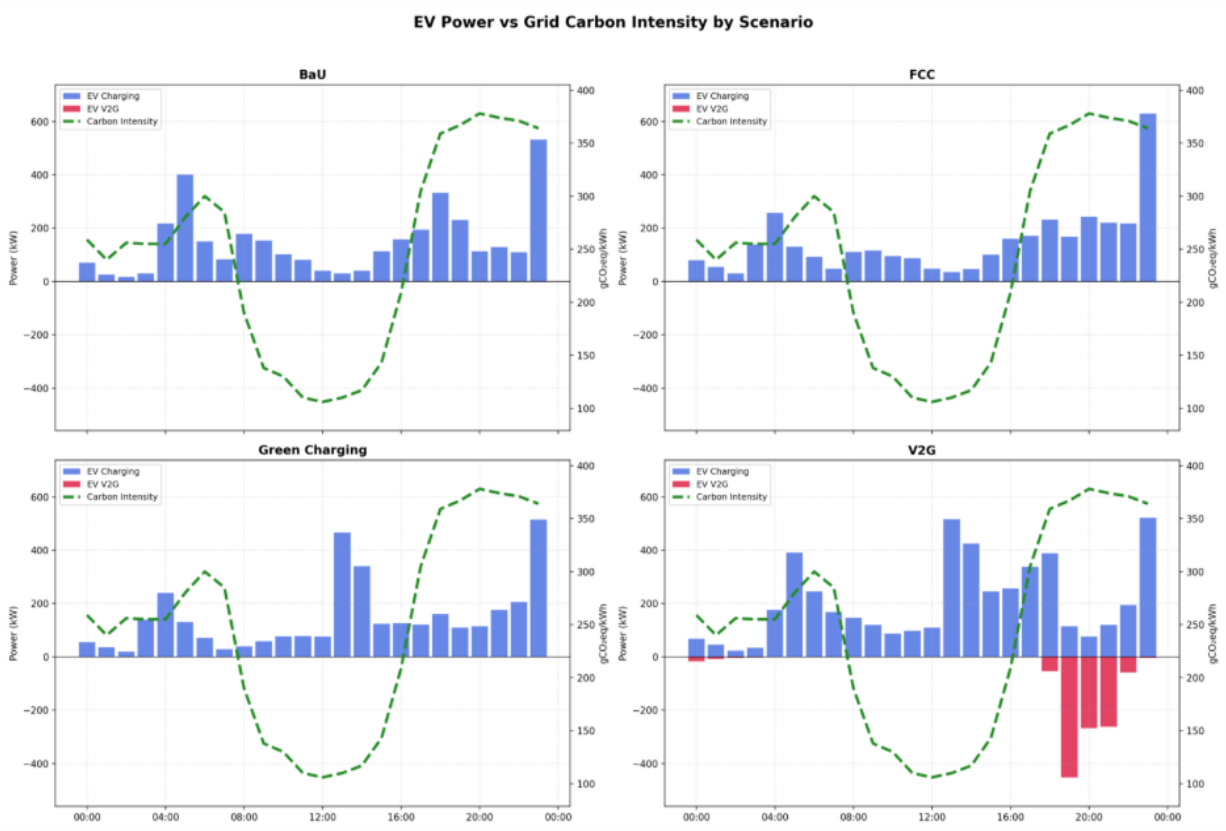

Figure 51: EV charging/discharging power versus carbon intensity for each scenario.

The EV user cost KPI shows that FCC performs essentially the same as BaU, with no meaningful cost benefit for users. While BaU results in a total user cost of 952.35, the FCC scenario remains the same indicating that capacity-based control does not create economic incentive for users to reduce their charging costs. In contrast, Green Charging lowers total user cost to 865.42, corresponding to a 9.1% reduction relative to BaU, showing that dynamic tariffs allow users to shift charging toward cheaper periods. The strongest economic performance is observed in V2G, where user cost decreases to 750.88, a 21.2% improvement compared to BaU. This is consistent with the scenario design, as users can both avoid expensive charging periods and benefit economically from discharging when V2G compensation and tariff conditions make this profitable.

RES Curtailment

To investigate the effect of flexibility services on RES curtailment, we simulate a case where RES curtailment is allowed by the DSO. In fact, such a case is examined in [19], since allowing limited curtailment can be a practical way to accommodate higher RES capacities in distribution networks under stressed operating conditions, especially when local voltage or thermal constraints would otherwise restrict further integration.

In the present implementation, this condition is reproduced by ranking substations according to the total time of EVs parked there during the solar window and assigning a significantly higher PV capacity to **the top 10%**. In this way, these substations are more likely to experience excess PV generation during peak solar hours, where there is the EV potential to harvest the effect.

The RES curtailment results show that the BaU case leads to a total technical PV curtailment of 1,137.56 kWh, while the Green Charging case reduces this value to 1,028.98 kWh. Although this confirms that

flexibility can mitigate curtailment, neither case is able to eliminate it to a substantial extent, which is reasonable given that the total PV curtailment before the EV simulation, 1,153.6 kWh, is already a considerable amount of energy compared with the total charging demand of 3,527.4 kWh. In other words, the available EV demand is not large enough to absorb the surplus PV generation. Still, the **Green Charging case achieves a clear RES curtailment reduction of 108.58 kWh, corresponding to about 9.5%** relative to BaU, indicating that dynamic tariffs can improve the temporal alignment between EV charging and PV surplus and therefore contribute to reducing RES curtailment. It should also be noted that the BaU curtailment results are identical to those of FCC, and the Green Charging results are identical to those of V2G; therefore, this is the only meaningful comparison for the RES curtailment analysis.

6 Discussion

This section discusses the main findings of the Greek demonstration by combining the evidence from the field activities, the measured KPI results, and the supporting simulation analysis. The discussion aims to interpret the results beyond a purely descriptive presentation of the data, highlighting what was effectively demonstrated under real operating conditions, what was validated through KPI assessment, and what could only be explored through simulation. In this way, the discussion provides an integrated view of the pilot's achievements, the factors that limited some aspects of the demonstration.

6.1 Demo Activities

The Greek demonstration confirmed that the pilot was able to move beyond a purely technical setup and operate as an integrated field trial in which grid monitoring, charging infrastructure, digital platforms and EV users interacted under real conditions. Although the charging infrastructure was operated within a controlled pilot framework and not as a continuously open public network, the demonstrator still generated real operational data on substation and feeder behaviour, charging sessions, tariff application, wallet transactions and user responses to smart charging signals. In that sense, the demo successfully validated the interoperability between the LV monitoring equipment, the DSS, the O-V2X-MP platform, the charging infrastructure and the participating EV users.

A key aspect of the field activities was the detailed LV monitoring of the substations and feeders supplying the chargers. The pilot achieved visibility at both substation and feeder level, allowing the assessment of EV charging impacts on the local LV grid. The results also showed different electrical conditions across the three charging areas used during the demonstration. While the substations feeding the 2nd Elementary School and Eleftherias Square appeared over-dimensioned relative to the observed winter loading, Papasideris Stadium operated closer to a potentially critical range, reaching around 75% of transformer capacity. At the same time, no major voltage quality violations were observed, indicating that the demo did not create power quality problems under the current EV penetration and usage levels.

The BUC activations should be interpreted in the context of the actual network conditions. Since the monitored transformers did not naturally exceed their operational limits during the demo period, the pilot could not rely on real congestion or overvoltage events to test the services. For this reason, the project applied a forced activation logic based on forecasted and historical transformer behaviour, using transformer- and month-specific thresholds. This approach allowed the demonstrator to test the communication chain, tariff logic and charger response despite the limited grid stress. It also showed that reliable forecasting, supported by robust data processing and continuous data quality checks, is essential for enabling flexibility services in practice.

Moreover, the Greek pilot demonstrated the technical, operational, and economic viability of smart EV charging infrastructure integrated with dynamic pricing and grid-responsive functionality. During the pilot period, the charging system operated reliably, with stable energy transfer and no major technical disruptions. Session profiles confirmed consistent power delivery, meeting expectations for public AC charging in an urban environment. A total of 13 active users engaged with the system, including a core group of recurring users. Charging behavior was characterized by medium-sized sessions (around 14 kWh on average), indicating opportunity charging and early user acceptance. From an economic perspective, revenues were proportional to energy consumption, while billing remained

transparent. The breakdown of charging costs into energy and network tariff components confirmed correct tariff implementation, and variations in average cost per kWh reflected dynamic pricing.

An important contextual factor is that employee participation may have led to more disciplined charger use and parking behaviour than would typically be expected in a fully public setting. This may have positively influenced operational smoothness and user compliance during the pilot.

A key outcome was the validation of smart charging capability. When tariff signals alone were not sufficient to reduce peak demand, a DSO flexible capacity triggered active power modulation, reducing charging power without interrupting service. In addition, spatial analysis showed uneven utilization across charging locations, with Papasideris Stadium emerging as the main demand hub. These findings provide useful guidance for future infrastructure planning.

V2G Limiting Factors

The ISO 15118-20 standard has recently been finalized, enabling bidirectional communication between EVs and charging infrastructure. However, certified commercial deployments remain limited. Although support for OCPP 2.0.1 is gradually emerging, only a very limited number of EV charging stations in Greece currently support this protocol. While several EVSEs are technically capable of enabling V2G functionality, their communication interfaces are not fully certified or interoperable with commercially available V2G-capable vehicles.

At the vehicle level, OEM adoption of V2G technology is increasing, with manufacturers such as Nissan, Hyundai, Volkswagen and Renault introducing V2G-ready products. Nevertheless, no V2G-capable EVs are currently commercially available in the Greek market, preventing the practical demonstration of bidirectional charging.

From a regulatory perspective, V2G services in Greece are currently permitted only for behind-the-meter applications, typically in installations with existing PV or storage capacity. Consequently, EV integration in the Greek market is presently limited to unidirectional charging and participation in flexibility services as controllable demand, without provisions for bidirectional energy exchange.

Overall, the aforementioned technical, regulatory and market constraints constituted the key limiting factors that prevented the practical demonstration and validation of the V2G interfaces of the O-V2X-MP within the Greek demonstration site.

6.2 KPIs

The measured KPI results suggest that the Greek demo performed well in terms of deployment maturity and operational readiness, even if its scale remained limited. In general terms, the demonstration succeeded in putting into operation a non-trivial set of charging and monitoring assets and in attracting enough users to test the complete service chain. The four electrified locations show that the infrastructure rollout objective was largely achieved, even though the accessibility limitations at one site reduced its practical usability. Likewise, the user participation target was exceeded, and the very high satisfaction results indicate that the demonstrator was not only technically functional but also positively received by the participating EV users.

A second group of findings concerns the quality and robustness of the digital and monitoring backbone. Here the KPIs are consistently strong. Data acquisition and storage accuracy reached 99.58%, clearly

above the 95% threshold. Sampling rates were also comfortably aligned with operational needs: charger heartbeat messages were available every 10 seconds, meter values during transactions every 5 seconds, and the LV monitoring system at 1-minute resolution. Together, these results indicate that the pilot had a sufficiently dense and reliable data stream to support near-real-time observation and flexibility activation.

The KPIs also show a positive picture regarding platform performance and interoperability. The O-V2X-MP platform demonstrated scalability up to 28 simultaneously connected chargers, surpassing the target of 25, while service availability during the examined January 2026 interval was reported at 100%, above the >99.9% target. In addition, the average DSO-to-platform latency was measured at 250 ms, which is a strong result for the practical deployment of flexibility signals. These values suggest that the digital platform was not a bottleneck in the Greek demo. On the contrary, they indicate that the communication layer between the DSO logic and the charging infrastructure was mature enough to support coordinated smart charging actions. Even if the field trial itself remained limited in size, the KPI results imply that the platform architecture can already accommodate a somewhat larger deployment without fundamental redesign.

The forecasting-related KPIs strengthen this conclusion further. The short-term forecasting model achieved an average MAPE of 8.41% for the 4-hour horizon, remaining below the 10% target, while retraining time was reported at about 2.74 seconds, well below the 15-second target. These results are especially relevant because the forced BUC activations depended on forecasting and trigger logic rather than on naturally emerging overload conditions. Therefore, the value of the forecasting KPIs is not only methodological but operational: they show that the pilot had the analytical capability to support timely and data-driven flexibility actions. In other words, even though the field conditions did not produce severe natural stress, the pilot demonstrated that the intelligence layer needed to respond to such stress is already technically viable.

The cost KPIs should be interpreted somewhat differently from the performance KPIs. The reported ICT costs confirm that achieving this type of integrated demonstrator requires substantial software and systems investment on both the DSO and CPO sides. The DSS development cost on the DSO side and the O-V2X-MP-related costs on the CPO side underline that flexibility services are not enabled by chargers alone; they depend on a broader digital ecosystem involving communication, servers, software development and platform integration. This does not weaken the pilot's results, but it does highlight an important replication issue: scaling such solutions beyond pilot mode will require careful consideration of who bears these digitalization costs and how they are recovered in future market or regulatory arrangements.

Overall, the measured KPIs paint a coherent picture. The general KPIs show that the demonstration was sufficiently populated with infrastructure and users to produce meaningful observations, while the technical KPIs indicate a highly reliable monitoring, forecasting and platform environment. Taken together, these results suggest that the Greek pilot was particularly successful as a systems integration **demonstrator**. Its strongest evidence is not that it solved a severe real-world congestion problem during the demo window, but that it proved the readiness of the monitoring, communication and control chain needed to address such problems when they emerge more clearly in future deployments.

6.3 Simulations

The simulation work plays an essential complementary role in this deliverable because it extends the analysis beyond what could be physically observed during the limited demo period. This is particularly important in the Greek case, where the field deployment did not experience naturally critical

transformer loading and where V2G could not be demonstrated physically. The simulations therefore provide the analytical space to test the relative effects of Business as Usual, Flexible Capacity Contracts, Green Charging and V2G under a broader and more systematic set of conditions. In that respect, the simulations are not secondary to the demonstration; they are the mechanism through which the project can discuss flexibility impacts that the field trial alone could not expose.

A key modelling limitation is the assumption of perfect foresight. Since users are assumed to know their future trips, energy needs, and price signals in advance, the resulting flexibility performance should be interpreted as an upper-bound estimate rather than a directly achievable real-world outcome.

The simulation results support a plausible progression across scenarios. The FCC case mainly smooths and constrains charging power, confirming its role as a direct congestion-management mechanism. Green Charging produces a more visible temporal reshaping of charging demand, especially by shifting activity toward periods associated with PV generation and favourable DUoS signals. The V2G case has the strongest effect, including periods of net discharge, showing the theoretical potential of bidirectional flexibility when it is economically enabled. This staged structure is useful because it separates the effects of simple physical power limitation, price-based behavioural steering, and bidirectional services, rather than conflating them into a single “smart charging” result.

At the same time, we have to underline that the results of the simulations are intended to demonstrate trends and trade-offs rather than exact predictions of operational performance. This is a critical point. The simulated indicators for desired flexibility, utilised flexibility, CO2 emissions, EV users’ economic impact and RES curtailment depend on assumptions regarding travel behaviour, charger availability, battery characteristics, tariff design, transformer loading, and PV production. Therefore, they should be read as showing the relative direction and magnitude of possible effects.

The KPI results make this progression more concrete. The simulated desired flexibility in the system is estimated at 192.84 kWh, which defines the volume of charging demand that would ideally be shifted away from stressed periods. Against this benchmark, FCC utilises 46.11 kWh, corresponding to 23.9% of the desired flexibility, showing that direct curtailment can provide some support but with a relatively limited effect. Under Green Charging, utilised flexibility rises to 152.18 kWh, or 78.9% of the desired flexibility, indicating that dynamic tariffs are much more effective in steering charging demand toward more beneficial periods. The V2G scenario reaches the same utilised flexibility value, 152.18 kWh (78.9%), which suggests that its additional value does not come from shifting more charging demand, but from enabling discharge during system-relevant periods.

A similar ranking appears in the environmental and economic KPIs. Net CO_2 emissions decrease from 998.92 $kgCO_2eq$ in BaU to 875.05 $kgCO_2eq$ in Green Charging and 795.27 $kgCO_2eq$ in V2G, while FCC slightly increases emissions to 1021.31 $kgCO_2eq$. In parallel, the average EV user cost remains unchanged in FCC at 952.35, but falls to 865.42 in Green Charging and to 750.88 in V2G, corresponding to improvements of 9.1% and 21.2%, respectively. Overall, these results show that FCC mainly delivers technical grid support, whereas Green Charging and especially V2G provide broader benefits by combining flexibility activation with lower emissions and improved user economics.

7 Conclusions

The Greek DEMO has shown that the pilot is mature enough to be assessed not only as a technical prototype, but as an operationally integrated smart charging ecosystem. The combined evidence from the field activities and the simulation analysis indicates that the project has established a solid implementation basis for coordinated EV charging, grid visibility and flexibility-oriented service provision. At the same time, the results show that the greatest value of the DEMO lies not only in the infrastructure deployed, but also in the successful interaction between monitoring, forecasting, control and user-facing charging services.

The first main conclusion is that the core building blocks of the DEMO are operationally ready and capable of supporting real service implementation.

- **LV monitoring system**
- **DSS and forecasting services**
- **O-V2X-MP**
- **Smart chargers**

The LV monitoring system provided the observability needed to assess transformer and feeder behaviour under charging activity, confirming that the grid side of the DEMO can support data-driven decision making. The DSS, including its forecasting services, demonstrated that flexibility activation can be supported through a structured operational logic rather than through ad hoc control actions. This is particularly relevant for future scaling, since it shows that smart charging services can be linked to grid conditions in a systematic way. The O-V2X-MP proved to be a reliable integration layer, supporting charging management, billing functions and service execution with solid overall performance. In parallel, the smart chargers provided the physical interface through which these services could be implemented in practice, confirming the readiness of the hardware layer for coordinated and controllable charging operation. Taken together, these components form a coherent and sufficiently mature technical ecosystem, able to support future expansion and more advanced service deployment.

The second main conclusion concerns the assessment of the business models and service concepts examined through state-of-the-art simulations.

- **Flexible Capacity Contracts**
- **Green Charging**
- **V2G**

The analysis shows that these three approaches provide different forms of value and should not be seen as interchangeable options. Flexible Capacity Contracts mainly serve as a grid protection mechanism, offering a direct means of limiting charging demand when network conditions require intervention. Green Charging extends this logic by using dynamic DUoS tariffs to influence charging behavior more proactively, creating benefits not only for grid operation but also for renewable energy utilization. V2G represents the most advanced concept among the analyzed cases, as it expands flexibility from managed consumption to bidirectional energy exchange, thereby increasing the potential contribution of EVs to system support.

From this perspective, simulations are important because they demonstrate that the same technical ecosystem can underpin multiple service layers with different operational objectives. FCC is closer to a technical flexibility product for local congestion management, Green Charging is closer to a market-oriented and user-facing flexibility mechanism, and V2G points toward a future model in which EVs

can act as distributed energy resources. The KPI results reinforce this interpretation, as they show a progression from more limited local network support toward broader environmental, economic and system-level benefits.

Ultimately, the Greek pilot demonstrated, the enabling components required for smart and flexible EV charging are already in place and operationally credible. Second, the service assessment indicates that the value of this architecture can grow substantially when moving from basic control mechanisms toward more advanced charging strategies and, in the longer term, V2G flexibility schemes.

References

[1] P. Pediaditis *et al.*, "UC Specifications and Demonstrator Deployment Plan," EV4EU Project, Deliverable D8.1 D8.1, Nov. 2023. [Online]. Available: https://ev4eu.eu/resources/

[2] G. Papadakis, A. Koutounidis, I. Manitaris, and P. Pediaditis, "Open V2X Platform Validation and Commissioning Tests." 2024. [Online]. Available: https://ev4eu.eu/resources/

[3] G. Papadakis, V. Melissianos, A. Koutounidis, P. Pediaditis, and I. Manitaris, "Open V2X Management Platform Test Report." 2025. [Online]. Available: https://ev4eu.eu/resources/

[4] A. Koutounidis *et al.*, "Services Activation in Greek Demonstration Report," Electric Vehicles Management for carbon neutrality in Europe (EV4EU), Deliverable D8.4 D8.4, Aug. 2025. [Online]. Available: https://ev4eu.eu/resources/

[5] N. Velosa *et al.*, "V2X Use Cases Repository." 2023. [Online]. Available: https://ev4eu.eu/resources/

[6] C. P. Guzman *et al.*, "Deliverable D4.5 Demand Response Programs Design for EVs." Accessed: Mar. 26, 2026. [Online]. Available: https://ev4eu.eu/resources/

[7] N. Ilioupoulos, C. Dalamagkas, and G. Papadakis, "Open V2X Management Platform," Electric Vehicles Management for Carbon Neutrality in Europe (EV4EU), Deliverable D5.5 D5.5, Feb. 2024. [Online]. Available: https://ev4eu.eu/resources/

[8] "Υπολογισμός ρυθμιζόμενων χρεώσεων ηλεκτρικής ενέργειας." Accessed: Mar. 26, 2026. [Online]. Available: https://www.protergia.gr/spiti/oikiako-reuma-proionta/ypologismos-rythmizomenon-xreoseon/

[9] "GitHub - SAP/e-mobility-charging-stations-simulator: OCPP-J charging stations simulator · GitHub." Accessed: Mar. 13, 2026. [Online]. Available: https://github.com/sap/e-mobility-charging-stations-simulator

[10] P. G. Tzouras, P. Delialis, and C. Iliopoulou, "Assessing the Impact of Micromobility Measures on Last-Mile Network Resilience Using Agent-Based Simulation," *Procedia Comput. Sci.*, vol. 257, pp. 945–950, Jan. 2025, doi: 10.1016/j.procs.2025.03.121.

[11] "Δημοσίως Προσβάσιμα Σημεία Φόρτισης." Accessed: Mar. 12, 2026. [Online]. Available: https://electrokinisi.yme.gov.gr/public/ChargingPoints/

[12] "Στατιστικές - ELSTAT." Accessed: Mar. 12, 2026. [Online]. Available: https://www.statistics.gr/el/statistics/-/publication/SAM05/-

[13] "Pyomo," Pyomo. Accessed: Mar. 12, 2026. [Online]. Available: https://www.pyomo.org

[14] "Standard Load Profiles," RMDS Prd CM. Accessed: Mar. 12, 2026. [Online]. Available: https://rmdservice.com/reference/standard-load-profiles

[15] S. Sagaria, M. van der Kam, and T. Boström, "Vehicle-to-grid impact on battery degradation and estimation of V2G economic compensation," *Appl. Energy*, vol. 377, p. 124546, Jan. 2025, doi: 10.1016/j.apenergy.2024.124546.

[16] C. Vagdatli, V. Petraki, J. Roussou, and G. Yannis, "Economic Assessment of Free Public Transport in Athens," in *Transport Transitions: Advancing Sustainable and Inclusive Mobility*, C. McNally, P. Carroll, B. Martinez-Pastor, B. Ghosh, M. Efthymiou, and N. Valantasis-Kanellos, Eds., in Lecture Notes in Mobility. , Cham: Springer Nature Switzerland, 2025, pp. 647–653. doi: 10.1007/978-3-031-85578-8_87.

[17] S. Djurhuus, H. S. Hansen, M. Aadahl, and C. Glümer, "Individual Public Transportation Accessibility is Positively Associated with Self-Reported Active Commuting," *Front. Public Health*, vol. 2, p. 240, Nov. 2014, doi: 10.3389/fpubh.2014.00240.

[18] J. Li, E. Rombaut, and L. Vanhaverbeke, "Agent-based digital traffic model generation for regions facing data scarcity using aggregated cellphone data: a case study for Brussels," *Int. J. Digit. Earth*, vol. 17, Sep. 2024, doi: 10.1080/17538947.2024.2407046.

[19] V. Sharma, M. H. Haque, S. M. Aziz, and T. Kauschke, “Reducing Overvoltage-Induced PV Curtailment Through Reactive Power Support of Battery and Smart PV Inverters,” *IEEE Access*, vol. 12, pp. 123995–124008, 2024, doi: 10.1109/ACCESS.2024.3454313.